PROCESSING OF COMMERCIAL PURITY TITANIUM, ALUMINIUM AND Al-5Zn-1Mg ALLOY BY EQUAL CHANNEL ANGULAR PRESSING

Thesis

Submitted in partial fulfilment of the requirements for the degree of

DOCTOR OF PHILOSOPHY

by

JAMES VALDER

DEPARTMENT OF METALLURGICAL AND MATERIALS ENGINEERING
NATIONAL INSTITUTE OF TECHNOLOGY KARNATAKA, SURATHKAL, MANGALORE - 575025

July, 2014

D E C L A R A T I O N

I hereby declare that the Research Thesis entitled **"Processing of Commercial Purity Titanium, Aluminium and Al-5Zn-1Mg Alloy by Equal Channel Angular Pressing"** which is being submitted to the **National Institute of Technology Karnataka, Surathkal** in partial fulfilment of the requirements for the award of the Degree of **Doctor of Philosophy** in Metallurgical and Materials Engineering is a bonafide report of the research work carried out by me. The material contained in this **Research Thesis** has not been submitted to any University or Institution for the award of any degree.

JAMES VALDER

Register No.:**MT07P01**

Department of Metallurgical and Materials Engineering

Place: NITK Surathkal,Srinivasnagar

Date: 18.07.2014

C E R T I F I C A T E

This is to certify that the Research Thesis entitled, **"Processing of Commercial Purity Titanium, Aluminium and Al-5Zn-1Mg Alloy by Equal Channel Angular Pressing",** submitted by **James Valder** (Register Number: **MT07P01**) as the record of the research work carried out by him, is accepted as the **Research Thesis** submission in partial fulfilment of the requirements for the award of the degree of **Doctor of Philosophy**.

Prof. A.O. Surendranathan
Research Guide

Prof. Jagannatha Nayak
Chairman – DRPC
(Signature with Date and Seal)

ACKNOWLEDGEMENT

ABSTRACT

Severe plastic deformation (SPD) is a metal forming process in which a very large plastic strain is imposed on a billet in order to make an ultra-fine grained metal. Among all SPD processes, equal channel angular extrusion or pressing (ECAE/P) is an attractive processing method because of its simplicity and the possibility to scale up the technique for use in industrial applications. ECAE/P was originally developed by Segal et al. in the beginning of the 1980s' to introduce a homogeneous simple shear deformation into billets without any change in its dimensions. There are various types of ECAP that have been developed and applied in the production of fine grained structures like ECAP of rods, bars, tubes etc. Many industrially important materials such as commercially pure (CP)-Ti and its alloys, CP-Al and its alloys, etc. have been processed by ECAP.

In the present study, ECAP of CP-Ti rod in the wrought form, CP aluminium rod and tube in cast and wrought forms and Al-5Zn-1Mg alloy rod and tube in cast form using a die channel angle of 150° were investigated for various passes using four fundamental processing routes: route A where the sample is pressed repetitively without any rotation, route B_A where the sample is rotated by 90° in alternate directions between consecutive passes, route B_C where the sample is rotated in the same sense by 90° between each pass and route C where the sample is rotated by180° between passes. Mechanical properties of as-received and as-pressed billets after each pass were determined by Vickers hardness and tensile tests. Frictional property was determined by ring compression testing. The as-received microstructure and its evolution due to ECAP were characterized by optical microscopy. Failure analysis of fractured billets was characterized by scanning electron microscope (SEM). Compression testing was carried out for as-received and as-pressed billets to determine the flow properties before and after ECAP. Peak extrusion pressure was estimated for each pass for various routes by carefully recording the peak force for each pass.

Processing of CP-Ti at room temperature resulted in improved strength with reduction in ductility. In spite of increased strength the peak punch pressure decreased as the number of passes was increased to three. Processing of CP-Al rod in the cast form at room temperature resulted in improved strength. Flow properties like strength coefficient (K) and strain hardening exponent (n) were also found to increase as number of passes was increased to two. The peak punch pressure increased for second pass compared to the first pass. CP-Al rod in the cast form failed in the third pass. A failure analysis of the same was carried out with the help of SEM. Processing of CP-Al rod in the wrought form at room temperature resulted in improved strength with reduction in ductility. The peak punch pressure increased as the number of passes was increased to four. Al-5Zn-1Mg rod in the cast form failed during the second pass for all the temperatures selected for the study (303-673K). Friction factor (m) for Al-5Zn-1Mg was determined in the temperature range of 303-673K. The maximum plasticity was observed in the temperature range of 373-573K where a hardness improvement is also seen. Processing of CP-Al tube in the wrought form at room temperature resulted in improved hardness. The peak punch pressure increased as the number of passes was increased to three. CP-Al and Al-5Zn-1Mg tube in cast form could not withstand even a pass. Failure analysis was carried out and crack propagation was observed clearly. Out of the four routes employed in the study route B (B_A or B_C) showed superior mechanical properties in all the chosen metals and alloy. As far as peak punch pressure is concerned route A showed the least punch pressure for CP-Ti after three passes, whereas for CP-Al, route C showed lowest punch pressure except in tubular form where route A showed the minimum punch pressure. From the present study it is clear that the different microstructural parameters for grain refinement criterion may give rise to different conclusions on the effectiveness of deformation route.

CONTENTS

iv

LIST OF FIGURES

LIST OF TABLES

NOMENCLATURE

ABBREVIATIONS

AISI	:	American Iron and Steel Institute
CP	:	Commercially Pure
DSA	:	Dynamic Strain Ageing
ECAE/P	:	Equal Channel Angular Extrusion or Pressing
FEM	:	Finite Element Method
HSS	:	High-Speed Steel
SDF	:	Shape Difficulty Factor
SEM	:	Scanning Electron Microscope
SPD		Severe Plastic Deformation
XRD	:	X-Ray Diffraction

SYMBOLS

D	:	Diameter of the billet
d_o	:	Outer diameter of the ring specimen
d_i	:	Inner diameter of the ring specimen
h_0/d_0	:	Ratio of initial height of the compression test specimen to the diameter
K	:	Strength Coefficient
L	:	Length of the Billet
m	:	Friction factor
n	:	Strain hardening exponent
t_0	:	Thickness of the ring specimen
γ	:	Shear strain
ε	:	Equivalent Plastic Strain
φ	:	Die channel angle or angle of intersection
ψ	:	Outer corner angle or angle of curvature
σ	:	Flow Stress

CHAPTER 1

INTRODUCTION

The primary objective of metal working is to change billet shape and dimensions by various forming operations such as forging, rolling, extrusion and so forth. Simultaneously, plastic deformation is also recognized as an effective method for structure alteration and property improvement of metals and alloys. Until recently, traditional forming processes have been used to attain both goals. Multiple reductions of a billet cross section associated with traditional processing require high pressures and loads, powerful machines and expensive tooling.

There are especially difficulties to be overcome when producing large or massive products in the processing of new materials with stringent requirements for structure, texture and other properties. In these cases, the conventional processes are not optimal and special deformation methods must be developed with advanced technologies to solve many metallurgical and industrial problems. As a scientific concept, such an approach may be linked to the work in the 1930s' and 1940s' of Bridgeman who used torsion combined with compression to attain very large plastic strains. Although Bridgeman's anvils could be applied only to thin discs, this technique realizes intensive simple shear under high hydrostatic pressure that was essential for later developments [Segal, 2006].

Grain refinement is one of the techniques, which provides finer grains and hence ultra high strength and ductility combination demanded for ambient and cryogenic temperature applications. On the other hand, severe plastic deformation (SPD) is an effective tool for producing bulk nanostructured metals. As a new materials processing technology, severe plastic deformation (SPD) was introduced by Segal et al. in the beginning of the 1970s' at the Physical Technical Institute in Minsk, Russia. The main advantage of these SPD processes is that very high strain can be imparted to a specimen by repeatedly processing the material several times using the same die. This leads to the accumulation of plastic strain in the material. Conventional metal

forming processes do not provide such high levels of strain to the material without failure. Materials produced by severe plastic deformation are 100% dense, contamination free and sufficiently large for use in real commercial structural applications. These fine grained materials are found to have excellent super plasticity, high wear resistance, enhanced high cycle fatigue life and good corrosion resistance. They exhibit higher strength and hardness along with optimum values of ductility. The superior properties of these materials are derived from their unique microstructures which control deformation mechanisms and mechanical behavior. These characteristics of SPD process make themselves a novel technique in material processing. Several SPD processing methods are now available. These include high pressure torsion (HPT)[Sakai et al.,2005], equal channel angular pressing or extrusion(ECAP/E)[Segal et al.,1981], equal channel angular drawing(ECAD)[Chakkingal et al.,1998], multiple forging[Salishchev et al.,1993] and cylic extrusion and compression (CEC) [Korbel and Richert, 1985]. For sheet metals, accumulative roll bonding (ARB) [Saito et al., 1998], repetitive corrugation and straightening (RCS) [Huang et al., 2001], constrained groove pressing (CGP)[Shin et al., 2000] and constrained groove rolling [Lee and Park, 2002]. Among all these processes, ECAP/E is an attractive processing method because of its simplicity and there is a possibility to scale up the technique for use in industrial applications [Langdon, 2007].

Equal channel angular pressing or extrusion (ECAP/E) was originally developed by Segal et al. (1981) in the beginning of the 1980s' in the last century to introduce a homogeneous simple shear deformation into billets without any change in its dimensions. Since the early 1990s', the method was spreading out worldwide and has been improved by many research groups [Matthias Hockauf et al., 2008]. Equal channel angular extrusion is a material processing technique through which an ingot in the form of either cast or wrought are subjected to intense plastic straining, through two channels of equal cross-section intersecting at an angle 2φ that varies between 60°-150˚, which produces submicron grain structure without residual porosity. Since the two sections of the channels within the die are equal in cross section, there is no change in the billet dimensions during processing [Saravan et al., 2006]. This

facilitates repetitive extrusion through the ECAP channels. The intense plastic straining of the billets takes place at the intersection line between the two channels, where the material is subjected to simple shear strain, the magnitude of which depends on the angle 2φ. One important characteristic of ECAP is its ability to fragment the bulk materials structure by simple shear into a very fine grain size of one order of magnitude less than that produced by any conventional processing method.[Segal, 1995,Chakkingal and Thomson, 2001,Cornwell et al., 1996,Stolyarov et al., 2001, Horita et al., 2000 and 2001].

A schematic diagram of ECAP die with round corner intersections is shown in Fig. 1.1. A well-lubricated billet of almost same cross section is placed in the top channel and extruded into the intersecting channel by a punch [Segal, 1995 and Langdon et al., 2000]. It is believed that the stress characteristics are uniform in the cross section of the billet and that this uniformity of the stress-strain distribution ensures the uniformity of microstructure and mechanical properties in the processed billet [Lapovok, 2005].
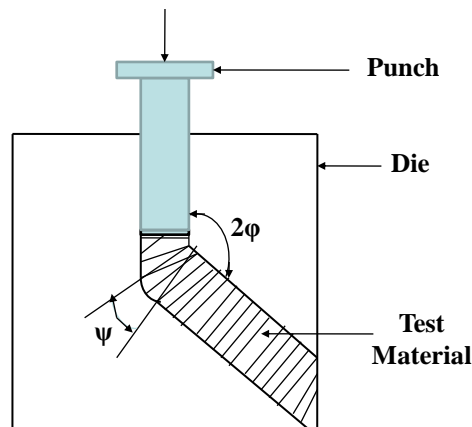
Fig. 1.1 Schematic diagram of equal channel angular pressing (ECAP) die with round corner

ECAP employs different processing routes for the deformation. Four fundamental processing routes have been identified: these are route A where the sample is pressed repetitively without any rotation, route B_A where the sample is rotated by 90°in alternate directions between consecutive passes, route B_C where the sample is rotated

in the same sense by 90˚ between each pass and route C where the sample is rotated by180˚ between passes [Nakashima et al., 2000].

The various types of ECAP that have been developed and applied in the production of fine grained structures are conventional ECAP of rods and bars [Nakashima et al., 2000 and Segal, 1995], ECAP of plate samples [Kamachi et al., 2003],ECAP with rotary dies, side-extrusion and multi-pass dies[Ma et al., 2005, Azushima and Aoki, 2002 and Nakashima et al., 2000],ECAP with parallel channels[Raab, 2005], continuous processing by ECAP [Han et al., 2002,Nam et al., 2003 and Park et al., 2004], ECAP–conformed process[Raab et al., 2004],consolidation by ECAP[Matsuki et al., 2000] and ECAP of tubular specimen[Nagasekar et al., 2006].

Many industrially important materials such as commercially pure Ti and its alloys, commercially pure Al and its alloys, commercially pure Mg and its alloys, steels, composites etc. have been processed by equal channel angular pressing.

After surveying the available literature, it was found that very less amount of data is available for ECAP using higher die angles. Most of the published research has dealt with fundamental issues in metallurgy such as development of sub-grain structures, grain refinement, formation of shear bands and development of texture in solid materials. Limited literature related to a die of channel angle 150° and property enhancement of rod and tubular specimen using ECAP have been reported. Not much study related to analysis of extrusion pressure during property enhancement of materials in the form of rods and tubes using ECAP have been reported. No work on commercially pure titanium rod was carried out with a die angle of 150°whereas Nagasekhar et al. (2006) conducted studies in the ECAP of tubular CP-Ti using same die angle. No work on ECAP of commercially pure aluminium and Al-5Zn-1Mg in the cast and wrought form either as rod or tube with die angle of 150° is reported yet.

1.1 SCOPE OF THE PRESENT WORK

The scope of the present work is to study the candidature of the ECAP process for commercially pure Ti rod in the wrought form, commercially pure aluminium rod and tube in cast and wrought form and Al-5Zn-1Mg alloy rod and tube in cast form using a die channel angle of 150˚.

1.2 OBJECTIVES

The objectives of the present research work were as follows:

1. To analyze the stress for forming commercially pure Ti using ECAP and its influence over the mechanical properties and microstructural evolution.
2. To analyze the stress for forming commercially pure aluminium in the cast and wrought form for rods and tubes using ECAP and its influence over the mechanical properties.
3. To analyze the stress for forming Al-5Zn-1Mg in the cast form for rods and tubes using ECAP and its influence over the mechanical properties and microstructural evolution.

1.3 STRUCTURE OF THE THESIS

A detailed review of the available literature on current knowledge of ECAP processing along with some remarks on the gap existing in the ECAP of titanium, aluminium and aluminium alloys are presented in Chapter 2.

Chapter 3 describes the ECAP die and testing methods to determine strength and ductility of ECAP processed samples. Experimental set ups and procedures followed for ECAP of rod and tube are also presented in the same chapter.

The results of mechanical property evaluation, microstructures, fractographs and analysis of punch pressure of all the chosen metals and an alloy are presented in Chapter 4.

A detailed interpretation and analysis of the results was carried out and the related discussions are presented in Chapter 5. The conclusions drawn based on these discussions are listed in Chapter 6.

CHAPTER 2

LITERATURE REVIEW

There are several well-established methods for subjecting metallic samples to an imposed strain, including the standard industrial metal-working processes like rolling, forging and extrusion. All of these methods demand a change in the physical dimensions of the sample. By contrast, equal channel angular extrusion/pressing (ECAE/P) differs from these conventional processes because the cross-sectional dimensions of the sample remain unaltered during straining.

Historically, ECAP was developed in the Soviet Union almost thirty years ago but the process has received significant interest in western countries only within the last fifteen years [Furukawa et al., 2001]. Several parameters in ECAP can be changed, such as route type, the number of passes, the extrusion temperature, and pre- or post-ECAP processing. Heat treatments, annealing, and cold working can be applied before or after ECAP. Thus, ECAP provides a vast selection of parameters, which in turn, can yield a wide range of material properties and microstructures. It has also been suggested that the use of back pressure during ECAP, in which pressure is applied at the opposite end of the billet as it is pressed through the extrusion channel, can provide high hydrostatic pressure levels [Cathleen Ruth Hutchins, 2007].

2.1 PRINCIPLE OF ECAE/ECAP

ECAP is a forming technique capable of producing uniform plastic deformation in various materials, without causing significant change in geometric shape or cross sectional area. It involves simple shear deformation which is achieved by passing the billet through a die containing two channels of equal cross section that meet at a predetermined channel angle usually between 60˚ to 150˚. The effective strain that is imposed on the specimen increases as the channel angle decreases. An important advantage of ECAP process is that a large amount of strain can be imposed without any major changes in the dimensions of the work piece. As the cross section of the

specimen is not altered, the material can be processed over and over again to achieve very large strain. Multiple pressing of specimen by ECAP also helps to achieve complex microstructures and textures by changing the orientation of the billet during successive pressings.

The schematic diagram of ECAP process is shown in Fig.2.1 [Tjong and Haydn, 2004]. It consists of two channels of equal cross sections intersecting at an angle φ. The billet placed in the first channel entry is extruded out of the second channel exit by the application of load using a punch. It has been demonstrated that, after extrusion, the entire billet is plastically deformed by simple shear except a small part at the ends.
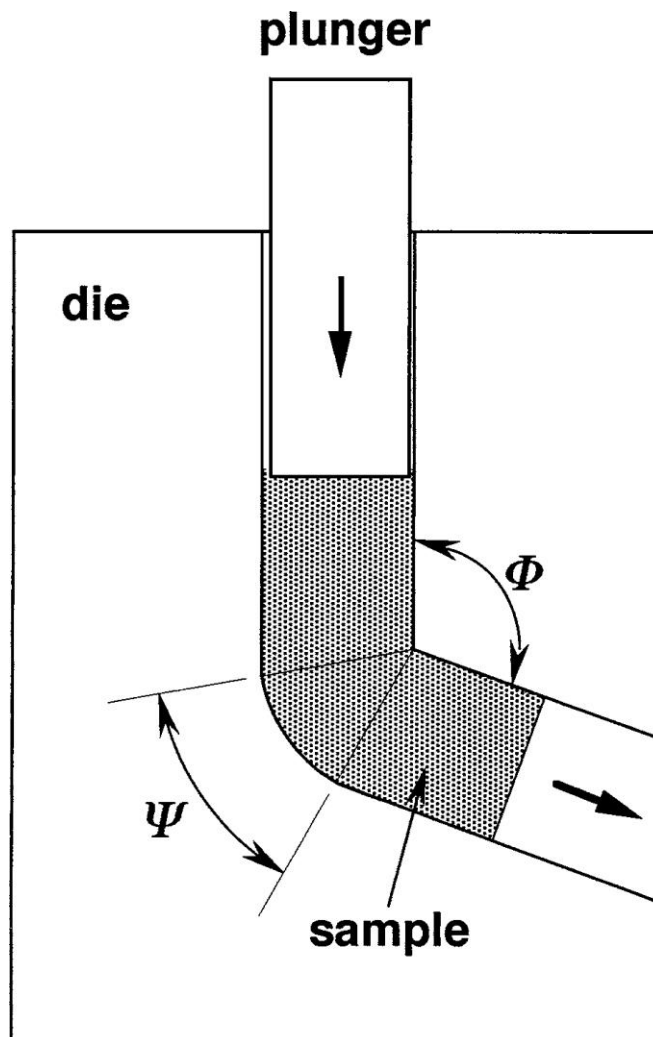
Fig.2.1 The schematic diagram of ECAP process

2.2 DEVELOPMENT OF PROCESSING USING ECAP

Various types of ECAP have been developed and applied in the production of fine-grained materials. They are described below

2.2.1 Conventional ECAP Of Rods And Bars

The sample, in the form of a rod or bar, is machined to fit within the channel and the die is placed in some form of press so that the sample can be pressed through the die using a plunger. In practice, many of the investigations of ECAP involve the use of bars with square cross-sections and dies having square channels. It is convenient to develop processing routes for these samples, in which the billets are rotated by increments of 90˚ between each separate pass. The same processing routes are also easily applied when the samples are in the form of rods with circular cross-sections [Nakashima et al., 2000 and Segal, 1995].

2.2.2 ECAP Of Plate Samples

For some industrial applications, such as the use of the ultra-fine-grained (UFG) materials produced by ECAP in super plastic forming operations, it is necessary that the as-pressed samples are in the form of thin metallic sheets. This requirement has prompted an interest in the possibility of applying ECAP to plate samples where the as-pressed materials can be readily prepared for use in conventional metal forming facilities. A limited number of reports are now available on the application of ECAP to plate samples [Kamachi et al., 2003, 2004, Ferrasse et al., 2004]. Unlike the bars and rods described in the preceding section, the number of possible rotations between passes is limited.

2.2.3 ECAP With Rotary Dies, Side-extrusion and Multi-pass Dies

An important limitation in conventional ECAP, as described in the preceding sections, is that the sample must be removed from the die and reinserted, with or without an intermediate rotation, in order to achieve large numbers of passes and a high imposed strain. These operations are both labor-intensive and time-consuming. Accordingly, several procedures are under development to avoid these limitations. A simple procedure that effectively eliminates the need for removing specimens from the die between each pass is to make use of rotary-die ECAP [Ma et al., 2005, Azushima and Aoki, 2002 and Nakashima et al., 2000].The facility consists of a die containing two channels, having the same cross-section, intersecting at the center of the die at an angle of 90˚. Three punches of equal length are inserted in the lower section of the vertical channel and in the horizontal channel .The sample is inserted in the vertical channel so that it rests on the lower punch and an upper punch is inserted to press the sample with a plunger. However, a significant advantage of this type of pressing is the simplicity of operation. For example, rotary-die ECAP has been used effectively for consecutive pressings up to a maximum of 32 passes [Ma et al., 2005]. However, a disadvantage of the process is that the aspect ratios of the sample are small so that end effects may lead to significant inhomogeneities [Ma et al., 2005]. An alternative but physically similar approach is the side-extrusion. This process uses four punch-pull cams which are capable of generating high forces during operation. This procedure has been used effectively for pressing up to 10 passes [Azushima and Aoki, 2002].

An alternative procedure, which does not require the acquisition of a complex pressing facility, is to construct a die having multiple passes. This type of die is useful in order to compare the microstructural characteristics in the same specimen after different numbers of passes.

2.2.4 ECAP With Parallel Channels

There is an important new development showing the potential for conducting ECAP using a facility containing two parallel channels. Some early results are available, which were obtained by making use of this approach [Raab, 2005] but the most recent

approach, combining a two-dimensional finite element method simulation and direct experiments, provides a very clear demonstration of the advantage of pressing with two parallel channels. A distinctive feature of ECAP with parallel channels is that, during a single processing pass, two distinct shearing events take place [Raab, 2005]. This means in practice that there is a considerable reduction in the number of passes required for the formation of an ultra-fine-grained structure.

2.2.5 Continuous Processing By ECAP

Continuous confined strip shearing, equal-channel angular drawing and conshearing processing by ECAP have attracted considerable attention because it produces ultra-fine-grained materials with unique physical and mechanical properties suitable for important applications in industry. Some initial effort has been made in developing processing technique for long metal strips. First, a process was developed using a rolling facility combined with the principles of ECAP [Han et al., 2002, Nam et al., 2003 and Park et al., 2004]. This process was variously designated as continuous confined strip shearing [Han et al., 2002], dissimilar-channel angular pressing (DCAP) [Nam et al., 2003] and equal-channel angular rolling (ECAR) [Nam et al., 2003 and Park et al., 2004]. Second, equal-channel angular drawing (ECAD) was proposed as a potential route for the processing of rod samples [Chakkingal et al., 1998,1999] but subsequent calculations, combined with experiments, demonstrated that ECAD entails a reduction in the cross-sectional area of the sample by >15% so that it cannot be used effectively for multi-pass processing [Alkorta et al., 2002]. Third, the conshearing method was proposed for use with metal strips [Saito et al., 2000, Utsunomiya et al., 2004] and this process, which employs a continuous rolling mill. Despite the apparent success associated with these various procedures, the results obtained to date cover only a very limited range of materials and they deal also with the processing of very small batches of each alloy.

2.2.6 ECAP–conformed Process

The conform extrusion process was developed over thirty seven years ago for the continuous extrusion of wire products but very recently it has been conveniently combined with ECAP in the ECAP–conform process [Raab et al., 2004]. In this process, the principle used is to generate a frictional force to push a work-piece through an ECAP die which is similar to conform extrusion process, but using a modified ECAP die design, so that the work-piece can be repetitively processed to produce UFG structures. It includes a rotating shaft in the center, which contains a groove, and the work-piece is fed into this groove. The work-piece is driven forward by frictional forces on the three contact interfaces with the groove so that the work-piece rotates with the shaft. However, the work-piece is constrained within the groove by a stationary constraint die and this die also stops the work-piece and forces it to turn at an angle by shear as in a regular ECAP process. In the current set-up, the angle is close to 90° which is the most commonly used channel intersection angle in ECAP. This set-up effectively makes the ECAP process continuous. Other ECAP parameters, such as the die angle and the strain rate, can also be incorporated into the facility.

2.2.7 Consolidations By ECAP

Although ECAP is generally associated with the processing of solid metals, it may be used also for the consolidation of metallic powders too [Matsuki et al., 2000]. An important difficulty in the pressing of powders is that cracking occurs readily on the surface of the pressed samples. To avoid cracking during ECAP consolidation, the powders were inserted into a tight-fitting outer jacket of the same alloy and pressed at the required temperature. It was shown recently that the propensity for cracking can be significantly reduced, or even eliminated, by pressing under a confining back-pressure [Xia and Wu, 2005].These and other similar results confirm, the potential for using ECAP as a tool in powder consolidation for the production of UFG microstructures.

2.2.8 ECAP Of Tubular Specimen

Nagasekar et al. (2006) studied the candidature of the ECAP process for processing of materials in tubular form using commercially pure titanium (CP-Ti). The scientific parameter that characterizes the resistance to flow during extrusion is the shape difficulty factor (SDF). As the shape difficulty factor is high in tubular specimen geometries compared to solid shapes, significant differences are expected as far as extrusion/pressing pressures, microstructures, and mechanical properties are concerned. In general, higher the value of SDF, higher is the pressure needed for extrusion. In extrusion of tubes, an addition to the extrusion pressure arises due to the presence of the mandrel which is inserted inside the tube while ECAP is carried out. Nagasekhar et al. (2006) also investigated the potential of commercial grade aluminium alloy (6010) for the ECAP process for the processing of tubular specimen. They suggested, if mechanical property enhancement can be achieved through this process, it can be used for the processing of light weight tubular torque transmission shafts that are subjected to combined axial, torsional, and bending stresses. The study included the influence of ECAP on tubular specimen geometries in enhancing the properties with respect to conventional extrusion.

2.3 CONSTRUCTION OF ECAP FACILITY

Normally construction of a conventional ECAP facility is by machining a two-piece split die consisting of a highly polished smooth plate bolted to a second polished plate containing a channel on its side. This type of die is well suited for laboratories and can be used for multiple passes provided care is taken to manually tighten the bolts between each separate pass. A suitable lubricant such as MoS_2 is generally used to minimize frictional effects at the die walls.

However, an alternative approach for minimizing friction is to make use of more complex configurations incorporating moving die walls [Segal, 2003, 2004, Semiatin et al., 2000]. An alternative approach is to construct a solid die from tool steel. Solid dies have an advantage because they avoid any problems associated with the extrusion of as lender piece of material between the separate parts of a die.

However, solid dies require the use of a channel having a circular cross-section and, in addition, the die must be constructed with a finite outer arc of curvature at the point of intersection of the two parts of the channel so that ψ=0˚. When working with solid dies, it is important to note that it is necessary to remove each specimen from the die by pressing the next specimen into the die. In practice, therefore, the final specimen is generally removed using a dummy specimen which then remains within the die. The scaling of ECAP processing to incorporate large billets and the pressing of hard-to deform materials require more complex construction of the ECAP facilities in order to maintain enhanced loading during the pressing operation. This is true also for the development of ECAP processing for commercial use conditions. In the present study, a two-piece split die made of high speed steel of 150˚ die channel angle and outer angle of curvature of 30˚ is used.

2.4 FUNDAMENTAL CHARACTERISTICS IN ECAP

ECAP is a metal flow process operating in simple shear and characterized by several fundamental parameters such as the strain imposed in each separate passage through the die, the slip systems operating during the pressing operation and the consequent shearing patterns present within the as-pressed billets. Taken together, these various processes define uniquely the precise nature of the pressing operation.

2.4.1 Strain Imposed In ECAP

Iwahashi et al. (1996) have given the expression by analytical approach for the shear strain imparted per pass as,

$$\gamma = 2\cot\left(\Phi+\frac{\Psi}{2}\right)+\Psi\left(\Phi+\frac{\Psi}{2}\right) \tag{2.1}$$

where, 2Φ is the angle of intersection and Ψ is the angle of curvature.

This is derived for ideal conditions of pressing. In reality, several factors should be taken into account such as the friction in the channel walls, flow localization, material properties etc. For the situation where $\Psi = 0°$ (i.e. die has a sharp corner), the shear strain per pass is given by,

$$\gamma = 2\cot\Phi \qquad (2.2)$$

As the number of passes increases the amount of strain also increases. Segal et al. (1995) has given the expression for total equivalent strain per pass as

$$\varepsilon = \frac{2}{\sqrt{3}}\cot\Phi \qquad (2.3)$$

For N passes, the total equivalent stain is given by,

$$\varepsilon = \frac{2N}{\sqrt{3}}\cot\Phi \qquad (2.4)$$

2.4.2 Processing Routes In ECAP

There are four basic processing routes in ECAP and these routes introduce different slip systems during the pressing operation so that they lead to significant differences in the microstructures produced by ECAP [Nemoto et al.,1998, Horita et al., 2000, Furukawa et al., 2003]. The four different processing routes are summarized schematically in Fig. 2.2 [Nakashima et al., 2000]. In route A the sample is pressed without rotation, in route B_A the sample is rotated by 90° in alternate directions between consecutive passes, in route B_C the sample is rotated by 90° in the same sense (either clockwise or counterclockwise) between each pass and in route C the sample is rotated by 180° between passes. Various combinations of these routes are also possible, such as combining routes B_C and C by alternating rotations through 90° and 180° after every pass, but in practice the experimental evidence obtained to date suggests that these more complex combinations lead to no additional improvement in the mechanical properties of the as-pressed materials. Accordingly, for the simple

processing of bars or rods, attention is generally devoted exclusively to the four processing routes illustrated in Fig. 2.2.
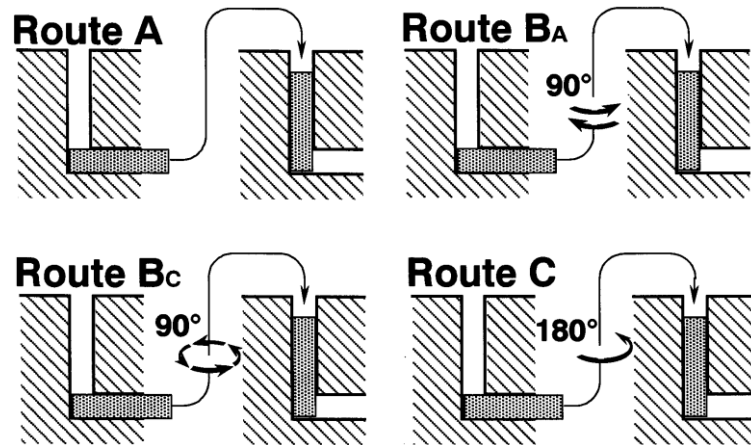
Fig.2.2. The four fundamental processing routes in ECAP

2.4.3 Slip Systems For The Different Processing Routes In ECAP

The different slip systems associated with these various processing routes were studied by Nemoto et al. (1998) and found that in route C, the shearing continues on the same plane in each consecutive pass but the direction of shear is reversed on each pass. Thus route C is termed a redundant strain process and the strain is restored after every even number of passes. Route B_C is also redundant strain processes because slip in the first pass is cancelled by slip in the third pass and slip in the second pass is cancelled by slip in the fourth pass. By contrast, routes A and B_A are not redundant strain processes and there are two separate shearing planes intersecting at an angle of 90° in route A and four distinct shearing planes intersecting at angles of 120° in route B_A. In routes A and B_A, there is a cumulative build up of additional strain on each separate pass through the die.

2.4.4 Shearing Patterns Associated With ECAP

The information available on shearing patterns in conventional ECAP using 90° and 120° dies for the pressing of plate samples where rotation occurs about the Y or Z axes by Furukawa et al. (2002) shows that the angular range is zero on all planes when using route C or when viewing the X or Z planes in route A. It is seen that route B_C yields the largest angular range after 4 passes. These angular ranges can be re-examined when considering the preferred route for developing an equiaxed and homogeneous microstructure.

2.5 EXPERIMENTAL FACTORS INFLUENCING ECAP

When materials are processed using ECAP, several factors influence the workability and the microstructural characteristics of the billets. These factors fall into three distinct categories. Firstly, there are factors associated directly with the experimental ECAP facility, such as die angle and the outer arc of curvature. Secondly, there are experimental factors related to the processing regimes where some control may be exercised by the experimentalist including, for example, the speed of pressing, the temperature of the pressing operation and the presence or absence of any back-pressure. Thirdly, there are also other processing factors which may play a role in influencing the extent of the grain refinement and the homogeneity of the as-received microstructure including the nature of the crystallographic texture and the distribution of grain misorientations in the initial material. Therefore it is important for the experimentalist to conduct a detailed characterization of the material prior to initiating the pressing operation. The first two sets of experimental factors are under consideration in the present study.

2.5.1 Influence Of Channel Angle

The channel angle, φ, is the most significant experimental factor since it decides the total strain imposed in each pass and thus it has a direct influence on the nature of the as-pressed microstructure. There are two separate literatures describing experimental

assessments of the significance of the channel angle. The first literature describes experiments on pure aluminum using a series of dies. Nakashima et al. (1998) conducted experiments using four separate dies having channel angles of 90˚, 112.5˚, 135˚ and 157.5˚: these four dies are illustrated schematically in Fig. 2.3 and the diagrams include the values for the arcs of curvature, Ψ. The second literature describes experiments on OFHC (Oxygen free high conductivity) copper pressed using two dies having channel angles of either 90˚ or 120˚ [Huang et al. 2001].
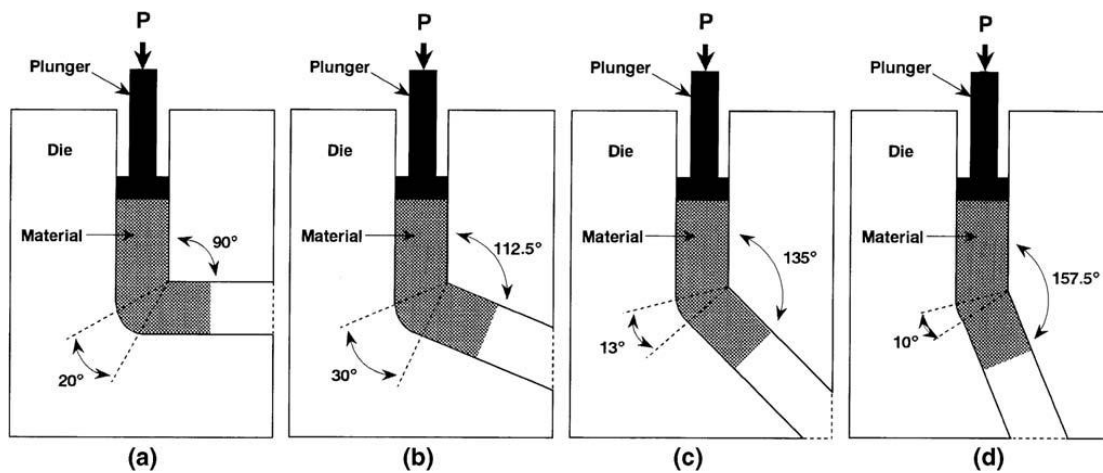
Fig. 2.3 Schematic illustration of the dies used to evaluate the influence of the channel angle, φ: the values of φ are (a) 90˚, (b) 112.5˚, (c) 135˚ and (d) 157.5˚[Nakashima et al. 1998]

Despite the efficiency of ECAP dies with channel angles of $\varphi = 90˚$, it is important to recognize that it is experimentally easier to press billets when using dies with angles that are larger than 90˚. For some very hard materials or with materials having low ductility, this may be an important consideration. For example, experiments showed that it was not feasible to press commercial purity tungsten through a die with a channel angle of 90˚ at a temperature of 1273 K because of cracking in the billets but excellent results were achieved at the same pressing temperature when the channel angle was increased to 110˚ [Alexandrov et al., 2000].

2.5.2 Influence Of Angle Of Curvature

The angle of curvature, ψ, denotes the outer arc where the two parts of the channel intersect within the die. This angle plays only a minor role in determining the strain imposed on the sample. The role of this angle is also important because, whereas conventional split two-part dies are easily constructed with ψ = 0˚, all solid dies will necessarily incorporate ψ> 0˚. The reason is because of the development of the corner gap or ''dead zone'' which is formed at the outer corner when the billets pass through the die. This means that the billet no longer remains in contact with the die walls at this outer corner [Wu and Baker, 1997 and Shan et al., 1999]. The angle subtended by the corner gap also depends on the rate of strain hardening of the material. From a practical point of view, however, incorporating an angle of curvature is difficult because split dies are easily constructed with no curvature at either the outer or inner points of intersection and in solid dies, where an outer arc of curvature is required, it is difficult to machine a die having equal fillet radii at both the inner and outer intersections. In view of these difficulties, it is reasonable to state that the most promising approach is to construct a die with an outer angle of curvature and with no arc of curvature at the inner point of intersection of the two parts of the channel.

2.5.3 Influence of pressing speed

Processing by ECAP is generally carried out by high-capacity hydraulic presses that operate with relatively high ram speeds. Typically, the pressing speeds are in the range of ~1–20 mm s^{-1}. It is also feasible to construct dies for use in conventional mechanical testing machines and which provides a range of pressing speeds. A study conducted by Berbon et al. (1999) shows that the pressing speed has no significant influence on the equilibrium size of the ultra-fine grains formed by ECAP but, since recovery occurs more easily when pressing at the slower speeds, these lower speeds produce more equilibrated microstructures. A similar conclusion was reached also in tests on pure Al and three Al-based alloys using pressing speeds of 18 and 0.18 mm s^{-1} where it was shown that there is an abrupt heating of the samples when testing at the faster rate but no significant heating at the slower rate [Yamaguchi et al., 1999]. In

addition, tests on titanium using pressing speeds of 0.2 and 2.8 mm s^{-1} revealed only minor microstructural differences in these specimens after pressing through only 1 pass [Kim et al., 2003].

2.5.4 Influence Of Pressing Temperature

The pressing temperature is a key factor in any ECAP process and it can be controlled relatively easily. A detailed investigation of the influence of temperature involved samples of pure Al, an Al–3%Mg alloy and an Al–3%Mg–0.2%Sc alloy with the pressing conducted from room temperature to 573 K. Yamashita (2000) revealed an increase in the equilibrium grain size with increasing temperature and from the examination of the selected area (electron) diffraction (SAED) patterns, it was found that the fraction of low-angle grain boundaries increased with increasing temperature. It was suggested, that faster rates of recovery at the higher temperatures which led to an increasing annihilation of dislocations within the grains and a consequent decrease in the numbers of dislocations absorbed into the subgrain walls. However, there was also a significant dependence on material because the transition to a high fraction of low-angle boundaries occurred at pressing temperatures of 473 K in pure Al and at 573 K in the Al–3%Mg alloy.

The tendency for larger grains or subgrains to form at the higher pressing temperatures was confirmed in several subsequent investigations [Shin et al., 2002, Chen et al., 2003, Huang et al., 2004 and Ma´lek et al., 2004] and detailed analyses using Kikuchi patterns also confirmed the tendency for a higher fraction of high-angle boundaries to form at the lower temperatures [Goloborodko et al., 2004 and Wang et al., 2004]. For the pressing of commercially pure Titanium, there was evidence for a change in the deformation mechanism from the formation of parallel shear bands to the formation of deformation twinning bands when the pressing temperature was increased from 473 to 523 K [Kim et al., 2003]. All of these results demonstrate that, although it is generally experimentally easier to press specimens at high temperatures, optimum ultra-fine-grained microstructures will be attained when the pressing is performed at the lowest possible temperature where the pressing operation can be

reasonably conducted without the introduction of any significant cracking in the billets.

2.5.5 Influence Of Back Pressure

The importance of using a back-pressure is an area of special interest in recent years [Raab et al., 2000, Stolyarov et al., 2003, Stolyarov and Lapovok, 2005]. ECAP die-sets can be designed to conduct the processing with a precise back-pressure which is computer-controlled. An important advantage in imposing a back-pressure is that it leads to a very considerable improvement in the workability of the processed samples. For example, during the ECAP of Cu in the absence of a back-pressure it is generally found that cracks appear on the billet surface after about 12–13 passes. However, when a back-pressure of only 300 MPa is imposed during ECAP, the same samples remain integral without any perceptible cracking even after 16 or more passes [Valiev et al., 2002]. Similarly, a sample of a quenched aluminum 6061 alloy failed in the first pass during ECAP at room temperature in the absence of a back-pressure but during pressing with a back-pressure of 450 MPa the sample was processed up to 4 passes without any cracking [Krasilnikov, 2005]. Another important advantage of back-pressure is the visible enhancement introduced in the uniformity of the metal flow during the ECAP operation. During ECAP there is an under filling of the outer angle of the die due to the formation of a dead zone and, especially in strain-hardenable materials, there can also be a change in the shape of the deformation zone from a pure shear line to a fan shape within the die [Semiatin and DeLo, 2000]. As a result, the microstructural refinement becomes less uniform, especially in the vicinity of the bottom surface of the billet. By contrast, the application of a back-pressure leads to a filling of this outer corner, and a consequent removal of the dead zone, regardless of the character of the material strengthening. Furthermore, the deformation zone becomes closer to a localized shear band which is typical of a rigid perfectly-plastic body [Lapovok, 2005]. A back-pressure can be imposed in several ways. The simplest procedure is to increase the level of friction in the exit channel or to make use of a viscous ductile medium [Raab et al., 2000]. However, an improved and more controlled procedure is to use special devices such as the application of a second

punch in the output channel [Lapovok, 2004, 2005]. In practice, an optimum condition may be achieved by using a computer-controlled ECAP die where it is possible to control not only the forward and backward pressures but also the velocities of both punches.

2.6 CHARACTERISTIC FEATURES OF METALS AND ALLOYS PROCESSED BY ECAP

The characteristics of the as-pressed microstructures are influenced by several variables including the total strain imposed in ECAP processing (number of passes through the ECAP die), the processing route (in terms of routes A, B_A, B_C and C) and the nature of the material (including the crystal structure, the stacking-fault energy and the rate of microstructural recovery). All of these features interact in different ways so that, when combined with experimental factors such as the values of the angles φ and Ψ within the die, the values of the pressing speed and temperature and the imposition of any back-pressure, there are a multiplicity of permutations which make it difficult to identify the precise requirement in order to achieve an optimum ultra-fine-grained microstructure. Nevertheless, there are some basic trends that provide very clear indications of the best procedures that maybe undertaken in order to achieve excellent microstructures after ECAP leading to exceptionally high strength and good mechanical properties. Few factors which influences the as-pressed microstructures are listed below.

2.6.1 Microstructural Features After ECAP

The characteristic of the microstructures introduced by ECAP have been evaluated in numerous investigations. However, almost all of these investigations employ transmission electron microscopy for determinations of the grain sizes produced by ECAP and the nature of any dislocation interactions occurring within the grains. An alternative approach is to employ optical microscopy to study the shearing of the original grains as they pass through the shearing plane within the die. An initial examination of shearing at the macroscopic level provides an opportunity to make

direct comparisons with the theoretical predictions both for the three-dimensional shearing behavior of large solid bodies and for the slip systems visible on orthogonal sections after ECAP processing. Iwahashi et al. (1998) in their study showed that the grains which were initially equiaxed have become elongated along the Y direction and flattened in the Z direction. In addition, slip was visible within these elongated grains lying approximately parallel to the Y direction. On the Y plane, the grains were elongated in a direction inclined, in an anti-clockwise rotation, through an angle of ~25–30˚ to the X direction. Within these grains, slip systems operate over a range of angles from ~29˚ to ~70˚ but primarily at an angle of 45˚ to the X direction. Finally, on the Z plane the grains remain reasonably equiaxed, they retain essentially the initial size and there is some slip parallel to the Y direction.

Various investigations on processing by ECAP showed significant distortions of the large equiaxed grains that are present in the unpressed alloy. This includes both the distortions of the grains at the macroscopic level and the predominant slip systems visible within the grains on three orthogonal planes of sectioning. Confirmation of these distortions at the macroscopic level was obtained by incorporating embedded solid inserts into the unpressed billets and then pressing these billets and examining the distortions of the embedded elements after ECAP [Kamachi et al., 2003]. Although the microscopic approach using optical microscopy provides very useful information in the early stages of deformation in ECAP, the approach is not feasible after multi passes because the grains get extremely distorted and it is difficult if not impossible to clearly differentiate the shapes of the individual grains.

2.6.2 Significance Of The Grain Size In ECAP

Iwahashi et al. (1998) determined the ultimate equilibrium grain size by measuring the width of the elongated cell or subgrain array which is formed on the first pass of ECAP. Fukuda et al. (2006) found that this array was developed such that the longer sides of the subgrain bands were oriented parallel to the primary slip plane. The deformation occurring in ECAP is analogous to higher strain deformation occurring in

conventional metal-working processes. The significant feature of ECAP is that, the billet retains the same cross-sectional area so that repetitive pressings are feasible. Materials processed by ECAP can be deformed to very high strains wherein the subgrain boundaries evolve into high-angle boundaries through the absorption of dislocations, thereby producing arrays of ultra-fine grains separated by high-angle grain boundaries. This evolution cannot be achieved in more conventional metal-working processes because of the natural limit imposed on the total strain introduced during deformation. It is possible to attain much smaller grain sizes by alloying but the production of an array of equiaxed grains may then require larger number of passes. The occurrence of smaller grain sizes on alloying with magnesium is attributed to the decreasing rates of recovery in the solid solution alloys [Iwahashi et al., 1998].

An alternative procedure for decreasing the grain size is to combine processing by ECAP with some other post-ECAP procedure. An alternative possibility is to cut small disks from the as-pressed billets for processing by high-pressure torsion (HPT). This combination of ECAP and HPT was successfully used both with CP-Ti where the grain size was reduced from ~300 nm after ECAP to ~200 nm after ECAP + HPT [Stolyarov et al., 1999] and high-purity nickel where the grain size was reduced from~350 nm to ~140 nm using these two processes, respectively [Zhilyaev et al., 2005]. Combination of ECAP + HPT decreases the fraction of low-angle boundaries. On the basis of the fragmentation theory, which states that the structure of a severely-strained metal represents a system of junction declinations [Rybin and Izvestiya, 1991], it was demonstrated that the ultimate grain refinement should depend both on the nature of the metal and on the straining regimes including the temperature, the rate of pressing and the applied pressure [Kopylov and Chuvil'deev, 2004].

2.6.3 Influence Of ECAP On Precipitates

The potential for precipitate fragmentation during ECAP was first recognized for $\theta`$ precipitates in an Al–Cu alloy [Murayama et al., 2001] and subsequently there were similar reports of the fragmentation of $\beta`$- precipitates [Oh-ishi et al., 2002] and

metastable β``- precipitates [Cabibbo et al., 2005] in Al–Mg–Si alloys and η-phase $MgZn_2$ precipitates in Al-7050 [Nam et al., 2003] and Al-7034 alloys [Xu et al., 2003 and 2005]. For the Al-7034 alloy the microstructure in the as-received condition revealed the presence of three different types of precipitates [Xu et al., 2005]. There were large rod-shaped precipitates which were identified as the η-phase ($MgZn_2$), an array of very fine particles which was identified as primarily representing the metastable hardening θ`-phase but with additional Al_3Zr particles that were identified through the presence of Ll_2 superlattice reflection spots in the SAED patterns. Microstructures after one and two passes of ECAP revealed that the large rod-shaped precipitates have become fragmented by the high pressure imposed in ECAP. By contrast, inspection showed the very fine spherical particles of Al_3Zr appeared to be unaffected by the ECAP processing but there were also arrays of fine and reasonably spherical precipitates having sizes in the range of ~30–100 nm. These spherical precipitates were also identified as the η-phase and it was concluded that, although many of the more irregular particles were formed by fragmentation of the larger precipitates, it was reasonable to assume that many of the smaller $MgZn_2$ precipitates formed through a direct transformation of the η`-phase into the η-phase with subsequent coarsening. Thus, it is anticipated that this transformation occurs easily at the ECAP temperature of 423 K.

2.7 MECHANICAL PROPERTIES ACHIEVED USING ECAP

The small grain sizes and high defect densities inherent in materials processed by severe plastic deformation lead to much higher strengths than in their coarse-grained counterparts.

2.7.1 Strength And Ductility

It has been widely demonstrated that a major grain refinement, may lead to a very high hardness in various metals and alloys but nevertheless these materials invariably exhibit low ductility under tensile testing [Koch, 2003]. Strength and ductility are the key mechanical properties of any material but these properties typically have

opposing characteristics. Thus, materials may be strong or ductile but they are rarely both. The reason for this dichotomy is of a fundamental nature. The plastic deformation mechanisms associated with the generation and movement of dislocations may not be effective in fine grains or in strongly-refined microstructures. This is equally true for ECAP -processed materials. Thus, most of the materials have a relatively low ductility but they usually demonstrate significantly higher strength than their coarse-grained counterparts. Despite this limitation, it is important to note that ECAP processing leads to a reduction in the ductility which is generally less than in more conventional deformation processing techniques such as rolling, drawing and extrusion. For example, experiments conducted to compare the strength and ductility of the 3004 aluminum alloy processed by ECAP and cold-rolling [Horita et al., 2000] revealed that the yield strength increased monotonically with the increasing equivalent strain imparted into the alloy by either cold rolling or ECAP [Zhu and Langdon, 2004]. However, it is apparent also that the overall ductility exhibits different trends for these two processing methods. After one ECAP pass, equivalent to a strain of ~1, the elongation to failure or the ductility of the alloy decreases from ~32% to ~14%. However, there is no additional reduction in the ductility with additional ECAP passes and therefore with the imposition of even larger strains. By contrast, cold-rolling decreases the ductility by a similar magnitude initially but thereafter the ductility continues to decrease with increasing rolling strain although at a slower rate. Consequently, processing by ECAP leads ultimately to a greater retention of ductility than conventional cold-rolling.

The extraordinary combination of high strength and high ductility for the nano structured Cu and Ti after processing by SPD clearly sets them apart from the other coarse-grained metals. Similar tendencies have been reported in a number of metals, including Al [May et al., 2005], Cu [Dalla Torre et al., 2004], Ni [Krasilnikov et al., 2005] and Ti [Valiev et al., 2003] after processing through various types of severe plastic deformation such as ECAP, high-pressure torsion or accumulative roll bonding. It has been suggested that this behavior is associated with an increase in the fraction of high-angle grain boundaries with increasing straining and with a consequent change in the dominant deformation mechanisms due to the increasing

tendency for the occurrence of grain boundary sliding and grain rotation. The ductility enhancement was also suggested to be due to the introduction of a bimodal distribution of grain sizes [Wang et al., 2002]. The reason for this behavior is that, while the nano crystalline grains provide strength, the embedded larger grains stabilize the tensile deformation of the material. Investigation of copper [Mughrabi et al., 2003] showed that bimodal structures may increase the ductility not only during tensile testing but also during cyclic deformation. An alternative approach has been suggested for enhancing strength and ductility based on the formation of second-phase particles in the nanostructured metallic matrix [Koch, 2003] where it is anticipated that these particles will modify the shear-band propagation during straining and thereby increase the ductility.

The principle of achieving high strength and high ductility through the introduction of intermediate metastable phases can be successfully realized from a commercial Al–Zn–Mg–Cu–Zr alloy [Islamgaliev, 2001] and an Al–10.8%Ag alloy subjected to ECAP and subsequent ageing [Horita et al., 2005]. It was shown, using scanning TEM, that the peak hardness achieved after ECAP and ageing for 100 h is due to precipitation within the grains of spherical particles with diameters of ~10 nm and elongated precipitates with lengths of ~20 nm. The spherical particles were identified as η-zones consisting of arrays of solute atoms lying parallel to the (001) plane sand the elongated precipitates were identified as the plate-like γ` particles. It was also shown that additional ageing up to 300 h led to a growth in the γ` particles and a very significant reduction in the density of the fine η-zones, thereby giving a consequent loss in hardening at the longest ageing time recorded. The introduction of ageing after ECAP has an important influence on the stress–strain behavior at room temperature. For the ECAP condition, the strength is high in the absence of ageing but there is a negligible region of uniform strain and no significant strain hardening.

2.8 ADVANTAGES AND DISADVANTAGES OF ECAP

ECAP has the following advantages:

(i)   Homogeneity in structure and properties are developed throughout the worked materials.

(ii)   A high equivalent deformation per pass and a higher total effective deformation after multiple passing occur without any appreciable change in the cross section of the initial billet.

(iii)   Relatively low pressure sand loads are sufficient for pressing at a higher die angle and temperature.

(iv)   Complicated structures and textures are possible because of careful control over the direction of shear, the homogeneous stress-strain state, the capacity for extremely large deformations in massive products and the opportunity to modify the shear lane and direction during a multiple extrusion sequence.

(v)   The simulation of different mechanisms of structure formations and phase transformations are possible using this metal working procedure.

(vi)   The process is not expensive to set up with standard metal working equipment fitted with inexpensive devices and tools.

(vii)   The process can be applied to various metals and alloys, including high strength and difficult to deform materials under cold, warm and hot working conditions.

The disadvantages are:

(i)   Designing a die suitable to process a variety of engineering materials has been identified as a major difficulty in commercialization of the process.

(ii)   **ECAP** is a batch process and is limited by the length of the material it can handle.

In spite of these limitations, there are many potential and promising applications of this deformation method in material synthesis and processing. Breakdown of cast ingots, consolidation and bonding of powders and grain refinement by intensive **ECAP** with subsequent recrystallisation treatments can be used to produce submicron grained mechanical properties. Extensive studies are being carried out in many research laboratories all over the world on the use of the process for developing exotic materials such as nanocrystalline materials, in situ composites, ultra-fine-grained materials, processing of intermetallics etc.

2.9 DEFORMATION BEHAVIOR OF ALUMINIUM AND ITS ALLOYS

Of all the metals, aluminum occupies the predominant role in terms of both production volume and value based on the annual volume of production of primary and secondary metal, aluminum is placed directly after iron. Major amount of aluminium goes to be produced as wrought alloys and semi-finished products. The working temperature depends on the flow stress variations and the friction across the tooling. Alloys and quality requirements determine the necessary exit temperature of the product. The flow stress of aluminum alloy is very much dependent on the temperature and composition. The control of processed aluminium alloy grain structures is being driven by many applications and is the immediate and future requirements for aerospace as well as automotive industries. Aluminium provides the characteristics of good strength to weight ratio, machinability, corrosion resistance, attractive appearance, high thermal conductivity and high electrical conductivity. Aluminium alloys are low density materials which do not react chemically with a wide range of liquid fuels and oxidizers and experience no sudden transition from ductile to brittle behavior at low temperatures.

The physical and metallurgical properties of aluminium and its alloys make them particularly suitable for ECAP. The face centered cubic (FCC) structure with 12 slip systems combined with a high stacking fault energy makes aluminum and its alloys good for cold, warm and hot working. The hot working temperature of aluminium alloys falls in the range of 350 to 550°C, which the tools made from the hot working

steels can easily withstand. Aluminium forms age hardening alloys with low alloying additions that combined good hot workability with a high strength after heat treatment.

Iwahashi et al.(1997,1998) and Nemoto et al. (1999) processed pure Al with ECAP routes A, B_C and C using a die with $\emptyset = 90°$. They concluded that route B_C is the most effective in refining grain size and route A is least effective. Oh-Ishi et al. (1998) processed pure Al with routes B_C and B_A using a 90˚ die. Collectively, they found that route B_C is the most effective in grain refinement while route C is intermediate and routes A and B_A are least effective. These results are different from the observations of Prangnell et al. (1999) who found that the most effective method of forming a sub micron grain structure is to maintain a constant strain path. While no satisfactory explanation has been found to interpret the above observations, shearing strain path generated by different processing routes [Iwahashi et al., 1997, 1998] and accumulative strain [Prangnell et al., 1999] are believed to play major roles. Zhu and Lowe (2000) suggested that the interaction of shear path with crystal structure and deformation texture, which has not been well understood, play a major role in the grain refinement. The crystal structure largely determines the deformation system under a certain deformation mode.

The age hardenable wrought aluminium alloy compositions include alloys of the 2XXX (Al-Cu, Al-Cu-Mn and Al-Cu-Mg), 6XXX (Al-Mg-Si) and 7XXX (Al-Zn-Mg) series. The high strength 2XXX and 7XXX series are used extensively in airframe construction due to their superior strength, high fracture toughness, good fatigue resistance and acceptable corrosion properties. In a typical commercial aircraft structure, aluminium alloys of the 2XXX and 7XXX series comprise 80-85 percent of the structural weight. Among aluminium alloys Al-Zn-Mg system is the hardest of all. Early research on the processing of Al and its alloys by ECAP generally focused on the process of grain refinement [Wang et al., 1996, Stolyarov et al., 1997, Iwahashi et al., 1997, 1998]. More recently, there has been a growing interest in controlling the precipitation microstructures of Al alloys and thereby achieving a combination of strengthening from both grain refinement and precipitation hardening [Nakashima et

al., 2000]. The evidence to date suggests that processing by ECAP has a relatively complicated effect on precipitate evolution. Thus, conducting ECAP at room temperature generally suppresses precipitation in Al alloys because no precipitation was reported in the as-quenched samples during the process [Zhao et al., 2004 and Horita et al., 2005] and there was dissolution of pre-existing θ` precipitates in the matrix after eight passes of ECAP [Murayama, 2001]. On the other hand, when the ECAP is conducted at higher temperatures, such as 473 K, precipitation is promoted in an Al–Zn–Mg alloy [Gubicza et al., 2007]. Experiments on an Al–Cu–Mg alloy showed that one pass of ECAP at room temperature initiated a rotation of pre-existing large h_0 precipitates, whereas four passes led to the fragmentation of h_0 plates and the formation of spherical nanoparticles [Murayama, 2001]. In an Al–Zn–Mg–Cu (Al-7034) alloy, processing by ECAP at 473 K produced spherical precipitates by fragmentation of the pre-existing larger platelet precipitates [Xu et al., 2005]. To date, only fragmentation of the larger precipitates has been identified as a mechanism dominating precipitate evolution for materials containing pre-existing large precipitates [Murayama, 2001 and Xu et al., 2005] and accordingly it is not clear at present whether other mechanisms may be involved and, if so, whether they are equally important in precipitate evolution. The results to date have established that the high strains imposed by SPD are effective in altering the precipitate orientations within the matrix. This potentially may provide an effective method for manipulating the precipitate morphology and obtaining unique microstructures that are significantly different from those formed by conventional ageing treatments.

2.10 DEFORMATION BEHAVIOR OF CP-TITANIUM

Commercial purity titanium (CP-Ti) is an attractive candidate material for a wide range of applications. It is widely used for medical implants and as a structural metal for high performance applications. There have been several studies on the ECAP of CP-Ti. The possible application of ECAP to HCP metals, such as titanium and its alloys, is challenging because the deformability of these materials is normally inferior to that of cubic metals. It depends on physical mechanisms such as crystallographic texture, density of twinning, morphology of grain and dynamic strain aging. Plastic

behavior of CP -Ti depends not only on the current state of deformation but also on the deformation history. CP-Ti is usually processed by ECAP at warm working temperatures in the range of 350˚C to 500˚C. However there are reports of successfully pressing the CP-Ti material at lower temperatures and room temperatures. Raab et al. (2004) successfully pressed Ti at 200˚C using a back pressure of 640 MPa. Zhao et al. (2008) had shown that ECAP of CP-Ti at room temperature is possible using an increased channel angle of 120˚ within the ECAP die and relatively a low ram speed of 0.5 mm/s. Xirong et al. (2009) showed that CP-Ti can be processed by multipass ECAP process at room temperature. Zeipper et al. (2002) have noticed that one to eight passes of ECAP results in a homogeneous microstructure formation with an increasing amount of high angle grain boundaries. Stolyarov et al. (2001) processed Ti through ECAP routes B_C, B_A and C to study the effect of shearing strain path on its microstructures. They also studied surface quality, microhardness, tensile properties, anisotropy and thermal stability. Stolyarov et al. (2008) also combined ECAP and cold rolling to create UFG CP-Ti and thereby obtained yield and ultimate strengths as high as 1020 MPa and 1050 MPa respectively.

The mechanical behavior of CP-Ti has been systematically investigated by Nasser et al. (1999). They have found that true stress- true strain curves of CP-Ti show two stages of deformation pattern at low temperatures, three stages at temperatures above 296 K and only one stage at temperatures exceeding 800 K, although all three stages may exist even at 1000 K for very high strain rates where the dislocation motion is still the major cause for plastic deformation. The loss in ductility and the variation of flow stress, the strength coefficient and the strain hardening exponent with variation in temperature characterize the onset of strain aging. A sudden increase in the work metal temperature due to adiabatic heating also contributes to occurrence of strain aging. At lower test temperatures in the range 100˚C - 250˚C dynamic strain ageing phenomenon is observed [Venugopal et al., 1990].

Due to its limited number of slip systems, plastic deformation of CP-Ti is usually accommodated by a combination of deformation twinning and slip by dislocation

motion [Kim et al., 2003].This behavior is mainly due to the fact that slip occurs primarily only on basal or prism planes along the close-packed **a** direction. Yoo (1981) revealed, a slip in titanium along $\langle 11\bar{2}0 \rangle$ direction primarily on $\{10\bar{1}0\}$ planes and less frequently on the $\{0001\}$ planes. Since a slip does not induce a plastic strain along the **c** axis of the crystal, deformation twinning or **c+a** slip on pyramidal planes have been observed to accommodate the plastic strain imposed by conventional deformation processes [Paton and Backoften, 1970, Akhtar, 1975, Minonishi et al., 1982]. The twinning planes in titanium are $\{11\bar{2}1\}$ and $\{11\bar{2}2\}$ at ambient temperatures and $\{10\bar{1}1\}$ at temperatures above 673K [Numukura and Koiwa, 1998]. Furthermore deformation twins have been found to enhance slip along the $\langle 11\bar{2}3 \rangle$ direction (**c+a** slip) on $\{\bar{1}011\}$ or $\{\bar{1}\bar{1}22\}$ planes [Minonishi et al., 1982, Numukura and Koiwa, 1998].

Bozzolo et al. (2007) pointed out that multiple twinning is an effective mechanism of grain fragmentation at the beginning of deformation and that the refined grains are mainly deformed by prismatic slip. Shin et al. (2003) examined microstructure evolution during ECAP of Ti. In the first pass of ECAP, titanium was observed to deform by deformation twinning. TEM analysis revealed that twinning occurred on $\{10\bar{1}1\}$ planes. During the second pass ECAP, strain was accommodated primarily by dislocation glide processes. The specific slip system was strongly dependent on the processing route i.e. route A, B or C. Alternating twin bands containing prism **a** and **c+a** dislocations characterized deformation via route C but basal **a** slip with deformation micro twins comprised the mechanism via route A. However, prism **a** slip was the main deformation mechanism in every twin band in route B. Furthermore Shin et al. (2003) suggested that the texture formed during the first pass and the resolved shear stress for each slip system determine the deformation mechanism during the second pass ECAP and thus must be carefully considered in understanding the microstructure development.

Strain hardening behavior of CP-Ti is a very complex process and many aspects of it are still intensely debated. Salem et al. (2003) investigated strain hardening behavior of CP-Ti with emphasis on the role of deformation twinning; they have observed three

stages of strain hardening in α Ti. Biswas (1973) did the comparison of strain hardening behavior of HCP α Ti with strain hardening behavior of other cubic materials. Furthermore he demonstrated that Ti deformed by wire drawing shows a decreasing hardening rate upto equivalent strain of 2 and beyond this strain a linear stress-strain relationship was observed upto the largest equivalent strain of 4.

CHAPTER 3

EXPERIMENTAL PROCEDURES

3.1 MATERIAL

This research was conducted on commercially pure titanium, aluminium and Al-5Zn-1Mg.

3.1.1 Commercially Pure Metals

3.1.1.1 Commercially pure metals in the wrought form

Commercially pure titanium was processed in the as-received wrought form after homogenization at 973 K for 3 hours in the electric resistance furnace. This material was supplied by Indira Gandhi Centre for Atomic Research, Kalpakkam, India. Commercially pure aluminium was also processed in as-received wrought form after homogenization at 623 K for 3 hours in the electric resistance furnace.

3.1.1.2 Casting of commercial pure metal ingots

Melting of the metal was carried out in electric resistance furnace of 3 kg capacity with automatic temperature controller, which had allowed the variation of ± 5°C. Pure aluminium pieces were charged into silicon carbide crucible. The charge was melted and held at a temperature of 973 K. Slag was removed from the surface of molten aluminium after complete melting. The melt was degassed with hexachloroethylene tablets.

3.1.2 Al-5Zn-1MgAlloy

Nominal composition of the above-mentioned alloy used in the present study is presented in Table 3.1.

Table 3.1 The nominal composition of the alloy used for the study

Alloy	Al (Wt. %)	Zn (Wt. %)	Mg (Wt. %)
Al-5Zn-1Mg	94	5	1

3.1.2.1 Melting of Al-5Zn-1Mg

Pure aluminium pieces were charged into silicon carbide crucible along with appropriate addition of zinc granules. The charge was melted and held at a temperature of 1023 K. The melt was degassed with hexachloroethylene tablets. Magnesium in the pure elemental form was added to the melt just before pouring. In order to avoid the loss by flaring, magnesium was packed in aluminium foil with a few pieces of aluminium. The package was immersed into the superheated melt using graphite pusher rod. The melt was mildly stirred; surface dross is skimmed off and immediately poured into the mold. In order to get homogeneous composition, the solidified alloy was remelted and poured into an appropriate mold.

3.1.3 Pouring

The melt was poured into a mild steel die. The dimensions of the mold cavity are presented in Fig.3.1. The cast billets were homogenized at 623 K for 3 hours in an electric resistance furnace.

3.2 SAMPLE PREPARATION

From the cast and wrought cylindrical billets, the following types of samples were prepared:

(i)   Cylindrical billet samples for ECAP - The schematic diagram of the samples are shown in Figure 3.2. L/D ratio for all the samples were fixed at 3 where L= 60 mm and D = 20 mm except for titanium where L/D ratio was fixed at 2.5 where L= 50 mm and D = 20 mm. Cylindrical billet samples for ECAP were made with all the materials used for the present study.

All dimensions in mm
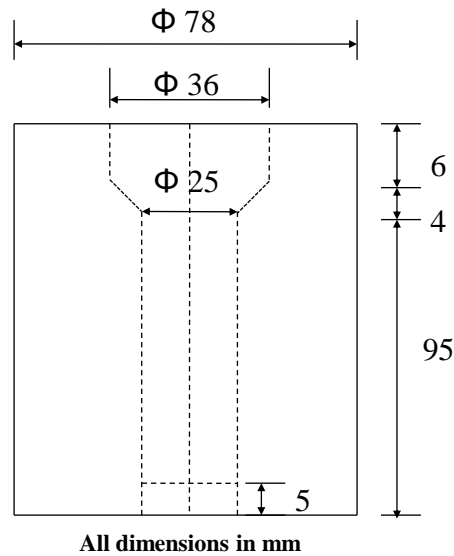
Fig. 3.1 The dimensions of the mold cavity used to produce billets

(ii) Tubular samples for ECAP - The schematic diagram of this sample is shown in Fig.3.3. The Cylindrical billet samples were further machined to tubular form with outer diameter 20 mm, inner diameter 13 mm and length 60 mm. The end thickness (t) of 3 mm and a 30°taper were made at one end of the specimen. Tubular samples for ECAP were made with all the material except titanium in the present study.

(iii) Ring compression test samples - The schematic diagram of this sample is shown in Fig.3.4. The proportion (d_O: d_I:t_0) was fixed at 6: 3: 2 where d_O = 24 mm, d_I = 12 mm and t_0 = 8 mm respectively. Ring compression test samples were made out of Al-5Zn-1Mg to study the frictional property before ECAP.

(iv) Axisymmetric compression test samples – The schematic diagram of this sample is shown in Fig.3.5. h_0/d_0 ratio for the samples were fixed at 1.5 where h_0 = 18 mm and d_0 = 12 mm. Axisymmetric compression test samples were made out of commercial purity (CP) aluminium in the cast form to study the flow properties after ECAP.

37

(v) Tensile testing samples after ECAP - The schematic diagram of this sample is shown in Fig.3.6. Tensile testing samples were made out of CP aluminium and CP titanium in the wrought form to study the improvement in mechanical properties after ECAP.
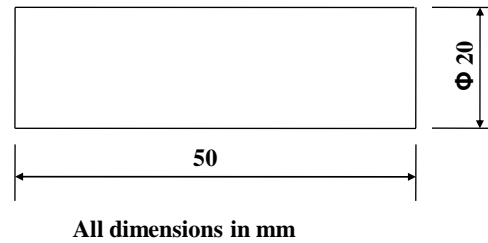
(a)
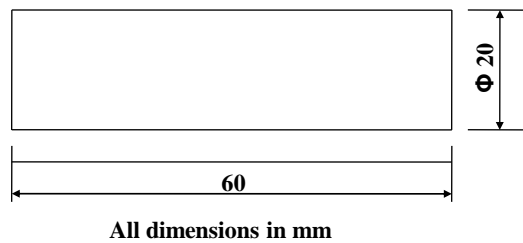
(b)

Fig. 3.2 Schematic diagram of cylindrical billet samples with diameter 20 mm and length (a) 50 mm for titanium, (b) 60 mm for aluminium and its alloy

3.3 CHARACTERIZATION

3.3.1 Chemical composition

Samples were taken from the top and bottom of the material received and from the cylindrical cast ingots to chemically analyze using optical emission spectroscope. The chemical compositions of the materials are presented in Tables 3.2 to 3.4. From the various values presented in Tables 3.2 to 3.4, it can be seen that all the materials and ingots meet the specified requirement and can be taken for further investigation.
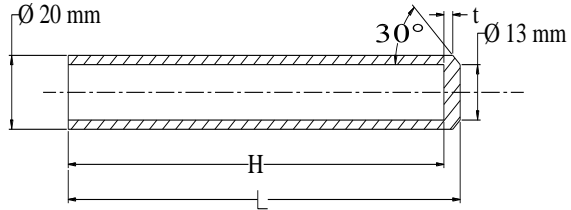
Fig. 3.3 Dimensions of the tubular specimen used for equal channel angular pressing (L= 60 mm, H=57 mm, t = 3 mm).
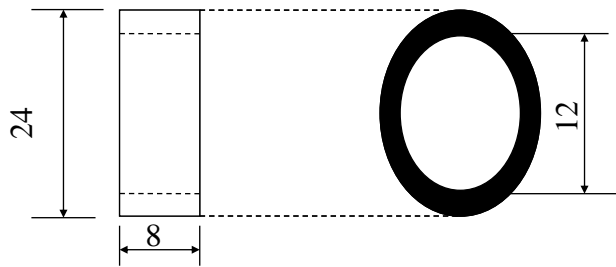
All dimensions in mm

Fig.3.4 Schematic diagram of ring compression testing sample
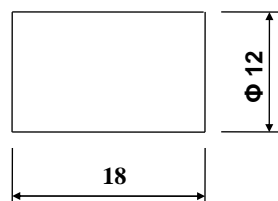
All dimensions in mm

Fig.3.5 Schematic diagram of compression testing sample
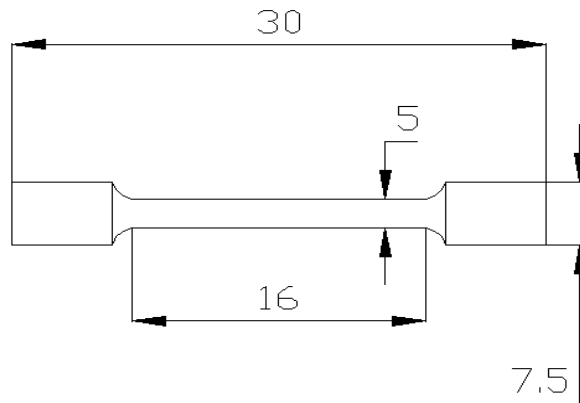
All dimensions in mm

Fig. 3.6 Schematic diagram of tensile testing specimen

Table 3.2 Chemical composition of commercial purity titanium

Elements	C	O	N	H	Fe	**Ti**
Wt %	0.035	0.05	0.05	0.02	0.001	99.844

Table 3.3 Chemical composition of commercial purity aluminium

Elements	Si	Fe	Cu	Mn	Mg	Ti	**Al**
Wt %	0.860	0.158	0.0160	0.580	0.760	0.0140	97.612

Table 3.4 Chemical composition of Al-5Zn-1Mg alloy

Elements	Si	Fe	Cu	Mn	Cr	**Mg**	**Zn**	**Al**
Wt %	0.860	0.238	0.0160	0.560	0.0069	1.46	5.72	91.139

3.3.2 Microstructural analysis

3.3.2.1 Characterization by optical microscopy

Standard metallographic technique was resorted to polish the sample for microstructural analysis. The polished samples of aluminum and its alloy were etched with Keller's reagent[*] whereas titanium was etched with Kroll's reagent[**]. Their microstructures were studied under a Zeiss Axioimager optical microscope.

3.3.2.2 Characterization by scanning electron microscopy

The detailed investigations of the samples after fracture were conducted using scanning electron microscope (SEM, JEOL JSM 6380LA). Details of the final fracture and the evolution of damage were studied.

3.3.3 Hardness measurement

Vickers microhardness tester was used to find out the hardness of the materials: it was measured on the polished surface of the samples, both in transverse and vertical direction, with 300 gmf and 1 kg load. Average of minimum ten readings were taken in each field.

3.4 AXISYMMETRIC COMPRESSION TESTING

Axisymmetric compression testing was used to determine the flow of stress of all the materials.

3.4.1 Flow stress determination

The compression test was carried out using 40 T universal testing machine (Fuel Instruments & Engineers Pvt. Ltd. Model – UTN/E40). The schematic setup of compression test is shown in Fig. 3.7. The test was carried out at room temperature. Samples were lubricated with MoS_2. All the samples were tested with a constant ram speed of 3.3×10^{-4} m/s. Experiments were carried out in the following steps:

---

[*] 5% HNO_3, 5% HCl, 3% HF and 87% H_2O

[**] 6% HNO_3 (conc.), 2% HF and 92% H_2O

(i) Extent of compression at different loads was found out for all the categories of the samples at room temperature.

(ii) From the above experimental data force – stroke diagrams were generated.

(iii) Force – stroke diagrams were converted to engineering stress - strain curves.

(iv) From the stress – strain diagrams true stress – true strain diagrams were derived and plotted on log – log scale.

(v) Finally these flow curves were fitted into well-known Hollomon equation, i.e.

$$\sigma = K\varepsilon^n$$

Where σ = true stress, K= material strength coefficient and n denotes the strain hardening exponent. K and n were determined for different samples processed during various passes and routes employed in each pass.

(vi) Using these values plots were drawn which show the variation of K and n with respect to equivalent plastic strain.

3.5 RING COMPRESSION TEST

Schematic diagram of the sample for ring compression test is shown in Fig.3.4. Samples were lubricated with MoS_2. The test was carried out using 40 T universal testing machine (Fuel Instruments & Engineers Pvt Ltd. Model – UTN/E40). Fig. 3.8 shows the schematic set up for the ring compression test. The test was carried out at a constant load of 11000 Kgf and the reduction in height $(t - t_0)$ and the reduction in internal diameter $(d - d_0)$ were noted down. Using the calibration chart (Fig.3.9) developed by Male and Cockroft (1964-65) friction factor (m) for various temperatures in the range of 303 – 673 K was determined. A plot of the friction factor v/s temperature was developed.
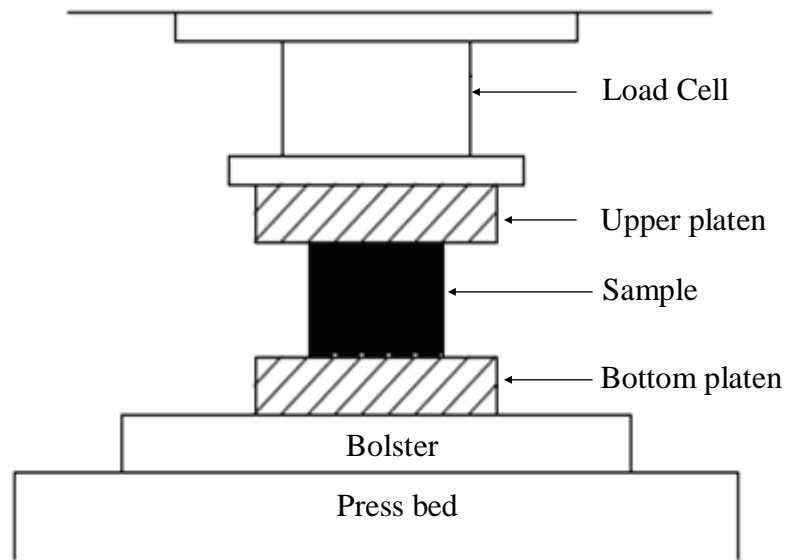
Fig. 3.7 Schematic set up for compression testing
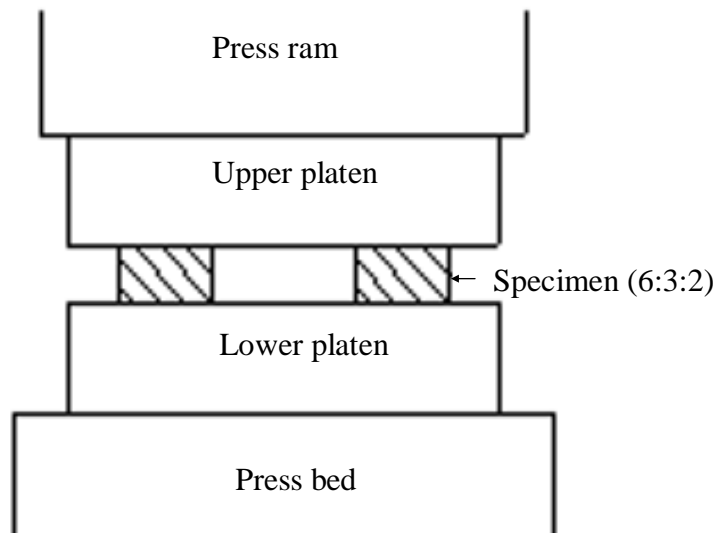
Fig. 3.8 Schematic set up of ring compression test
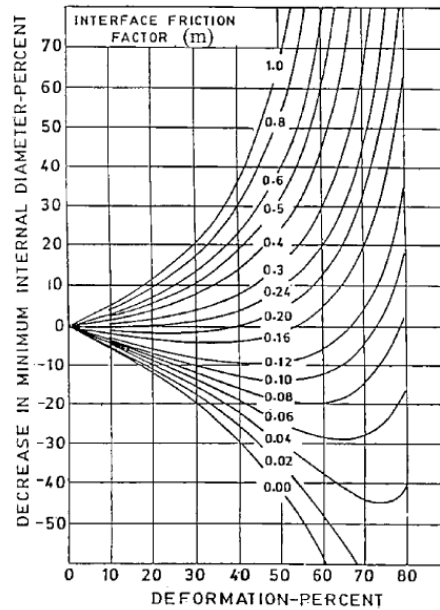
Fig.3.9 Calibration chart to determine friction factor (m)

3.6 ECAP

3.6.1 Design of die

Conventional design of dies for performing ECAP is extremely difficult due to the complexity of the shape of the dies. Further, designing the dies by trial and error is expensive. Therefore, finite element method (FEM) has been resorted to for the design of dies. A split die was designed for a load of 60 T with FE software ANSYS for the ECAP of Ti and its alloys. 200 mm breadth x 300 mm height x 150 mm thickness is the minimum dimension of the die to work safely with a displacement of 50 mm. It induces a Von–Mises stress of 1197MPa with a factor of safety of 1.67. The present die was designed for 250 mm breadth x 250 mm height x 250 mm thickness (Fig. 3.10) which gives a Von–Mises stress of 1390MPa with a factor of safety of 1.43.Basically the die is composed of two channels, the entrance and exit channels intersecting at an angle of $2\varphi = 150°$. Fillet radius of 3 mm was given to all the sharp corners in the die as well as in the punches.

The design details of the punch are shown in the schematic diagram presented in Fig.3.11. It should be noted that a small reduction in cross section is provided on the stem. The reduced circular cross-section of 19.8 mm was chosen to reduce the friction between the die and the punch.

44

250

Ø20

250

250

150°

20

250

All dimensions in mm
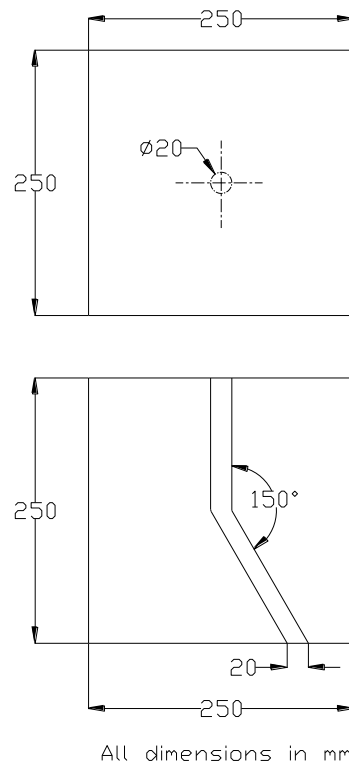
Fig. 3.10 Schematic diagram of the ECAP die;(top) top view, (bottom) Front view

25

20

105

19.8

20

20

All Dimensions in mm
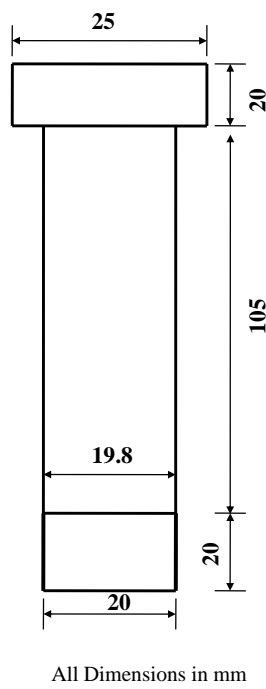
Fig. 3.11 Schematic diagram of punch used for ECAP

45

3.6.2 Die materials

AISI M2 HSS was used for making the punch and dies. The sample of the material was analyzed using optical emission spectroscope and its chemical composition is presented in the Table 3.5. The material was rough machined, close to the dimensions of die and punch. Then it was given the appropriate heat treatment. The time – temperature diagram of heat treatment is depicted in Fig. 3.12. The heat treatment in vacuum was carried out by Bhat Metals Research Pvt. Ltd., Bangalore. The final hardness after the heat treatment was determined and found to be R_C 62, which is appropriate for present experimental work. Having ensured adequate hardness the final fine machining was carried out to arrive at the correct dimensions of the die and punch.

Table 3.5 Chemical analysis of AISI M2 HSS used for making the die and punch

Alloy	C (%)	Si (%)	Mn (%)	Cr (%)	**W (%)**	**V (%)**	**Mo (%)**
AISI M2 HSS	0.8	0.4	0.4	4.3	**6.5**	**2**	**5**
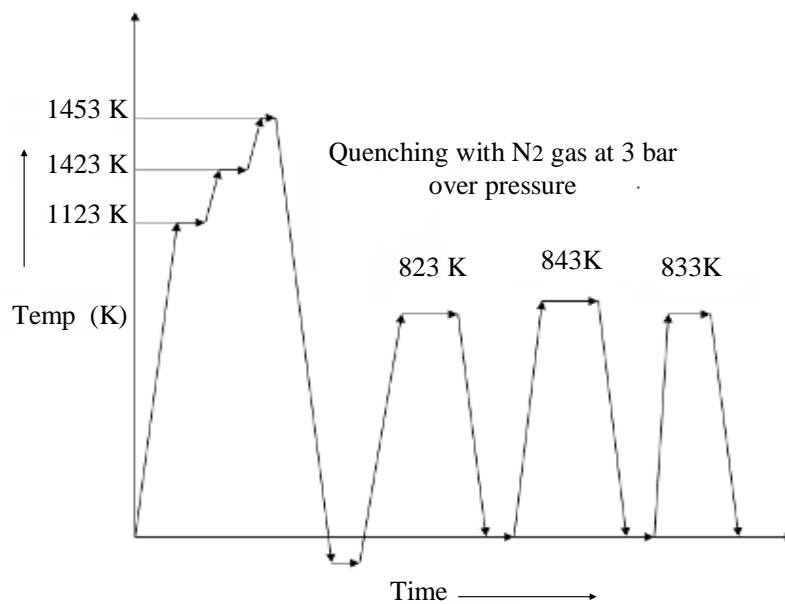
Fig.3.12 Heat treatment cycle of AISI M2 HSS for attaining a hardness of 61/62 R_c

46

3.6.3 Die assembly

The die assembly consisted of two split sections of the die. They were assembled with two pairs of roller bolts with nuts keeping them intact over a press bed. A guide rod was inserted through the channel to ensure proper alignment of the die. The schematic sketch of ECAP die assembly for extruding rod and tube is shown in Fig 3.13 and 3.14 respectively. The photograph of the die assembly including the load cell is shown in Fig.3.15.
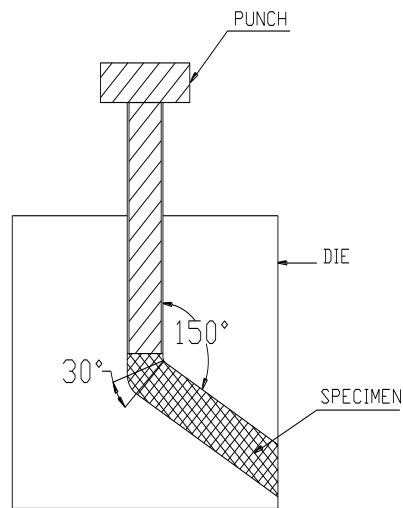
Fig.3.13 The schematic sketch of ECAP die assembly for extruding rod and tube
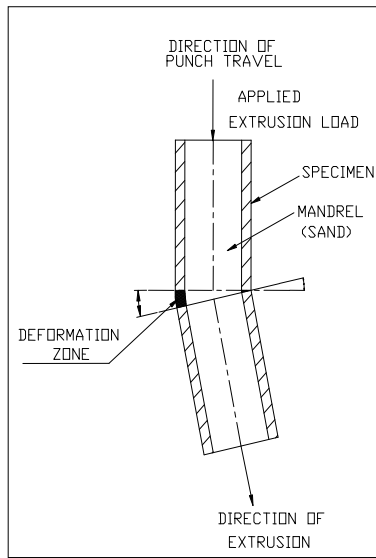
Fig. 3.14 Schematic diagram showing direction of punch travel, mandrel, deformation zone and exit direction of extrusion of the tubular specimen used for ECAP
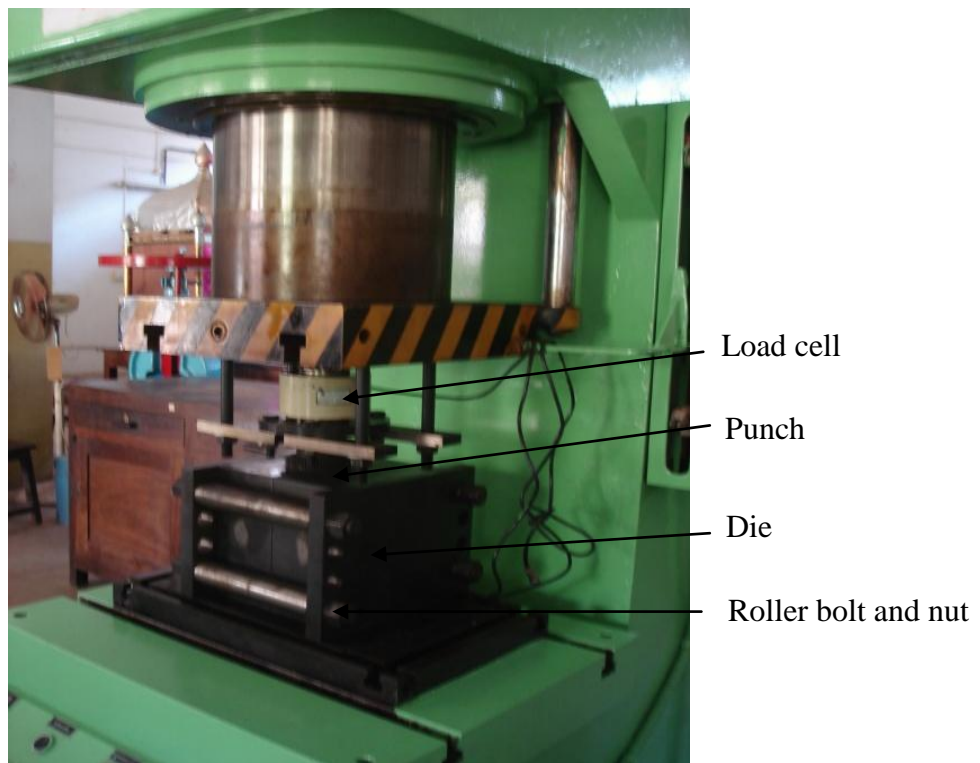
Fig.3.15 The photograph of the die assembly including the load cell

3.6.4 Preparation of ECAP specimen

From the metals and alloy chosen for the study, specimen of 50 mm and 60 mm length and 20 mm diameter were machined. The photograph of a billet sample before and after machining is shown in Fig. 3.16.

(a)

(b)

Fig.3.16 The photograph of an aluminium billet sample(**a**) before and (**b**) after machining

3.6.5 Testing

3.6.5.1 ECAP of solid cylindrical specimen

The ECAP was carried out using 250 T hydraulic press (Oriental Hydraulics–319/1987) with ram velocity of 13×10^{-3} m/s. The billet samples were coated with MoS_2 and heated to temperatures required for each material in a temperature controlled electric resistance furnace. They were taken out and inserted into the die and pressed immediately.

The specimens were pressed multiple times or till they fracture. The maximum passes were up to four in the present study. Routes A, B_A, B_C, and C were employed for pressing. After each pass the flash as well as the undeformed end part were cut off using abrasive cut off wheel and were machined to the required cross section and with reduced length for next pass, the specimen was reinserted to the channel and pressed again. The equivalent plastic strain is equal to approximately 0.31. ECAP was carried out by varying the load and measuring the stroke from which force-stroke diagrams were generated. Maximum punch pressure or stress is equal to the ratio of maximum punch load to the cross sectional area of the punch.

3.6.5.2 ECAP of tubular specimen

Tubular specimens with the dimensions shown in Fig.3.3 were used for the extrusions. The end thickness (*t*) of 3 mm was provided to support the mandrel which is made of sand in this study. A 30°taper was made at one end of specimen to facilitate easy start of ECAP. Various passes of ECAP were carried out with four different routes (Routes A, B_A, B_C and C) with molybdenum disulfide as lubricant. After each pass, the specimen ends (the unextruded portion) were cut off and faced in a lathe and the sample surface made smooth by using polishing papers. The specimens were then subjected to further pressing. The force–stroke diagram was recorded during the pressing and used in finding the maximum punch pressure during ECAP.

CHAPTER 4

RESULTS

4.1 MECHANICAL PROPERTY EVALUATION

Vickers hardness, tensile testing and compression testing were the tests carried out for evaluating the mechanical properties before and after ECAP. Vickers hardness was determined for all the materials whereas tensile testing was restricted to CP titanium and CP aluminium rods in the wrought form. Compression testing was confined to CP aluminum rod in the cast form.

4.1.1 VHN Before and After ECAP

4.1.1.1 CP titanium

Results of Vickers hardness measurement on CP titanium is presented in Table 4.1. From the values presented in the Table 4.1, it can be observed that hardness increased from 176 VHN in the annealed condition to 193 VHN after first pass at room temperature. Hardness value increased to 198, 206, 197 and 194 VHN for routes A, B_A, B_C and C respectively after second pass. Hardness further increased to 228, 213, 218 and 212 VHN for routes A, B_A, B_C and C respectively after third pass. This is illustrated by plot of Vickers hardness number v/s equivalent plastic strain in Fig. 4.1 This trend may be due to an increased twinning which may contribute to the overall hardness of a material [Kalidindi et al., 2003].

Table 4.1 Vickers hardness (VHN) data of CP-Ti in the annealed condition and after various passes at 623K for different routes

Processing condition	Vickers hardness number (VHN)			
	Route A	Route B_A	Route B_C	Route C
Annealed CP-Ti	176	176	176	176
Pass 1	193	193	193	193
Pass 2	198	206	197	198
Pass 3	228	213	218	212
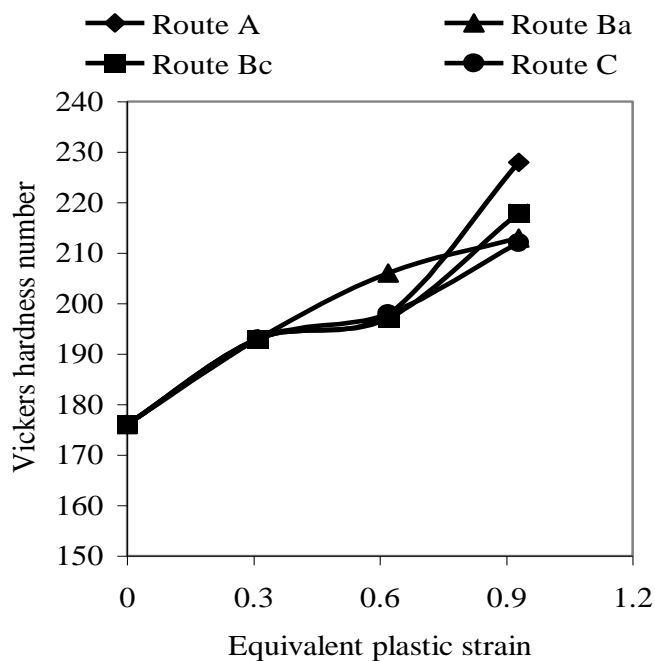
Fig.4.1 Variation in hardness (VHN) with equivalent plastic strain for CP titanium processed at 623K for different routes.

4.1.1.2 CP aluminium rod in the cast form

Results of Vickers hardness measurement on CP aluminium rod in the cast form is presented in Table 4.2. From the values presented in the Table it can be observed that hardness increased from 47 VHN in the annealed condition to 54 VHN after first pass at room temperature. Hardness value increased to 56, 57, 62 and 56 VHN for routes A, B_A, B_C and C respectively after second pass. This is illustrated by plot of Vickers hardness number v/s equivalent plastic strain in Fig. 4.2 This trend is may be due to severe breakdown of cast structure by changing the orientation of specimen from one pass to another. Studies carried out by EI-Danaf (2008), Saray and Purcek (2009) also show that ECAP caused mostly elimination of porosities by shear deformation.

Table 4.2 Vickers hardness (VHN) data of cast CP-aluminium rod in the annealed condition and after various passes at room temperature for different routes

Processing condition	Vickers hardness number (VHN)			
	Route A	Route B_A	Route B_C	Route C
Annealed CP-Al	47	47	47	47
Pass 1	54	54	54	54
Pass 2	56	57	62	56
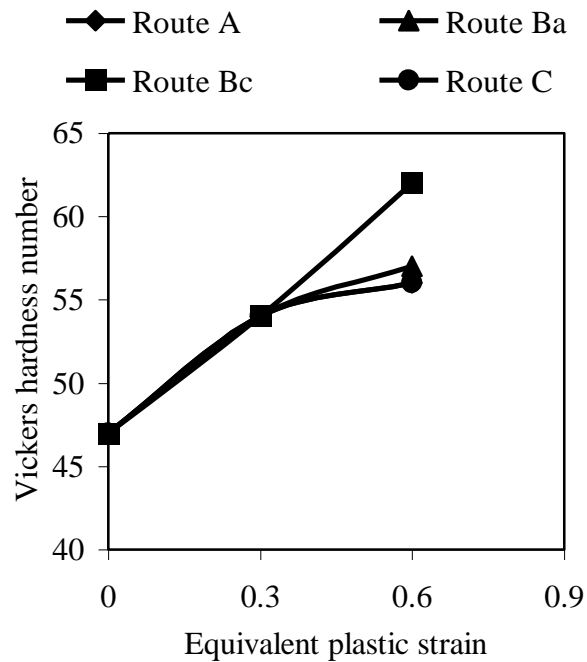
Fig.4.2 Variation in hardness (VHN) with equivalent plastic strain for cast aluminium rod processed at room temperature for different routes

4.1.1.3 CP aluminium rod in the wrought form

Results of Vickers hardness measurement on CP aluminium rod in the wrought form is presented in Table 4.3. From the values presented in the Table it can be observed that hardness increased from 50 VHN in the annealed condition to 58 VHN after first pass at room temperature. Hardness value increased to 61, 63, 67and 62 VHN for routes A, B_A, B_C and C respectively after second pass. Hardness value increased during third pass to 62, 64, 68 and 63 for routes A, B_A, B_C and C respectively. Hardness further increased to 66, 67, 69 and 65 VHN for routes A, B_A, B_C and C respectively after fourth pass. This is illustrated by plot of Vickers hardness number v/s equivalent plastic strain in Fig. 4.3. This trend may be due to the initial massive reduction in the grain size and grain breakup into bands of sub grains during first pass and subsequent passes. The present results are good comparison with earlier experiments [Iwahashi et al.,1997] on pure aluminium.

Table 4.3 Vickers hardness (VHN) data of CP-aluminium rod in wrought form in the annealed condition and after various passes at room temperature for different routes

Processing condition	Vickers hardness number (VHN)			
	Route A	Route B_A	Route B_C	Route C
Annealed	50	50	50	50
Pass 1	58	58	58	58
Pass 2	61	63	67	62
Pass 3	62	64	68	63
Pass 4	66	67	69	65
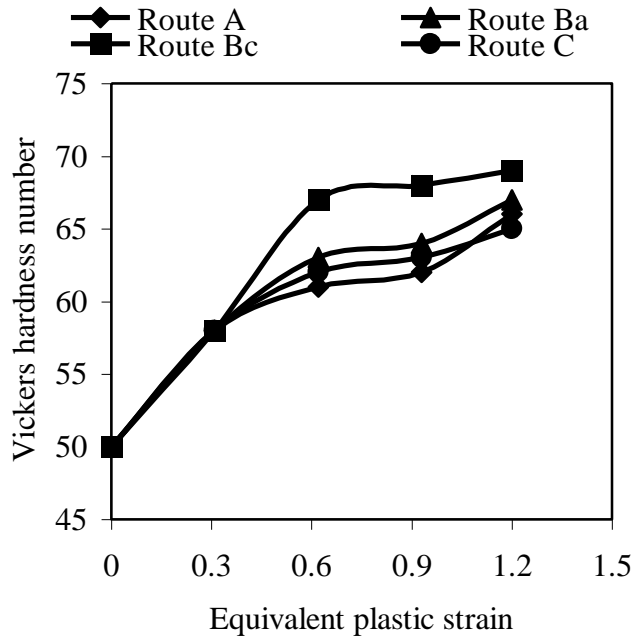
Fig.4.3 Variation in hardness (VHN) with equivalent plastic strain for wrought aluminium rod processed at room temperature for different routes.

4.1.1.4 Al-5Zn-1Mg rod in the cast form

Results of Vickers hardness measurement on Al-5Zn-1Mg rod in the cast form processed in the temperature range of 303 – 673 K are presented in Table 4.4. From the values presented in the Table it can be observed that hardness increased from 120 VHN in the annealed condition to 150, 145, 140, 130 and 155 VHN after first pass at 303 K, 373 K, 473 K, 573 K and 673 K respectively. This is illustrated by plot of Vickers hardness number v/s temperature in Fig.4.4. Al-5Zn-1Mg specimen couldn't survive further passes.

Table 4.4 Vickers hardness measurement on Al-5Zn-1Mg rod in the cast form processed in the temperature range of 303 – 673 K

Processing condition	Vickers hardness number (VHN)				
	303 K	373 K	473 K	573 K	673 K
Pass 1	150	145	140	130	155
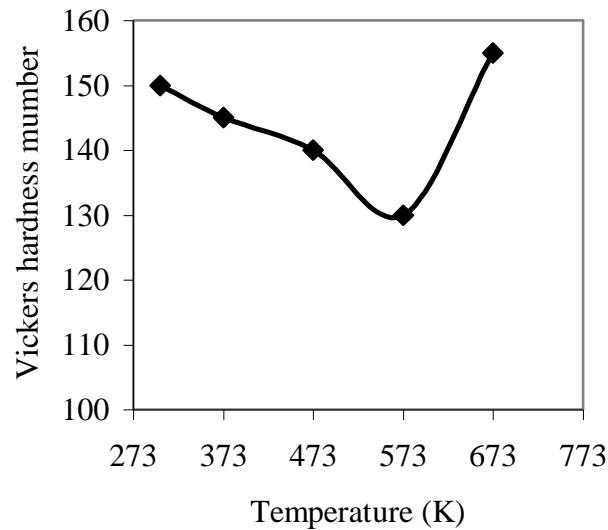
Fig.4.4 Effect of processing temperature on hardness of Al-5Zn-1Mg after first pass

4.1.1.5 CP aluminium tube in the wrought form

Results of Vickers hardness measurement on CP aluminium rod in the wrought form is presented in Table 4.5. From the values presented in the Table 4.5 it can be observed that hardness increased from 48 VHN in the annealed condition to 59 VHN after first pass at room temperature. Hardness value increased to 62 VHN for routes A, B_A, B_C and C respectively after second pass. Hardness further increased to 64, 66, 65 and 63 VHN for routes A, B_A, B_C and C respectively after third pass. This is illustrated by plot of Vickers hardness number v/s equivalent plastic strain in Fig. 4.5. This trend may be due to the strain hardening mechanism in the initial stage. Further ECAP promoted the formation of equiaxed grains accompanied with gradual decrease in dislocation density [Ferrase et al., 1997 and Iwahasi et al., 1997].

Table 4.5 Vickers hardness (VHN) data of CP-aluminium tube in wrought form in the annealed condition and after various passes at room temperature for different routes

Processing condition	Vickers Hardness Number (VHN)			
	Route A	Route B_A	Route B_C	Route C
Annealed	48	48	48	48
Pass 1	59	59	59	59
Pass 2	62	62	62	62
Pass 3	64	66	65	63
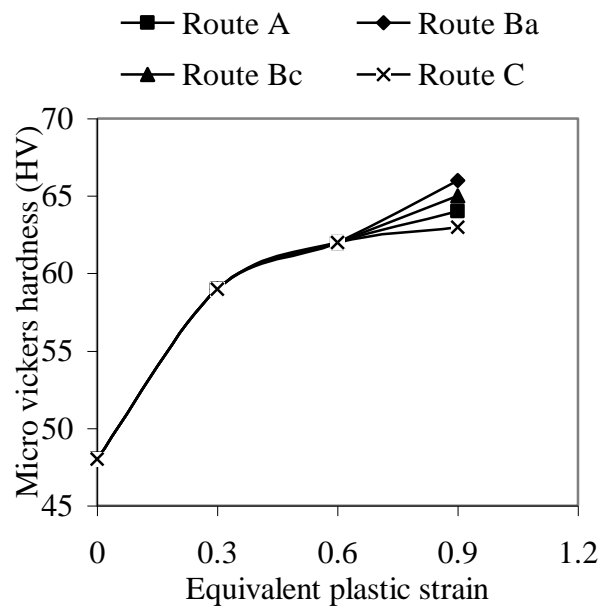
Fig.4.5 Variation in hardness (VHN) with equivalent plastic strain for wrought aluminium tube processed at room temperature for different routes

57

4.2 TENSILE TESTING

4.2.1 CP Titanium

Results of tensile testing on CP titanium rod in the wrought form are presented in Table 4.6. From the values presented in the Table 4.6 it can be observed that ultimate tensile strength shows a considerable improvement after the first pass. The UTS in the annealed condition was 562 MPa and it increased to 593 MPa after the first pass. UTS increased to 632, 812, 656 and 640 MPa for routes A, B_A, B_C and C respectively after second pass. UTS further increased to 742, 906, 703 and 671 MPa for routes A, B_A, B_C and C respectively after third pass. In contrast ductility decreased from 31 % to 30 % after first pass ECAP at room temperature. After second pass the percentage elongation to failure was 22 %, 22 %, 25 % and 17 % for routes A, B_A, B_C and C respectively. Percentage elongation to failure further decreased to 19 %, 17 %, 17 % and 22 % for routes A, B_A, B_C and C respectively. The profiles which depict the variation of ultimate tensile strength and elongation to failure with equivalent plastic strain are presented in Fig. 4.6 and 4.7 respectively. The superior properties attained after multi passes at room temperature reflect the increased densities of dislocation and twins introduced at the room temperature and the consequent increase in the rate of strain hardening [Xicheng et al., 2008].

Table 4.6   Tensile strength and percentage elongation to failure of different ECAP passes at 623K

Processing condition	Tensile strength (MPa)				% Elongation to Failure			
	Route A	Route B_A	Route B_C	Route C	Route A	Route B_A	Route B_C	Route C
Annealed CP-Ti	562	562	562	562	30	30	30	30
Pass 1	593	593	593	593	30	30	30	30
Pass 2	632	812	656	640	22	22	25	17
Pass 3	742	906	703	671	19	17	17	22
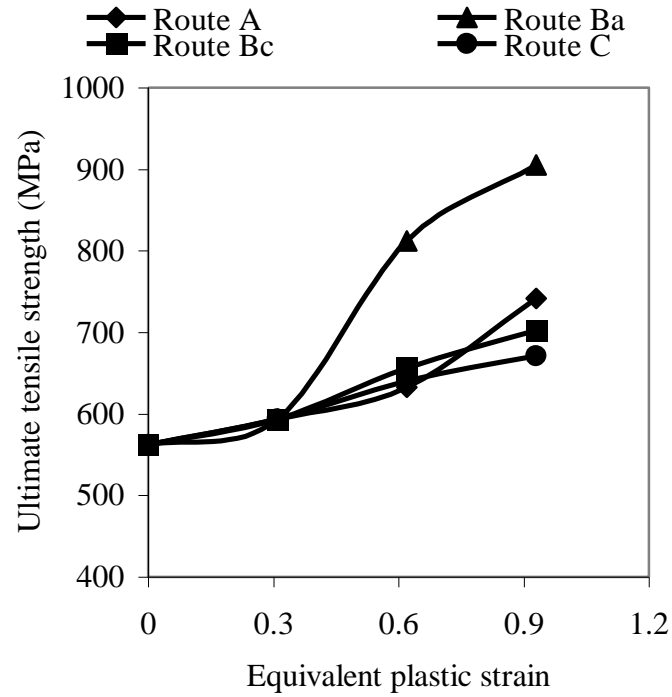
Fig. 4.6 The variation of ultimate tensile strength with equivalent plastic strain for CP titanium for various passes
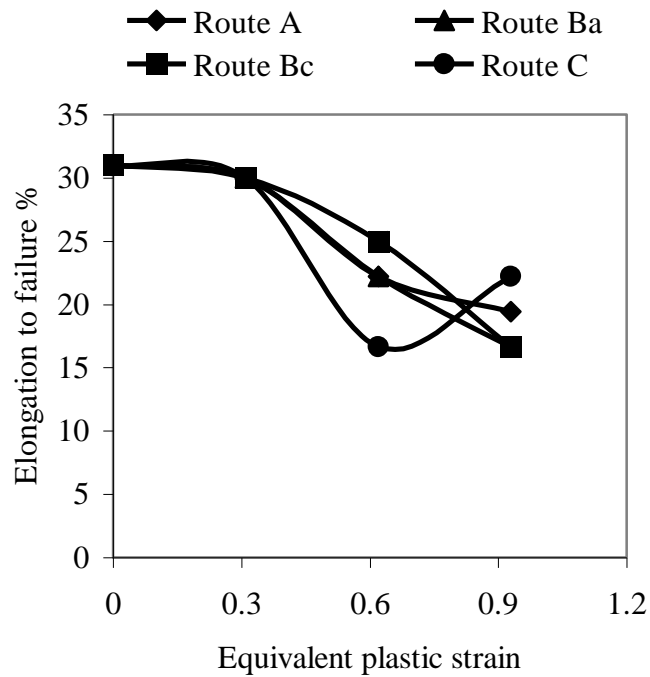
Fig. 4.7 The variation of elongation to failure with equivalent plastic strain for CP titanium for various passes

4.2.2 CP Aluminium Rod In The Wrought Form

Results of tensile testing on CP aluminium rod in the wrought form are presented in Table 4.7. From the values presented it can be observed that ultimate tensile strength shows a drastic improvement after the first pass. The UTS in the annealed condition was 227 MPa and it increased to 273 MPa after the first pass. UTS increased to 277, 281, 277 and 281 MPa for routes A, B_A, B_C and C respectively after second pass. UTS increased to 285, 289, 289 and 285 MPa for routes A, B_A, B_C and C respectively after third pass. UTS further increased to 289, 305, 293 and 289 MPa for routes A, B_A, B_C and C respectively after fourth pass. In contrast ductility decreased from 19 % to 18 % after first pass in ECAP at room temperature. Percentage elongation to failure further decreased to 17 % and 14 % for all the routes after the second and third passes respectively. Percentage elongation to failure remained same for route A and C while it further decreased to 11 % for route B_A and B_C. The profiles which depict the variation of ultimate tensile strength and elongation to failure with equivalent plastic strain are presented in Fig. 4.8 and 4.9 respectively. After ECAP, CP aluminium processed at room temperature may contain dislocations and long range internal stresses as well as a significant fraction of low angle boundaries, all of which can influence the UTS [Mallikarjuna et al., 2009].

Table 4.7 Tensile strength and percentage elongation to failure of different ECAP passes at room temperature for aluminium rod in the wrought form

Processing condition	Tensile strength (MPa)				% Elongation to Failure			
	Route A	Route B_A	Route B_C	Route C	Route A	Route B_A	Route B_C	Route C
Annealed CP Al	227	227	227	227	19	19	19	19
Pass 1	273	273	273	273	18	18	18	18
Pass 2	277	281	277	281	17	17	17	17
Pass 3	285	289	289	285	14	14	14	14
Pass 4	289	305	293	289	14	11	11	14
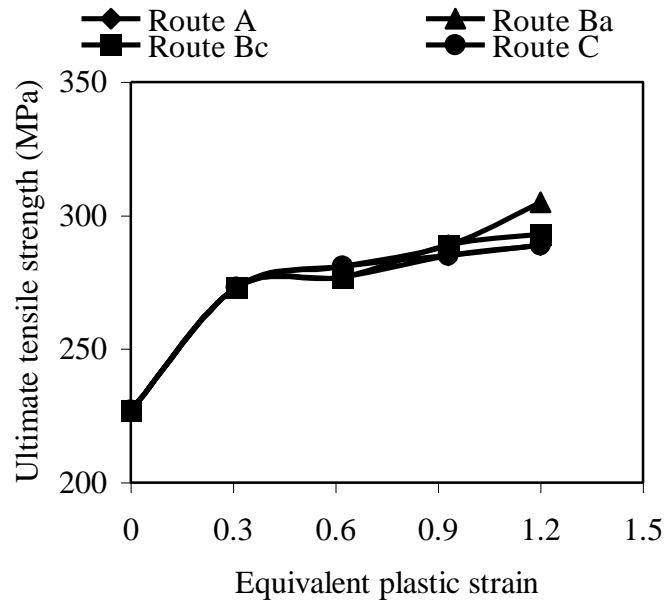
Fig. 4.8 The variation of ultimate tensile strength with equivalent plastic strain for CP aluminium rod in the wrought form for various passes
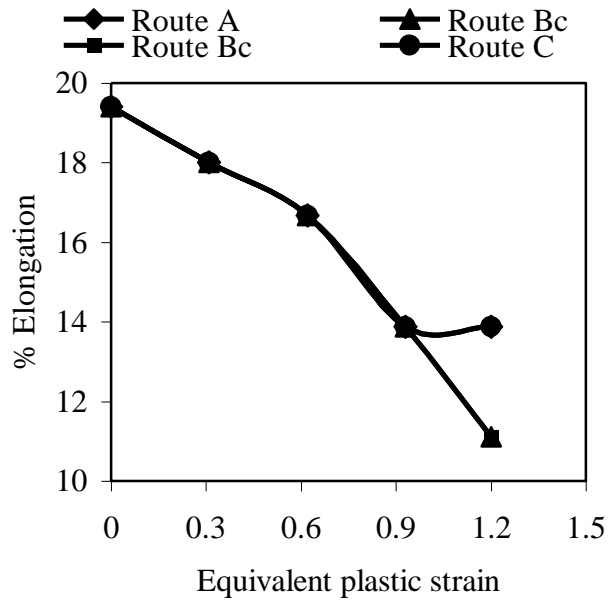
Fig. 4.9 The variation of elongation to failure with equivalent plastic strain for CP aluminium rod in the wrought form for various passes

4.3 COMPRESSION TESTING

4.3.1 CP Aluminium Rod In The Cast Form

After first, second and third passes of ECAP at room temperature, values of strength coefficient K and the strain hardening exponent n were determined from the flow stress data obtained from compression test. Results of tensile testing on CP aluminium rod in the wrought form were presented in Table 4.8. The K and n values of annealed CP aluminum was found to be 221 MPa and 0.18 respectively. K and n values increased to 245 MPa and 0.21 after first pass. K and n was further increased to 260, 270, 285, 257 MPa and 0.22, 0.28, 0.29, 0.22 for routes A, B_A, B_C and C respectively after second pass. The profiles which depict the variation of strength coefficient and strain hardening exponent with equivalent plastic strain are presented in Fig. 4.10 and 4.11 respectively. This suggests extensive strain hardening during deformation. The deformed microstructure strain hardens considerably leading to higher values of n and K.

Table 4.8   Strength coefficient and strain hardening exponent of different ECAP passes at room temperature for aluminium rod in the cast form

Processing condition	Strength coefficient **K** (MPa)				Strain hardening exponent **n**			
	Route A	Route B_A	Route B_C	Route C	Route A	Route B_A	Route B_C	Route C
Annealed CP Al	221	221	221	221	0.18	0.18	0.18	0.18
Pass 1	245	245	245	245	0.21	0.21	0.21	0.21
Pass 2	260	270	285	257	0.22	0.28	0.29	0.22
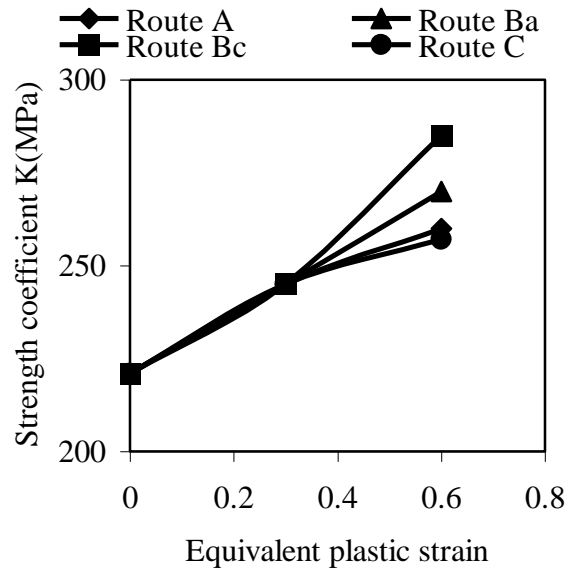
Fig. 4.10 The variation of strength coefficient with equivalent plastic strain for CP
aluminium rod in the cast form
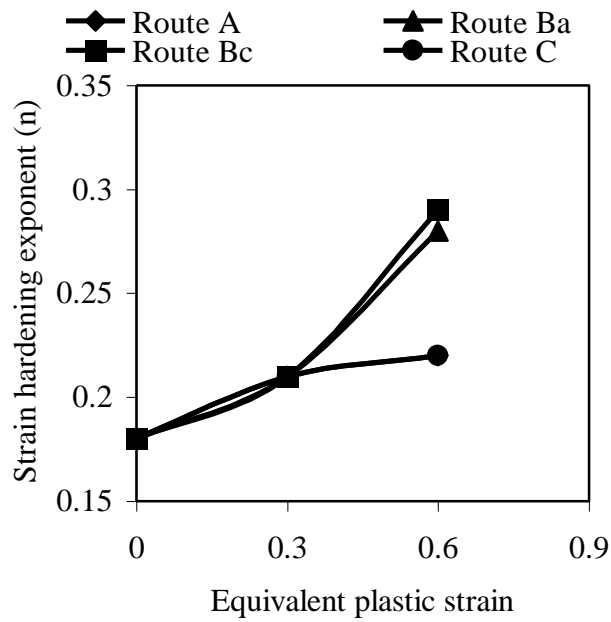
Fig. 4.11 The variation of strain hardening exponent with equivalent plastic strain for
CP aluminium rod in the cast form

4.4 ANALYSIS OF FRICTION

Results of friction factor measurement on Al-5Zn-1Mg are presented in Table 4.8. From the values presented in the Table 4.9 it can be observed that friction factor increased from 0.42 to 0.44, 0.62, 0.75 and 0.9 as temperature was increased to 373, 473, 573 and 673 K respectively. This is illustrated by plot of friction factor v/s temperature in Fig. 4.12. It is seen that friction factor increases as temperature increases in the case of MoS_2 lubricant.

Table 4.9 Friction factor (m) of Al-5Zn-1Mg alloy with MoS_2 lubricant at various temperatures

Temp (K)	Friction factor (m)
303	0.42
373	0.44
473	0.62
573	0.75
673	0.9
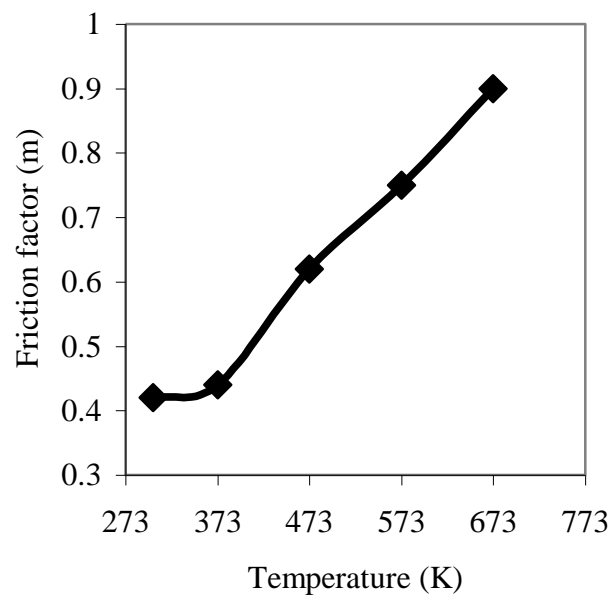
Fig.4.12 Plot of friction factor against temperature for Al-5Zn-1Mg alloy with MoS_2 lubricant

4.5 MICROSTRUCTURAL CHARACTERISTICS

4.5.1 Characterization By Optical Microscopy

4.5.1.1 CP titanium

Microstructure of CP titanium specimens annealed at 973 K for 3 hrs is shown in Fig.4.13. The microstructure consists of fairly equiaxed grains. It was used as a starting material for ECAP. The deformed microstructure after first pass ECAP which is extensively refined is shown in Fig. 4.14. In addition, a large number of both micro as well as macro twinning in grains can be found. The twinning direction is nearly parallel to the elongation direction which is in accordance with the study of Xirong et al. (2009), Shin et al. (2003) and Kim et al. (2003). Fig. 4.15 shows the microstructures after second pass where more volume fraction of elongated grains are seen. Fig. 4.16 shows the microstructures after third pass where no significant grain refinement is apparent when compared with initial annealed condition.

4.5.1.2 CP aluminium rod in the cast form

Microstructure of CP aluminium specimens annealed at 673 K for 3 hrs that was used as a starting material for ECAP is shown in Fig. 4.17. Dendrites and porosities are clearly visible. Fig. 4.18 shows microstructure of CP aluminium after first pass in which dendrites have been partially broken and porosities were decreased to a large extent. In second pass due to the change in orientation of cast aluminium from one pass to other pass different microstructures with various combination of severity of breakdown of the cast ingot were observed (Fig. 4.19).
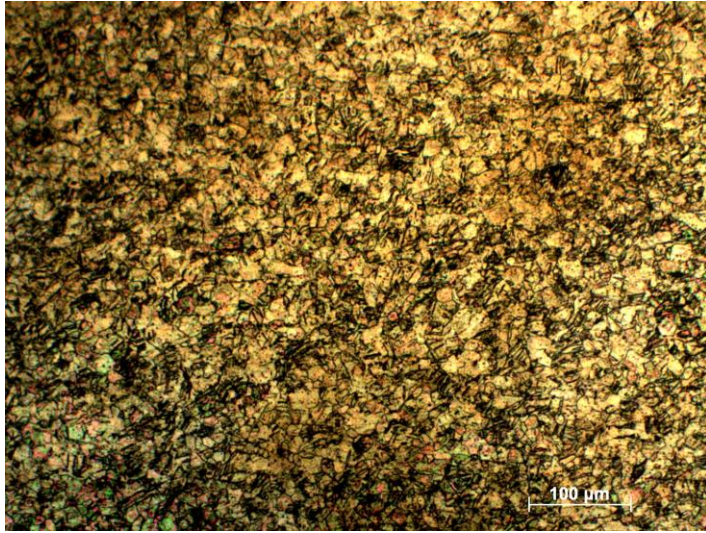
Fig.4.13 Optical microstructure of annealed CP-Ti
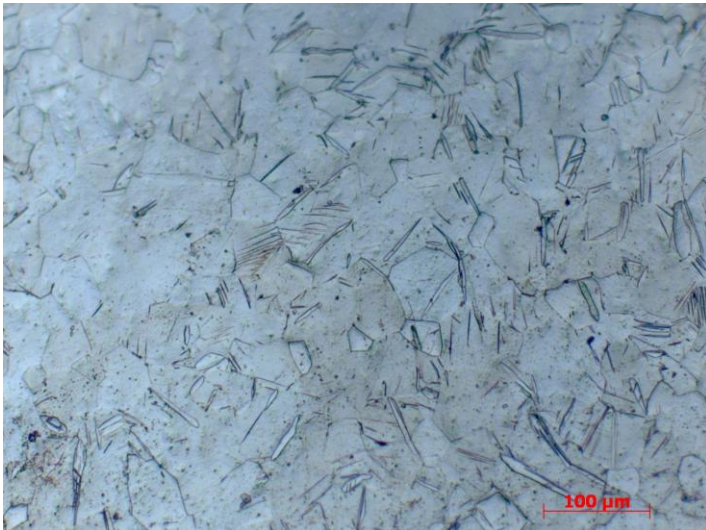
Fig.4.14 Optical microstructure of CP-Ti after first pass ECAP at 623 K
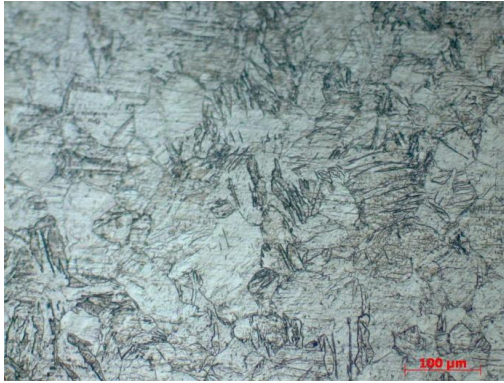
(a) Route A   (b) Route B_A
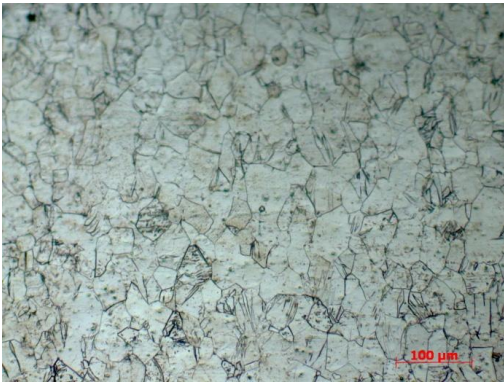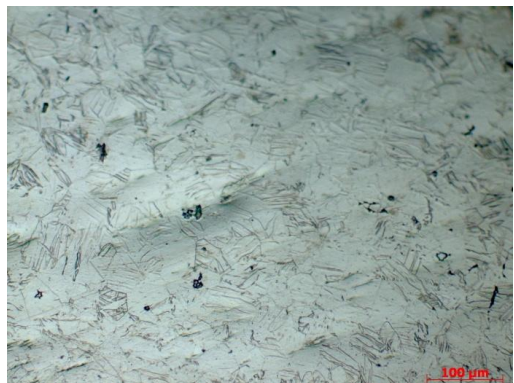
(c) Route B_C (d) Route C

Fig. 4.15 Optical microstructure of CP-Ti after second pass (a) Route A (b) Route B_A (c) Route B_C and (d) Route C by ECAP at 623K

a) Route A   (b) Route B$_A$
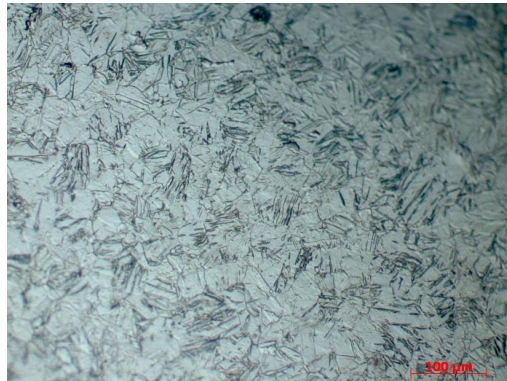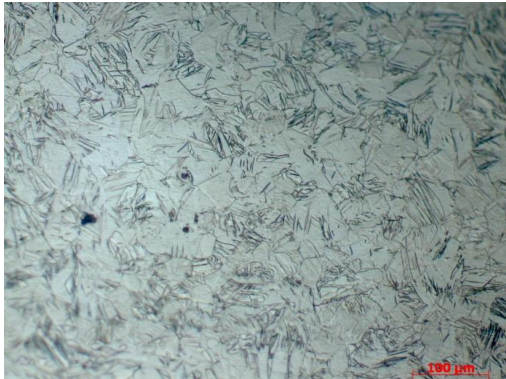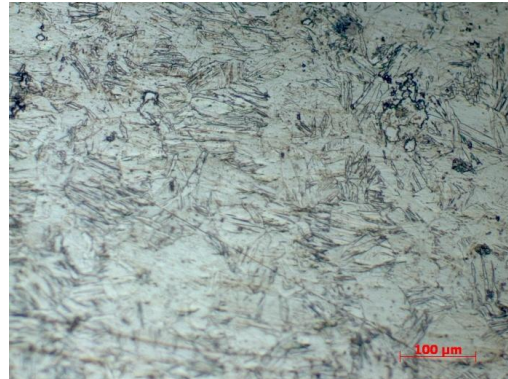
c) Route B$_C$ (d) Route C

Fig. 4.16 Optical microstructure of CP-Ti after third pass (a) Route A (b) Route B$_A$ (c) Route B$_C$ and (d) Route C by ECAP at 623K
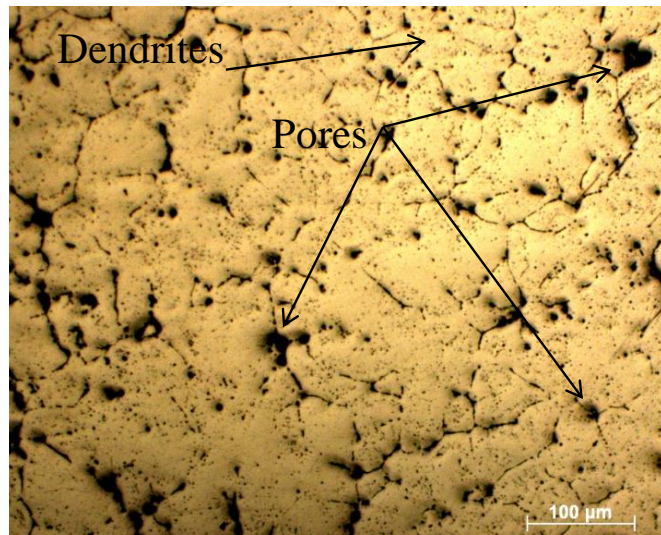
Fig.4.17 Optical microstructure of annealed CP-Al in the cast form
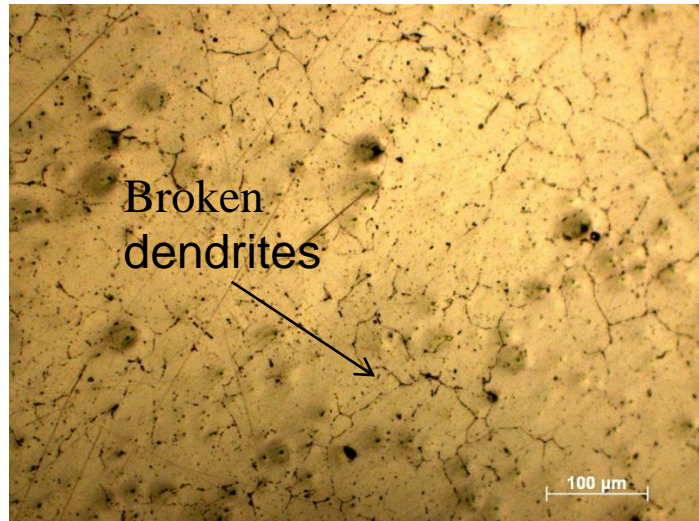
Fig.4.18 Optical microstructure of CP-Al after first pass ECAP at room temperature
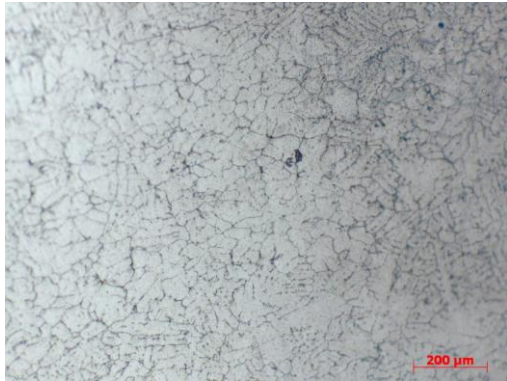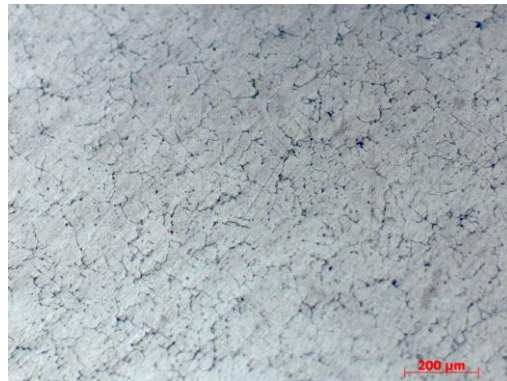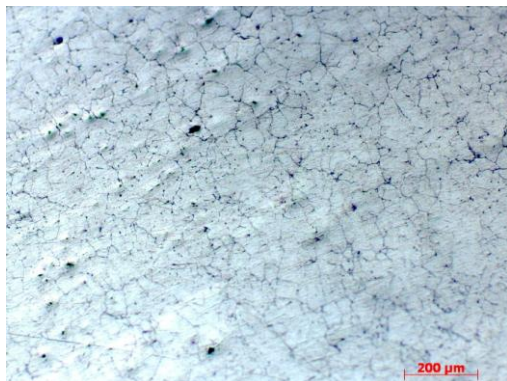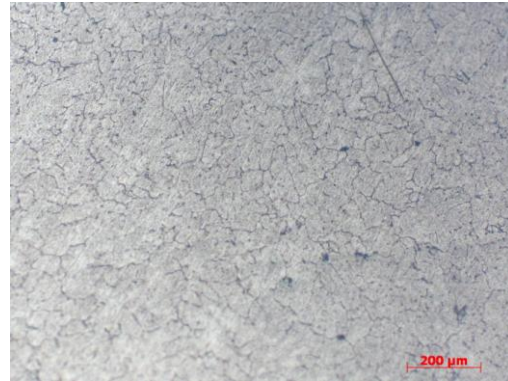
| a) Route A | (b) Route B$_A$ |

| c) Route B$_C$ | (d) Route C |

Fig.4.19 Optical microstructure of CP-Al after second pass (a) Route A (b) Route B$_A$ (c) Route B$_C$ and (d) Route C by ECAP at room temperature

4.5.1.3 Al-5Zn-1Mg rod in the cast form

The initial microstructure of Al-5Zn-1Mg before ECAP consisted of coarse grains in which η` precipitates were homogeneously distributed (Figure 4.20). Similar precipitates (η`) were identified by Zhang et al. (2010) as $MgZn_2$ intermetallic particle and matrix was semi-coherent. The local dislocation density is generally very high next to the precipitates.
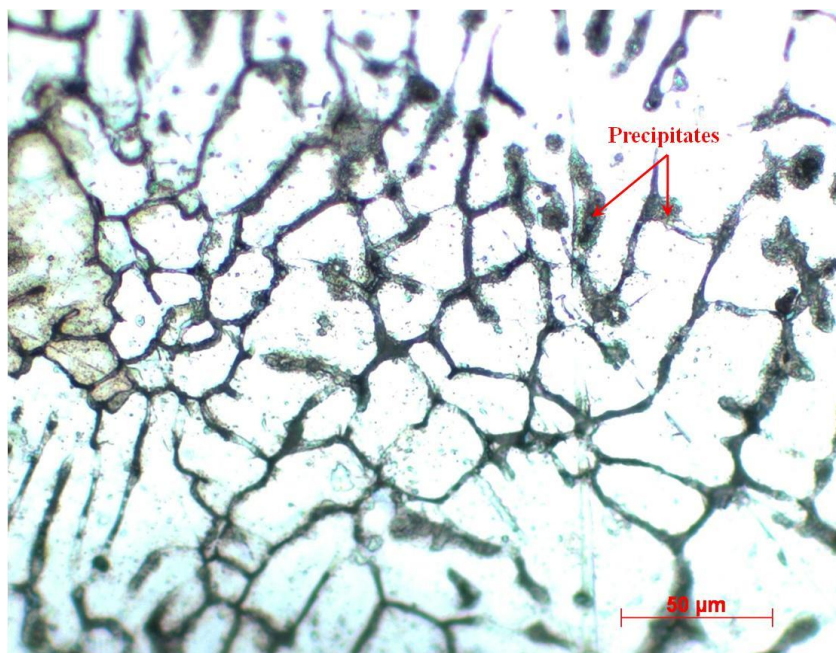
Fig. 4.20 The microstructure of Al-5Zn-1Mg tubular specimen before ECAP

4.5.2 Characterization By Scanning Electron Microscopy

4.5.2.1 CP aluminium tube in the cast form

The pores in cast aluminium microstructure instead of closing up propagated as a crack along the tube thickness of 3.5 mm. The smaller cross section can easily drive the crack due to elastic stored energy in the material. The fractograph showing the crack propagation in cast aluminium tube is shown in Fig. 4.21.
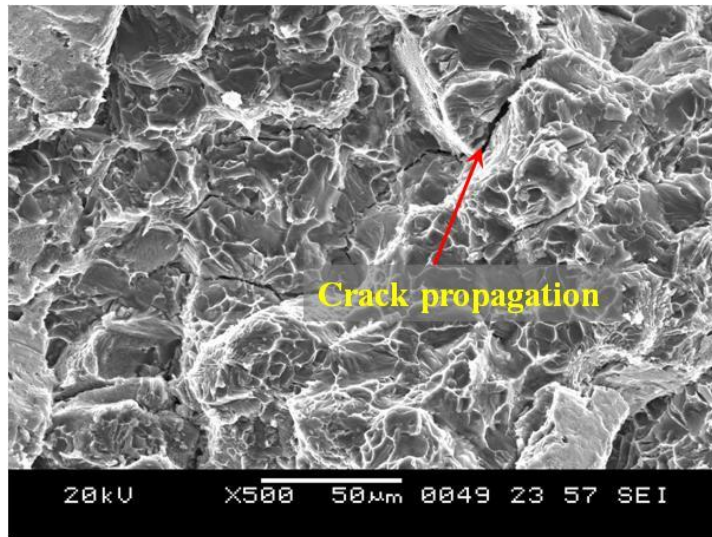
Fig. 4.21 Fractograph showing crack propagation in cast aluminium tube

4.5.2.2 Al-5Zn-1Mg tube in the cast form

Fractograph showing shallow dimples intermingled with microscopic cracks suggesting localized ductile and brittle deformation of Al-5Zn-1Mg alloy is shown in Fig. 4.22. Since the cross section of tubular section is less than a rod section the stored elastic strain energy can easily drive the microcrack to complete fracture.
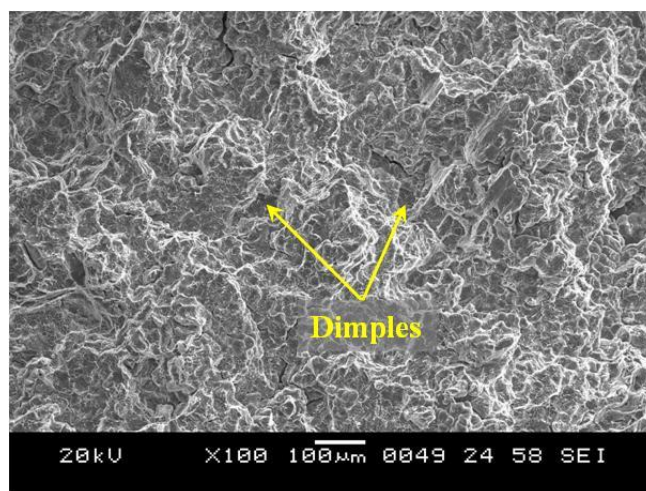
Fig. 4.22 Shallow dimples intermingled with microscopic cracks suggesting localized ductile and brittle deformation

4.6 EXPERIMENTAL ANALYSIS OF PEAK PUNCH PRESSURE

4.6.1 CP Titanium

Results of peak punch pressure while extruding CP titanium rod in the wrought form is presented in Table 4.10. From the values presented in the Table it can be observed that the peak pressure decreased from 232 MPa as equivalent plastic strain was increased from 0.31 to 0.93 for all routes selected for the study. This is illustrated by plot of extrusion pressure v/s equivalent plastic strain in Fig. 4.23. It was observed that for CP-Ti the pressure required for extrusion, is maximum in route C (150 MPa) and minimum in route A (94 MPa) after three passes.

Table 4.10 Comparison of peak extrusion pressure at comparable strains for CP Ti rod in the wrought form processed at various routes

Equivalent plastic strain	Average Peak extrusion pressure (MPa)			
	Route A	Route B_A	Route B_C	Route C
0.31	232	232	232	232
0.62	223	183	178	181
0.93	94	128	128	150
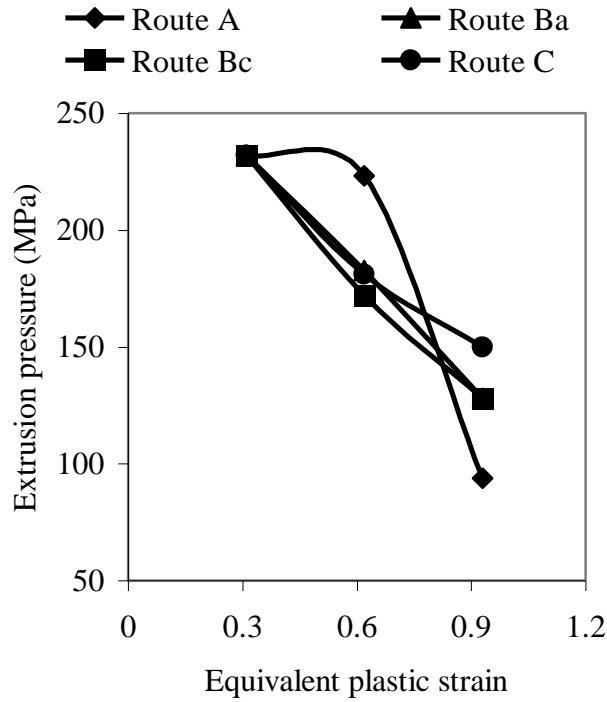
Fig.4.23 The variation of extrusion pressure with equivalent plastic strain for CP-Ti rod in the wrought form for various passes

4.6.2 CP Aluminium Rod In The Cast Form

Results of peak punch pressure while extruding CP aluminium rod in the cast form is presented in Table 4.11. From the values presented in the Table it can be observed that the peak pressure increased from 62 MPa as equivalent plastic strain was increased from 0.31 to 0.62 for all routes selected for the study. It was observed that for CP-Al the pressure required for extrusion, is maximum in route B_C (74 MPa) and minimum in route C (65 MPa) after two passes.

Table4.11 Comparison of peak extrusion pressure at comparable strains for CP-Al rod in the cast form processed through various routes

Equivalent plastic strain	Average Peak extrusion force (MPa)			
	Route A	Route B_A	Route B_C	Route C
0.31	62	62	62	62
0.62	68	71	74	65

4.6.3 CP Aluminium Rod In The Wrought Form

Results of peak punch pressure while extruding CP aluminium rod in the wrought form is presented in Table 4.12. The peak pressure increased from 74 MPa as equivalent plastic strain was increased from 0.31 to 1.24 for all routes selected for the study. This is illustrated by plot of extrusion pressure v/s equivalent plastic strain in Fig. 4.24. It was observed that for CP-Al the pressure required for extrusion, is maximum in route B_C (96 MPa) and minimum in route C (85 MPa) after four passes.

Table 4.12 Comparison of peak extrusion pressure at comparable strains for CP-Al rod in the wrought form processed through various routes

Equivalent plastic strain	Average peak extrusion pressure (MPa)			
	Route A	Route B_A	Route B_C	Route C
0.31	74	74	74	74
0.62	79	79	77	77
0.93	85	85	82	79
1.24	88	91	96	85
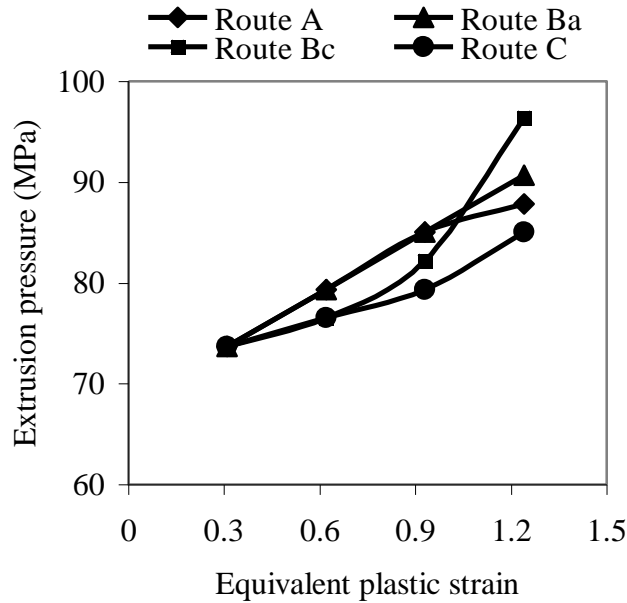
Fig.4.24 The variation of extrusion pressure with equivalent plastic strain for CP Al rod in the wrought form for various passes

4.6.4 Al-5Zn-1Mg Rod In The Cast Form

During ECAP, the force –stroke graphs were recorded. Typical extrusion force versus stroke diagrams corresponding to first pass are shown in Fig.4.25. The entry side of the specimens was little tapered and this is indicated in the force stroke graph by a change in slope in the initial stage. The transition of slope indicates end of extrusion of the tapered length. Results of peak punch pressure while extruding Al-5Zn-1Mg rod in the cast form is presented in Table 4.13. At room temperature the Al-5Zn-1Mg took 100 MPa to get extruded completely. As the temperature was raised the flow resistance of the material was decreasing. It showed maximum plasticity in the temperature range of 373-573 K. However, at 673 K peak pressure further increased to 97 MPa from 59 MPa at 573 K.

76
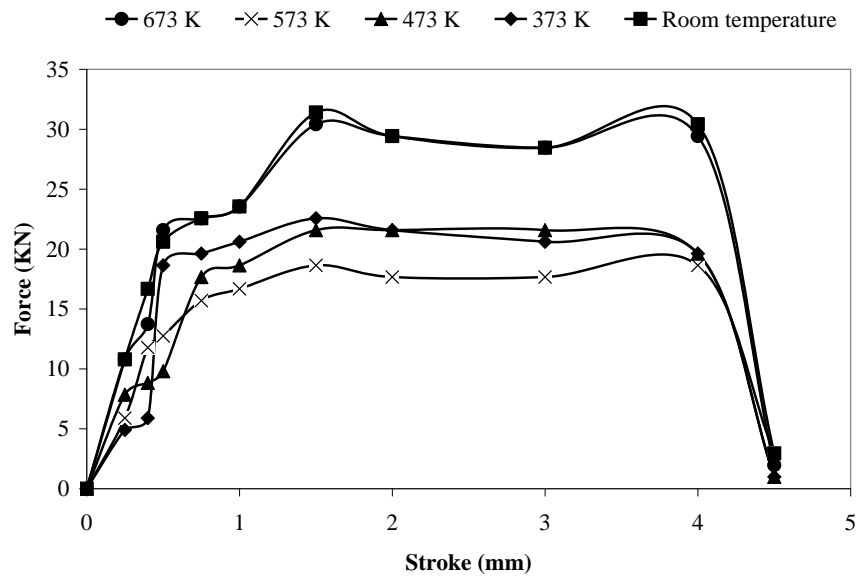
Fig.4.25 Force – stroke curves obtained during first pass at various temperatures for Al-5Zn-1Mg rod in the cast form during ECAP

Table 4.13 Comparison of peak extrusion pressure at various temperatures for Al-5Zn-1Mg rod in the cast form corresponding to first pass

Temperature (K)	Average peak extrusion pressure (MPa)
303	100
373	72
473	69
573	59
673	97

4.6.5 CP Aluminium Tube In The Wrought Form

Results of peak punch pressure while extruding CP aluminium tube in the wrought form is presented in Table 4.14. It can be observed that extrusion pressure for ECAP

increased from one pass to the next when processed through all routes. This is illustrated by plot of extrusion pressure v/s equivalent plastic strain in Fig. 4.26. The magnitude of the increase in load was reported to be higher in Route B_C and least in Route A. The rate of increase is not significant except for Route B_C. This may be due to the insignificant increase in shape difficulty factor from one pass to the next.

Table 4.14 Comparison of peak extrusion pressure at comparable strains for CP-Al tube in the wrought form with various shape difficulty factors processed through different routes

Equivalent plastic strain	Surface area/ volume ratio	Average Peak extrusion force (MPa)			
		Route A	Route B_A	Route B_C	Route C
0.31	0.604	28	31	33	30
0.62	0.608	30	33	38	31
0.93	0.611	31	38	45	35
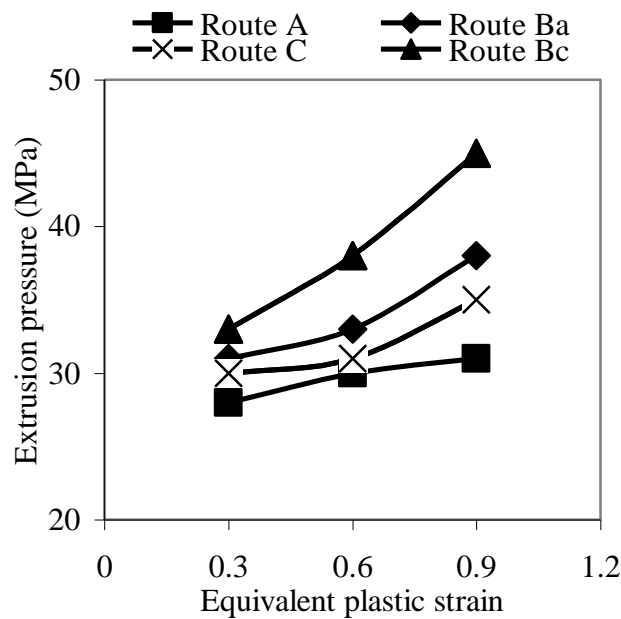
Fig.26 The variation of extrusion pressure with equivalent plastic strain for CP-Al tube in the wrought form for various passes

78

CHAPTER 5

DISCUSSION

5.1 ECAP OF COMMERCIAL PURITY TITANIUM

5.1.1 Effect Of Equivalent Plastic Strain And Processing Routes On Hardness Of CP Titanium

The high hardness obtained in CP-Ti is thought to originate from three primary factors. Firstly, the reduction in grain size and the presence of ultrafine grains in the microstructure are likely to have contributed to the observed strengthening via the well-known Hall–Petch mechanism [Stolyarov et al., 2003]. Secondly, the presence of a high density of dislocation networks and tangles is also a known factor that will contribute to strengthening [Courtney, 2000, Sergueeva, 2001]. Thirdly, there will likely be a solid solution strengthening effect as a result of increased amount of elements such as O, N, C, H and Fe [Donachie, 2000]. Overall contribution to increase in hardness is due to the contribution of second and third factors and not from first factor since the die angle is as high as 150˚.

The hardness after the first pass is higher than that in annealed CP-Ti, which may be connected with enhancement of the dislocation density. Deformation by twinning makes considerable contribution into strain hardening when deformed during first pass. The process of accumulation of dislocations in the cell walls is far more intensive than that in their interiors. On further passes through the die, the orientations across these boundaries increase as more dislocations move from the subgrain interiors and become absorbed in the subgrain walls, thereby refining the microstructure. After second pass it was found that route B_A showed the maximum hardness. This result indicates that the twin bands would have been rotated and distorted severely during the second pass by route B_A compared to other routes where there is no appreciable difference in the increased hardness. After third pass it was

found that route A showed the maximum hardness. This may be due to micro-twins aligned in longitudinal direction which is more pronounced and finer compared with the second pass. The increased alignment of shear bands to the longitudinal direction in aluminum alloys and carbon steels processed via route A has already been observed by Nemoto et al. (1998) and Kim et al. (2001). There is no appreciable difference in the increase of hardness in other routes after the third pass.

5.1.2 Effect Of Equivalent Plastic Strain And Processing Routes On Tensile Properties Of CP Titanium

Dealing with the tensile properties of CP-Ti, comparison with data shows that, although the present samples were submitted to a relatively low shear strain, they exhibit similar trend as specimens which are much more heavily deformed [Stolyarov et al., 2003, 2001 and Zhu et al., 2003]. Strain hardening may be the phenomenon that controlled the plastic deformation of annealed CP-Ti when tested at room temperature, which is associated with the dislocation accumulation in the material. As the metal was processed at 623 K during each pass the contribution of strain hardening mechanism is not intensified in further passes. Still it is noted that the ultimate tensile strength (UTS) of CP-Ti increased as the number of passes were increased for all routes. This may be due to the increased dislocation densities in the deformation band. The dislocations may have blocked at the twin boundaries. This indicates that twin boundaries acted as obstacles for dislocation movement and enhanced dislocation pinning [Serra et al., 2002]. This phenomenon has been generally observed in HCP metals that are plastically deformed by rolling or drawing [Christian and Mahajan, 1995].

This effect can be similar to that of second-phase particles and aid in the refinement of microstructure during SPD [Iwahashi et al., 1998]. Route B_A showed the maximum tensile strength after both second and third pass. This may be due to the fact that route B_A is not a redundant strain process and there are four distinct shearing planes intersecting at various angles. In routes B_A, there is a cumulative buildup of additional

strain on each separate pass through the die and thus higher UTS compared to other routes.

On the contrary ductility decreased after each pass till the third pass except in Route C where an increase in ductility was observed after third pass compared to the second pass. The percentage elongation to failure was decreased after the third pass compared to the first pass in all routes. This result is consistent with the classical mechanical behavior of metals that are deformed plastically with no significant grain size reduction. The plastic deformation mechanisms associated with the generation and movement of dislocations either by slip or twinning may be effective in improvement in strength but not in ductility enhancement. So it is expected that Route B_A which is having the highest UTS will have the least ductility. The increase in ductility after second pass by Route C may be due to an increase in the fraction of high-angle grain boundaries with increase straining and with a consequent change in the dominant deformation mechanisms due to the increasing tendency for the occurrence of grain boundary sliding and grain rotation.

5.1.3 Microstructural Analysis Of CP Titanium Before And After ECAP

The microstructure of as–received CP titanium showed equiaxed, coarse-grained structure which could be individually resolved. Observation of the fine features in titanium microstructure after first pass revealed elongated grain structures and a number of deformation twins (Fig. 4.14). At low strains, twinning can contribute significantly to accommodation of the deformation [Kim et al., 2003 and Minonishi et al.,1985]. In particular, grains with three distinct features were observed. Twins spanning the entire grain were formed parallel to the elongation direction; the twins inclined to the orientation of the deformation zone of the pressing and micro twins inside the grains were observed. Thus, the observations after the first ECAP pass revealed deformation twins either on a macro- or a micro-scale.

The micrograph after the second pass by route A revealed that most of deformation zone consisted of micro-twins which were aligned to the longitudinal direction. Some

of the twins, however, were aligned at an angle to the direction of the shear deformation. The alignments of the twins after the third pass was more pronounced and were finer compared with that after the second pass.

After the second pass by route B (B_A and B_C), alignment of the twins after the second pass remained almost the same as after the first pass except that their density (of twins) was increased. Micrograph after third pass route B revealed that most of the twins were aligned parallel to the orientation of the deformation zone of the second pass.

After the second pass by route C, the twins associated with the simple shear deformation of the first pass appeared to be randomly oriented, thus resulting in a relatively homogeneous microstructure. This observation is in accordance with the fact that the original macrostructure tends to be restored after every even pass of route C [Stolyarov et al., 2001, 2003, Zhu et al., 2003, Kim et al., 2003, Shin et al., 2003]. Micrograph after the route C third pass revealed remnants of micro-twins, which were distorted and segmented compared with those after the first pass (Fig. 4.16 d). The dislocation density may be slightly increased compared to that of first and second passes. Dislocation activity during the third pass must have rotated the twins developed during the second pass.

5.1.4 Effect Of Equivalent Plastic Strain And Processing Routes On Peak Punch Pressure While Forming CP Titanium

From the analysis of improvement in strength after the first pass, it can be predicted that the density of dislocations had increased significantly and from the microstructure it is clear that the density of twin bands is also increased. This suggests that plastic strain is mainly accommodated by a combination of slip, and deformation twinning. This result differs with previous findings that titanium deforms mainly by slip of a-type dislocations above ambient temperature and that twinning assists the activation of secondary slip systems [Yoo et al.,1981 and Paton and Backofen, 1970].

Thus an average peak extrusion pressure of 232 MPa may be a contribution to deformation both by slip and twinning.

The peak punch pressure decreased continuously for the second and third passes. This result also differs with previous findings that as titanium deforms, the twin boundaries act as obstacles for slip [Christian and Mahajan, 1995] and dislocations during ECAP were blocked by the twin boundaries. In such cases, the critical resolved shear stress (CRSS) for twinning must have increased much more significantly compared with that of dislocation slip, promoting the deformation by slip during the second pass. It is to be noted that there were significant grain size reduction during subsequent passes in the above study.

In the present study the relatively high deformation temperature (623 K) must have made the recovery and stress relaxation easier, which must have significantly relieved stress, caused by the deformation and dislocation density. With the number of passes increasing, annihilation processes intensify in the cell interiors and in the cell walls, which is connected with growing of annihilation during non-conservative dislocations motion. Therefore during the second and third pass since, the critical resolved shear stress (CRSS) for twinning may be less than dislocation slip and thus twinning must have dominated over deformation by slip. Since there is no appreciable grain size reduction in the present study, the rate of increase in the twinning stress need not be larger than that of dislocation slip.

After three passes Route A showed least punch pressure. This may be because of the same Schmid factor for basal slip system as that of the as-received CP-Ti since the texture will be retained in route A. Therefore, the grain size plays a dominant role but a significant increase in grain size is not observed and thus decreases in peak punch pressure. In other routes the Schmid factor for basal slip system varies and there will be coexistence of different modes of deformation is also reflected in the peak punch pressure.

5.2 ECAP OF COMMERCIAL PURITY ALUMINIUM ROD IN CAST FORM

5.2.1 Effect Of Equivalent Plastic Strain And Processing Routes On Hardness Of CP Aluminium Rod In The Cast Form

Porosities can result from several diverse mechanisms but are always related to casting. Entrapped gas can be present in the melt, evolve from the mould coatings or be present within fire cracks in the mould chill walls. Porosities decrease the strength of the material since they act as an area of stress concentrations. From the results it can be found that the increases in hardness are very profound in the first and second passes. This may be due to the closing of porosities during subsequent passes. By changing the orientation of cast aluminium from one pass to another, different combinations of severity of breakdown of cast ingots can be obtained. Varying the processing route effectively changes the strain path to which the material is subjected to deformation. The higher hardness obtained after processing by route B_C may be due to severe breakdown of dendritic structure which was observed in the samples. Previous studies carried out by EI-Danaf (2008) and Saray and Purcek (2009) also show that ECAP caused mostly elimination of porosities by shear deformation with superimposed hydrostatic pressure.

5.2.2 Microstructural Evolution Of CP Aluminium Rod In The Cast Form

It is well known that inherent in the casting process is the introduction of porosity, such as gas or shrinkage porosity, where the porosity size and shape distribution are dependent up on the casting process. If the porosity goes undetected and / or is not closed by the forming operation, it is often responsible for the failure of a component during metal forming operation or subsequent service life. After one pass of ECAP, the dendritic micro structure distorted through the way of shear stress acting during deformation. Increasing the number of passes caused further effect on the microstructure depending on the processing route. A severe break down of cast ingots was seen in the samples processed by route B_C where grains and grain boundaries were visible in some area, which is the characteristic of a wrought metal (Fig 4.19 c),

whereas in the case of samples processed by route C the breakdown of cast structure was not severe as B$_C$. This is in good comparison with result obtained by Saray and Purcek (2009) when they studied the microstructural evaluation in Al-40wt% Zn alloy. They also revealed significant grain refinement by samples processed through Route B$_C$.

5.2.3 Fracture Analysis Of CP Aluminium Rod In The Cast Form

It is evident from Fig. 5.1 that ECAP processing significantly changes the nature of the fracture surface. Interdendritic porosities that were formed during solidification lead to crack nucleation and fracture occurred with the propagation of crack through interdendritic region in the as-cast state. Fang et al. (2006) studied the fracture mechanisms of the as-cast Al-0.63%Cu and Al-3.9% Cu alloys processed by ECAP via route B$_C$ and found that shear fracture occurred and became more obvious with increasing ECAP pass. Phase boundaries and interdendritic shrinkage micro porosities formed as a result of dendritic solidification limit the ductility and strength of the aluminium due to increasing cracking tendency.
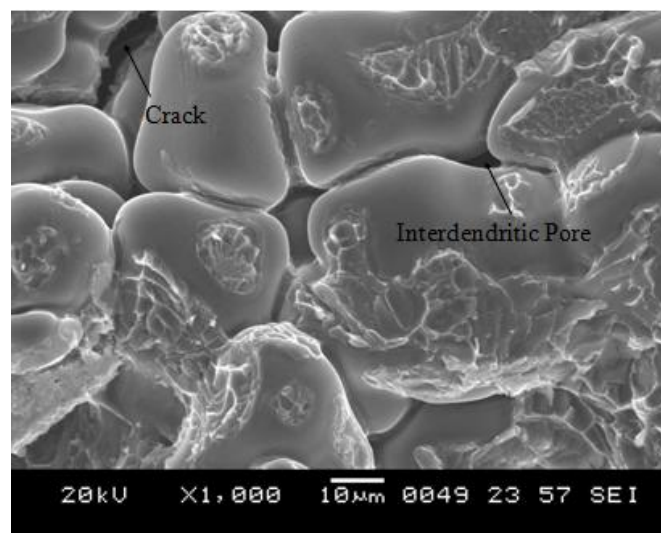
Fig. 5.1 Fractograph of cast aluminum rod fractured during third pass

5.2.4 Effect Of Equivalent Plastic Strain And Processing Routes On Strength Coefficient And Strain Hardening Exponent Of CP Aluminium Rod In The Cast Form

Mechanical properties of as-cast pure aluminium are strongly influenced by dendritic structures. Phase boundaries and interdendritic shrinkage micro porosities formed as a result of dendritic solidification limit the ductility and strength of the aluminium due to increasing cracking tendency. A significant increase in strength coefficient and strain hardening was observed in ECAP processed samples in comparison with as-cast structure. Strain hardening and strength coefficient are the result of dislocation accumulation and their interaction during deformation. Once a dislocation is emitted from a grain boundary, its path to transverse the grain interior is very short, and it may deposit on another grain boundary directly without intersecting other dislocations. This lack of strain hardening causes the onset of inhomogeneous deformation at small strains [Saray and Purcek, 2009].

From the results obtained it is clear that elimination of dendritic structure caused a simultaneous increase in both strength coefficient and strain hardening exponent. It is also seen that when processed by route A the increase in strain hardening was not significant due to the absence of strain reversal; instead the shear is accumulated continually on one plane. Route B showed a higher strength coefficient and strain hardening exponent due to the build-up of high dislocations densities and initiation of subgrains. This is in good agreement with the microstructure obtained in present study. It is evident that there is a gradual breakup of cast structure into subgrains [Nagasekhar et al., 2006]. The severity of breakdown of cast structure is more pronounced in route B_C.

5.2.5 Effect Of Equivalent Plastic Strain And Processing Routes On Peak Punch Pressure While Forming CP Aluminum In The Cast Form

The peak punch pressure was increased for second pass for all routes compared to the first pass. It is due to the breakdown of dendritic structure and closure of pores. As the

number of passes increases, the dislocation density increases which must be a reason for increase in peak punch pressure. Different combinations of severity of breakdown of dendrites were observed while changing the orientation of cast aluminium from one pass to another. These microstructural changes may be the reason for higher punch pressure to form using route B_C and lower punch pressure to form using route C during second pass. Furukawa et al. (2001) suggested that a wide angular range of slip traces might favor the formation of equiaxed grains. It may account for the present observations that among four routes studied, the grains developed in route B_C have the most equiaxed shape.

5.3 ECAP OF COMMERCIAL PURITY ALUMINIUM ROD IN WROUGHT FORM

5.3.1 Effect Of Equivalent Plastic Strain And Processing Routes On Hardness Of CP Aluminium Rod In The Wrought Form

It is a well established fact that processing by ECAP leads to an increase in the hardness, which is typically by a factor of ~1.5 - 2.0 for the first pass through a die with $\Phi = 90°$ where the imposed strain is ~1[Kamachi et al., 2003]. In the present study with a die angle of 150° where the severity is less, an increase in hardness as found in above study is not feasible yet an improvement in hardness can be expected. From the results it can be found that the enhancement in hardness is so profound in the first pass itself and then at a much lower rate in subsequent passes. This may be due to increased dislocation densities and grain refinement during the first pass. Generally aluminium and its alloys undergo grain refinement with increasing deformation, but these values normally stabilize in the submicron range with further deformation not leading to grain refinement. With larger initial grain sizes, a greater number of passes (i.e. more plastic deformation) would be required to achieve a stable micron or submicron sized grain [Khan et al., 2003]. In the present study since the commercially pure aluminium was having very fine initial grain structure, it was difficult to quantify the grain refinement by using SEM or optical microscope. But from the gradual increase in hardness after first pass suggests that a submicron sized

grain must have already formed from its first pass itself. It can be noted that Route B (B$_A$ and B$_C$) showed higher hardness compared to other routes and route C showed the least hardness after second, third and fourth passes. Because of the 90˚ rotation about the extrusion direction in route B, new deformation bands and cell blocks must have formed in each grain, deforming with a set of slip systems different from the previous passes. A similar situation occurs for all subsequent extrusion passes. Such an out of sequence strain reversal makes it more difficult for the cell blocks to rotate back to the initial state. Therefore, misorientation between cell blocks can accumulate strain quite effectively in route B$_C$. For route C, however, the shear strain reverses in the subsequent passes, thus there is generally a low efficiency for preservation of dislocations. Therefore increase in hardness by route C is not as high as other routes after multiple passes.

5.3.2 Effect Of Equivalent Plastic Strain And Processing Routes On Tensile Properties Of CP Aluminium Rod In The Wrought Form

The ultimate tensile strength of CP-Al processed by ECAP showed a substantial increase after first pass itself. This behavior may be due to the initial massive reduction in grain size achieved in the first pass and the original grains, break-up into bands of sub grains. These sub-boundaries subsequently evolve with further pressings into high angle grain boundaries, giving ultimately a reasonable equiaxed microstructure. As the number of passes increases up to 4 passes, the UTS increased for each pass for all the routes but not at the rate of increase shown after first pass.

It is to be noted that Route B (B$_A$ and B$_C$) showed the maximum UTS whereas there is no difference in UTS between route A and C after third and fourth pass. Previous works carried out by EI-Danaf (2008) also shows that route B$_C$ is the most effective way for the grain refinement of commercially pure aluminium. Similar results were observed by Sarvanan et al. (2006) too. In route B$_C$, where the sub-grain boundaries evolve most rapidly into high angle grain boundaries, the two shearing directions lie on planes which intersect at 150˚. As a result of this duality in the shearing directions, sub grain bands are developed on repetitive pressings along two separate and

intersecting sets of planes and this leads rapidly to an evolution in the boundary structure into a reasonably equiaxed array of high angle boundaries. Thus, it is reasonable to conclude that route B_C is the preferable procedure for use in ECAP experiments for CP-Al for higher tensile strengths.

5.3.3 Effect Of Equivalent Plastic Strain And Processing Routes On Peak Punch Pressure While Forming CP Aluminum

The peak punch pressure increased with the number of passes. This trend is expected since each pass showed superior mechanical properties compared to the previous pass. During plastic deformation, a grain tends to subdivide into blocks with different combination of slip systems, thus boundaries are generated between these blocks. As deformation progresses, the blocks will rotate to different end orientations and the boundaries between the blocks evolve into high angle grain boundaries. It is seen that route B (B_A or B_C) took maximum stress and route C took minimum stress to form after each pass till four passes. The low punch pressure for route C may be due to the shear strain reversal in the subsequent passes and due to the low efficiency for preservation of dislocations. Geometrically, route B_C is also a redundant strain process after four passes, but the shear strain reversed is way out of sequence, unlike the case of route C, where the shear is immediately reversed in the following pass. Because of the 90˚ rotation about the extrusion direction in route B_C, new deformation bands and cell blocks form in each grain, deforming with a set of slip systems different from those used in the previous pass. A similar situation occurs for all subsequent extrusion passes. Such an out of sequence strain reversal makes it more difficult for the cell blocks to rotate back to the initial state thus increasing the punch pressure for further passes. Therefore, misorientation between cell blocks can accumulate quite effectively in route B_C [Sun et al., 2004].

5.4 ECAP OF Al-5Zn-1Mg ROD

5.4.1 Effect Of Processing Temperature On Hardness Of Al-5Zn-1Mg After First Pass

The results show a significant increase in hardness after first pass of ECAP at all the selected temperatures. This may be due to elongated subgrains and high dislocation densities at the subgrain boundaries formed during the first pass. Second phase particles, such as $MgZn_2$, normally present in the Al-Zn-Mg alloy, can hinder the movement of dislocations and act as dislocation sources, which can affect the grain size refinement. Nam et al. (2003) showed that large platelet $MgZn_2$ precipitates can also act as obstacles to dislocations and provide favorable sites for the development of grain boundaries. During the first pass the alloy hardness may have increased due to the strain hardening too. As the temperature was increased for processing the strain hardening effect must have come down thus showing a decrease in hardness in the range of 303 – 573 K. The softening effects caused by the use of a pressing temperature of 303 – 573 K, can also be related to the recovery process and the dissolution of θ' phase with consequent transformation to stable θ phase. The increase in hardness at 673 K, which is against the general behavior, can be attributed to strain ageing. The diffusion coefficient increases exponentially with temperature and thus, an increase in temperature will result in an increase in diffusivity of the solute atoms which interact with the moving dislocations and influence the hardness.

5.4.2 Microstructure

A high magnification SEM image of the as-cast and homogenized microstructure of Al-5Zn-1Mg alloy is shown in Fig. 5.2. The α-Al phase with (α+τ) eutectic in inter dendritic regions and constitutive particles along the grain boundaries can be clearly seen. Shwe et al. (2008) reported as- cast structures of Al-5.8Zn-2.2Mg alloy Fig (5.3) which resembles the SEM images in the present investigation.
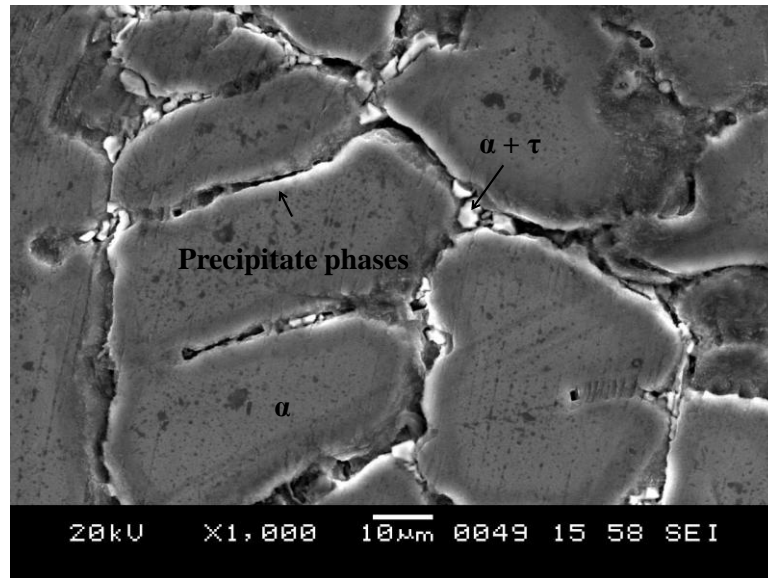
Fig. 5.2 SEM image of the as-cast and homogenized microstructure of Al-5Zn-1Mg alloy
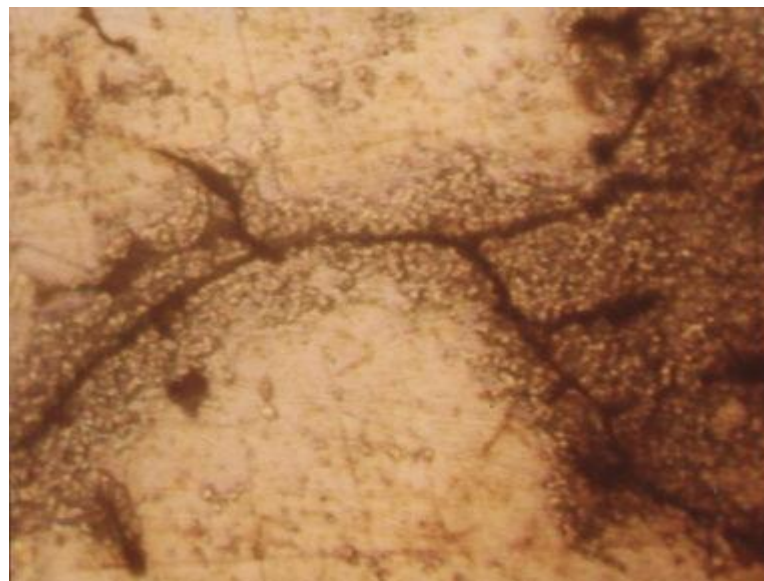
Fig. 5.3 Microstructure showing precipitate phases adjacent to the grain boundaries before solution treatment, 200X

During the solidification of the Al-Zn-Mg alloys some intermetallic particles such as $MgZn_2$ phases are formed [Rokhlin et al., 2004, Lim et al., 2006, Mondal and Mukhopadhyay, 2005, Gupta et al., 2006, Ahmed et al., 2008]. An X-ray diffraction (XRD, A JEOL JDX-8P-XRD) with a Cu K-alpha radiation over a range of $20^0 - 94^0$ at 2^0/min on the Al-5Zn-1Mg alloy in the present study reveals $MgZn_2$ phase, which is shown in Fig. 5.4 In addition, mutual dissolutions of different phases can result in the formation of new particles, for example, $Al_2Mg_3Zn_3$ compound (τ phase). Most of them have low melting points, which may result in incipient melting during hot deformation.
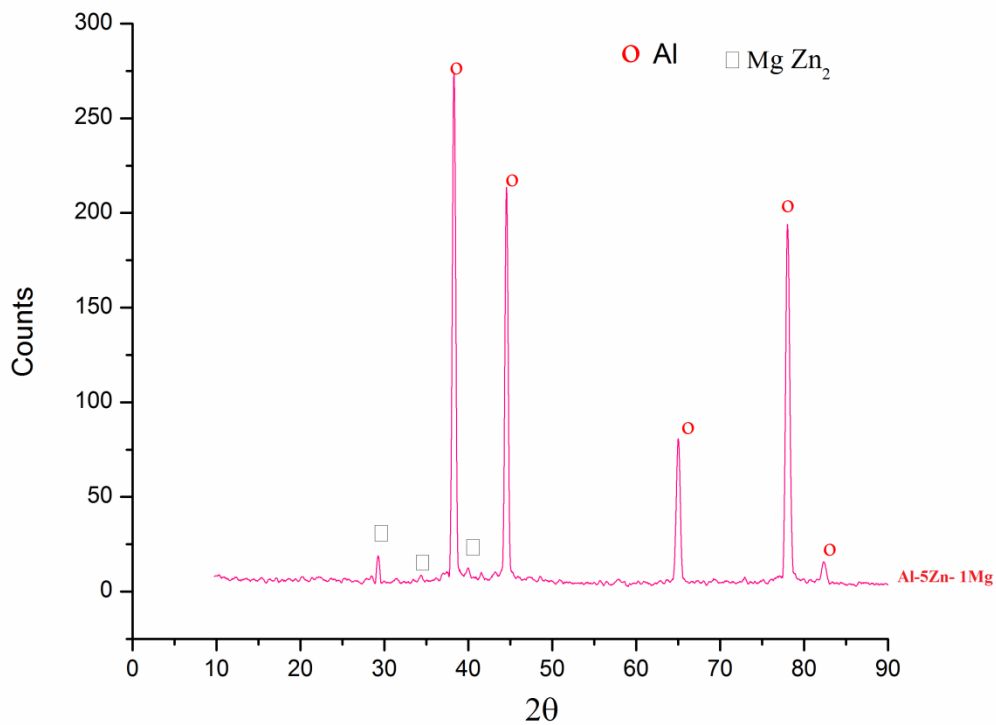
Fig. 5.4 X-Ray diffraction analysis of Al-5Zn-1Mg alloy

5.4.3 Analysis Of Forming Stress

This study was to analyze the forming loads required and how they vary during the processing temperatures. From the extrusion force versus stroke diagram it is observed that these curves show a maximum force between 10 – 20 mm stroke lengths. This value is taken to serve as the basis for comparison. As the temperature of ECAP was raised, a transition in flow was observed for the same extrusion speed. Flow resistance of the material was decreasing as the temperature was increasing. It shows maximum plasticity in the temperature range of 373-573 K and the stress required for deformation was more at 303 K. However at the highest extrusion temperature (673 K) flow stress increased and it is because of dynamic strain ageing (DSA) caused by substitutional elements in this temperature range. At room temperature, the elements have considerably lower diffusivities. They gain enough mobility, at high temperature such that the diffusivity approaches the dislocation velocity. Dynamic strain ageing increases the flow stress and decreases the ductility [Reed Hill and Reza Abbaschean, 1994]. DSA is totally undesirable during mechanical processing. Therefore this temperature range should be avoided while ECAP of   Al-5Zn-1Mg.

5.4.4 Role Of Friction

Friction coefficient has a noticeable effect on the magnitude of the punch pressure and this pressure/stress increases with increasing friction coefficient. For example, when friction coefficient decreases from 0.3 to 0.001 in the die channel angle of 110°, the magnitude of the punch pressure reduces by 60% [Djavanroodi and Ebrahimi, 2010]. For deformation to be uniform across the cross section of the billet, friction at the specimen-die interface has to be minimized. With moderate friction, a small dead end zone develops at the die corner. In the present study the friction factor **m** was found to increase from 0.42 to 0.9 at temperatures between 303Kand 673K which is a drawback when considering hot working.

5.5 ECAP OF WROUGHT ALUMINIUM IN THE TUBULAR FORM

5.5.1 Effect Of Hardness On Equivalent Plastic Strain During ECAP

The VHN of ECAP processed material increased for 0.3 and 0.6 strain but did not show pronounced difference between various routes but at 0.9 strain route B_A showed maximum hardness and route C showed the minimum hardness. The marginal difference existing in hardness is difficult to explain since the number of passes required to achieve a homogeneous microstructure in pure Al are subjected to many parameters including the impurity content. Iwahashi et al. (1998) and Xu et al. (2005) found that it is 4 passes for 99·99% pure Al whereas Sun et al. (2002, 2004) found that it is 8 passes for 99·5% pure Al. The grain refinement by ECAP has been explained by Valiev et al. (2000) the increase of dislocation density, formation of a cellular or sub-grain structure and subsequent formation of high angle grain boundaries by partial annihilation of dislocations. The present study and that of Sun et al. (2002) have used CP-aluminium having 0·158 and 0·2 wt% iron contents, respectively. Since the solubility of iron in solid state aluminium is very low (0·04 wt %), the iron appears as intermetallic second phase causing heterogeneities in plastic flow and more grain refinement thus increasing the hardness after each passes.

5.5.2 Effect Of Peak Extrusion Pressure On Equivalent Plastic Strain During ECAP

The magnitude of punch pressure is a major factor to be considered for selecting the suitable hydraulic press in designing the ECAP die. The force–stroke diagram for extruding a 60 mm length tubular CP-Aluminium was found. After each pass of ECAP, the end of the sample, i.e. un-extruded portion of 5 mm sample was cut off. This caused a reduction in length of the specimen after each pass. Therefore, to compare the three different passes (for the purpose of calculations and comparison between passes) calculations were carried out for a stroke of 60, 55 and 50 mm in each case. It can be observed that extrusion pressure for ECAP increased from one pass to the next when processed through all the routes. The observed high pressure is due to the higher strains generated along the sample by multiple passes. So, the existence of the high pressure assures homogeneous and reduced dead zone. Also,

friction coefficient has a noticeable effect on the magnitude of the punch pressure requirement and this pressure increases with increasing friction coefficient. The magnitude of the increase in extrusion pressure was reported to be higher in Route B_C and least in Route A. The rate of increase is not significant except for Route B_C. This may be due to the insignificant increase in SDF from one pass to the next.

5.5.3 Influence Of Shape Difficulty Factor (SDF)

Shape difficulty factor is defined as the ratio of the surface area to volume of the extruded specimen. In general, higher the shape difficulty factor, higher the forming pressures requirement. The comparison shown in Table 4.13 reveals that even though the ECAP specimen have high SDF, the peak pressing pressures recorded were very less compared to conventional extrusions of CP-Aluminium [Sivaraman and Chakkingal, 2008]. Even though the hardness of the material improved when processed though ECAP, the forming pressures required were lower when compared to conventional extrusion. This demonstrates that the ECAP process is advantageous in improving the properties for higher SDF specimen compared to conventional extrusion.

5.5 ECAP OF CAST ALUMINIUM AND Al-5Zn-1Mg ALLOY IN THE TUBULAR FORM

The equivalent plastic strain imparted would have been 0.3 if the samples survived a pass but the sample showed multiple fractures after the pass at room temperature [Fig. 5.5].

Fig. 5.5 Tubular specimens (a) Cast Al before ECAP (b) Cast aluminium (c) Al-5Zn-1Mg after first pass

Theoretical work required for ECA pressing of tubular specimens can be calculated according to work done principle. Fig. 5.6 shows the stresses and forces acting during ECA pressing of tubular specimen.
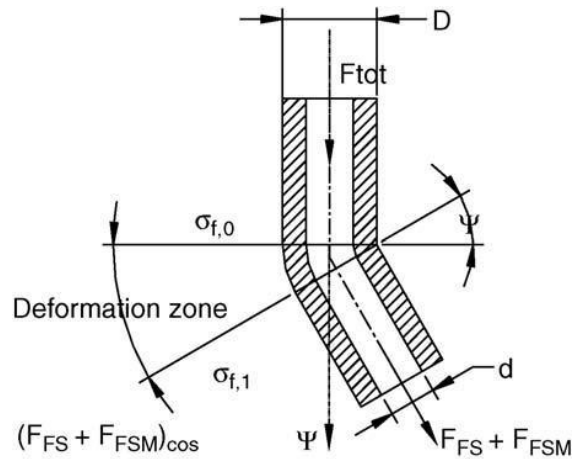
Fig 5.6 Stresses and forces during ECAP of tubular specimen geometries

Theoretical work required for ECAP of tubes is the addition of the following forces [similar to work done principle in metal forming (Lange K., 1985)]

$$F_{tot} = F_{Shear} + F_{FW} + F_{FS}\cos\psi - F\cos\psi - F_{FM} - F_{FSM}\cos\psi \qquad (5.1)$$

where F_{tot} is the total extrusion force needed for the ECA extrusion of the tube; F_{Shear}, the force required for shear deformation; F_{FW}, the force due to friction between the die wall and outer surface of the specimen (before entering deformation zone); F_{FS}, the force due to friction in the deformation zone between die wall and outer surface of the specimen (in the deformation zone); F_{FM}, the force due to friction between mandrel (sand) and inner surface of the specimen (in the deformation zone); F_{FSM}, the force due to friction in the deformation zone between mandrel (sand) and inner surface of the specimen (after leaving the deformation zone); ψ, the angular separation between the direction of application of load and the direction in which the pressed tube emerges. The friction factor of CP Al was determined using a ring compression test at

96

room temperature and reported as 0.34 by Vidyasagar et al. (2006). The friction factor of Al-5Zn-1Mg at room temperature was determined using ring compression test and was reported as 0.42 (Table 4.9). The strength coefficient and strain hardening exponent of Al-5Zn-1Mg was determined using a compression test at room temperature by Rijesh et al. (2011). The flow properties are given in Table 5.1.

Table 5.1 Flow properties of Al-5Zn-1Mg at room temperature

Strength coefficient, **K**(MPa)	Strain hardening exponent, **n**
611	0.54

5.5.1 Microstructural Analysis

5.5.1.1 Microstructure of cast Al tube

Microstructure of cast Al specimen showed dendritic arms and inter-dendritic porosities. Inter-dendritic porosities are typically irregular shaped cavities with rough dark interiors as shown in Fig.5.7. Porosities may be due to poor inter-dendritic feeding during solidification of the roll casting.
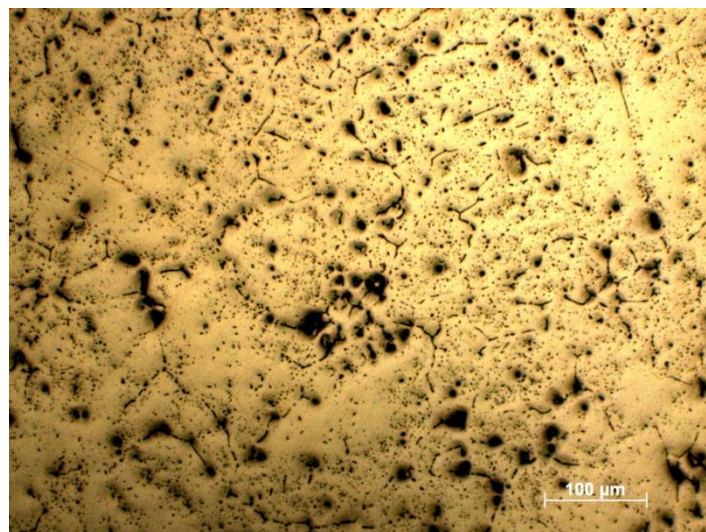
Fig.5.7 Optical microstructure of annealed CP-Al in the cast form revealing inter-dendritic pores

5.5.1.2 Microstructure of Al-5Zn-1Mg

The formation of precipitates in Al-5Zn-1Mg may be attributed to the super-saturation of the structure with alloying elements occurring during solidification at high cooling rates while solidifying in a metallic mould. When the as-cast alloy is exposed to a homogenization treatment at a low temperature (< 743 K), there is a tendency for the alloying elements to precipitate out. As the temperature increases (> 743 K), the solubilities of these elements in the α-Al matrix increase (Belov et al. 2005, ASM Handbook 1992) and the formation of new particles is not expected. In the present study homogenization treatment was given at 623 K thus formation of new particles is expected and the local dislocation density is expected to be very high next to the precipitates. The high strength coefficient (K) and strain hardening exponent (n) values reveal the same. Al-5Zn-1Mg contains precipitate phases along the grain boundaries and near the grain boundary as shown in Fig. 5.8.
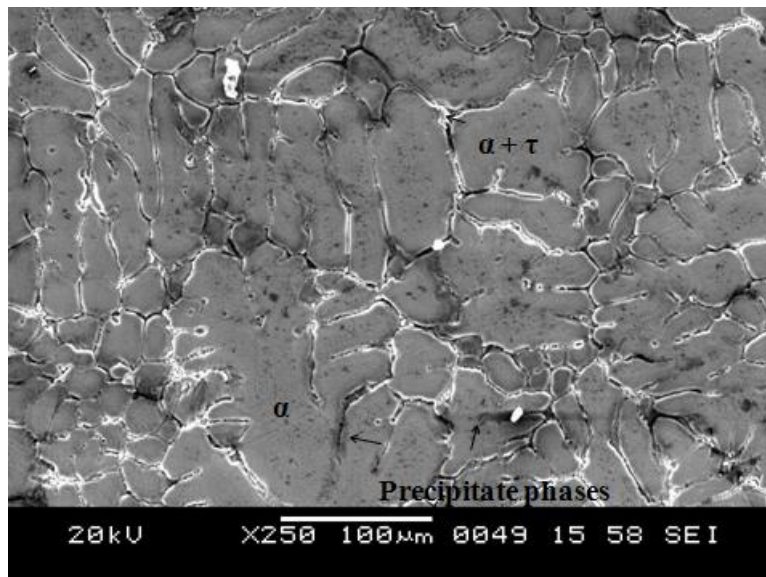
Fig.5.8 Scanning electron micrograph of as-cast and homogenized Al-5Zn-1Mg

5.5.2 Fracture Analysis

The process of brittle fracture consists of 3 stages: 1. Plastic deformation which involves pileup of dislocations along the slip planes at an obstacle, 2. The buildup of shear stress at the pileup to nucleate a microcrack, and 3. The stored elastic strain energy drives the microcrack to complete fracture without further dislocation movement or a distinct growth stage is observed in which an increased stress is required to propagate the microcrack [Dieter, 2001].

5.5.2.1 Cast Al tube

If the porosities are large, and extend to a measureable depth and/or are clustered together in a small area, the stress concentration effect can result in contact stress crack initiation and propagation which could eventually result in failure of tube walls. Cast aluminium tube has porosities as revealed from its microstructure, the pores in cast aluminium microstructure instead of closing up propagated as a crack along the tube thickness of 3.5 mm. The elastic stored energy can easily drive the crack along the tube thickness. Fig. 5.9 shows the fractograph revealing crack propagation along the tube thickness.
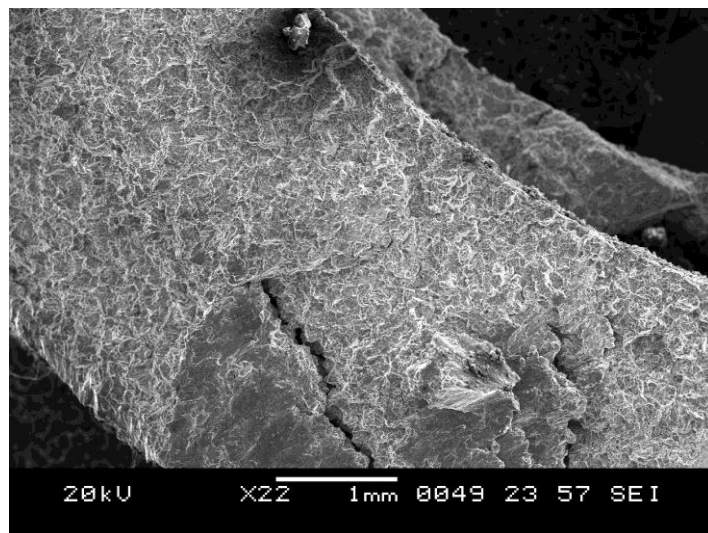
Fig.5.9 Fractograph showing crack growth along the wall thickness of CP-Al tube in the cast form

5.5.2.2 Al-5Zn-1Mg

In the present study, ECAP, which is a severe plastic deformation process, would have helped dislocations to pileup near $MgZn_2$ precipitates. ECAP is a material processing technology by simple shear stresses, which would help to build up shear stresses at the head of the pileup to nucleate many microcracks in Al-5Zn-1Mg alloy. Shallow dimples intermingled with microscopic cracks suggesting localized ductile and brittle deformation of Al-5Zn-1Mg alloy is shown in Fig.5.10. Since the cross section of tubular section is less than a rod section the stored elastic strain energy can easily drive the microcrack to complete fracture. Microcrack propagation into various sizes and shapes are shown in Fig. 5.10. Fig. 5.11 exhibits flat facets. The river markings are caused by the crack moving though the crystal along a number of parallel planes which form a series of plateaus and connecting ledges. These are indications of the absorption of energy by local deformation. The direction of the "river pattern" represents the direction of crack propagation.
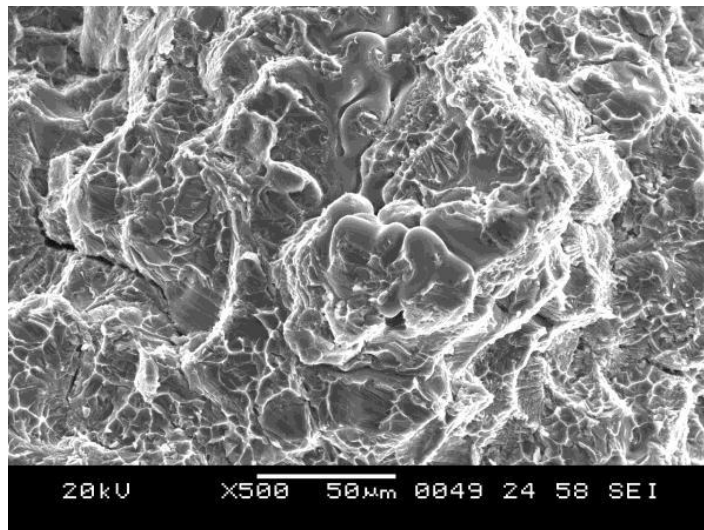
Fig 5.10 Microscopic cracks of varying size and shape and dimples
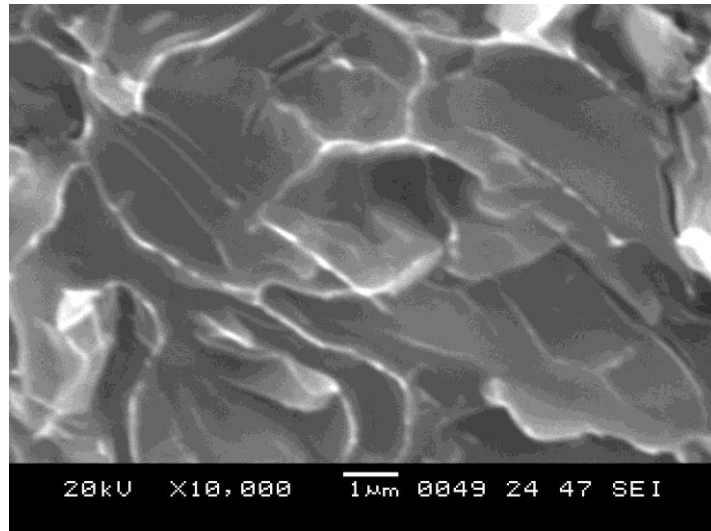
Fig. 5.11 Cleavage of Al-5Zn-1Mg caused by severe plastic deformation (ECAP) at room temperature

It is worth noting from the above study that cast aluminium and Al-5Zn-1Mg couldn't survive the required amount of passes even though they were deformed at a higher die angle where severity of deformation is less. Apart from the reasons discussed above it can be also interpreted from type of deformation during ECAP. While ECAP was believed to impart uniform simple shear deformation to the material while processing, many finite-element simulation and experimental works have shown that the actual stress–strain distribution is non-uniform and the deformation is not simple shear [Segal, 2003]. Uniformity of the stress and strain distributions can be improved, and an ideal simple shear deformation can be obtained with the application of back pressure during ECAP [Lapovok, 2005]. Another advantage of an imposed hydrostatic pressure during ECAP is the decrease of internal void initiation and improvements in the mechanical properties of cast billets. Application of back pressure would have helped cast aluminium and Al-5Zn-1Mg to survive more number of passes without cracking.

CHAPTER 6

CONCLUSIONS

1. Processing of CP titanium results in improved strength with reduction in ductility. Even though the hardness and ultimate tensile strength of the material was improved, the forming pressure decreased for each passes till 0.93 strains. This demonstrates that the ECAP using a 150° die angle is advantageous in improving the mechanical properties of CP titanium compared to other die angles with respect to lower punch pressure.

2. As received microstructure of cast aluminium is altered by ECAP. The casting defects like inter-dendritic porosities are reduced by changing the orientation of cast aluminium from one pass to another; different combinations of severity of breakdown of cast ingots were obtained. Processing via route B_A and B_C has a profound effect in breakdown of dendrites as compared to samples processed by route A and C. It is clear that altering the dendritic structure caused a simultaneous increase in flow properties like strength coefficient and strain hardening exponent. The severity of increase in strain hardening was more in first pass and at a lesser extent in the subsequent passes. VHN exhibit a significant increase with increase in equivalent plastic strain for cast aluminium rods. These enhancements in strength and hardness are profound in the first pass itself, but happen to increase at lower rate in next subsequent passes. Comparison of microstructure, flow properties and mechanical properties were carried out for different routes for multiple passes and the most effective route determined for cast aluminium rod in the present study was route B_C.

3. Comparison of UTS and hardness were carried out for all the four routes and the most effective routes determined for commercially pure wrought aluminium rod were found to be was B_A and B_C. UTS and VHN of CP aluminum rod in the wrought form exhibited a significant increase with increase in equivalent plastic strain. These enhancements in strength and hardness were profound in the first pass itself, but happen to increase at lower rate in next subsequent passes at the

expenses of reduction in ductility. The increase may be due to the buildup of high dislocation density and initiation of sub grain walls.

4. Al-5Zn-1Mg rod showed maximum plasticity in the temperature range of 373-573 K, where an improvement in hardness is also seen. The peak punch pressure was least when processed at 573K.

5. Tubular specimens of CP aluminium in the wrought form were subjected to three ECAP passes using four different processing routes. The VHN of ECAP processed material increased for 0.31 and 0.62 strain but didn't show pronounced difference between various routes. At 0.93 strain route B_A showed maximum hardness and route C showed the minimum hardness, whereas increase in forming pressures for three passes were insignificant except for route B_C. Thus it can be concluded that ECAP is a promising technique for improving properties of tubular specimen of CP aluminium in the wrought form.

6. Cast Al and Al-5Zn-1Mg tube cannot be processed at room temperature using ECAP without back pressure. A proper workability range where precipitates are dissolved and flow stresses are minimum is to be determined to process cast Al-5Zn-1Mg tube and a workability range where pores gets welded instead of propagating should be determined for cast aluminium tube. It also reveals that application of back pressure is a requirement even in the case of higher die angles when processing tubular specimen.

REFERENCES

Ahmed, H., Eivani, A.R., Zhou, J., and Duszczyk, J. (2008), "Proc. Symp. Aluminum Alloys: Fabrication, Characterization and Application", TMS Annual Meeting, New Orleans

Akhtar A. (1975), "Basal slip and twinning in α − Ti single crystals, Metallurgical Transactions A, Vol.6, 1105

Alexandrov, I.V. and Valiev R.Z. (2000), "Developing of SPD processing and enhanced properties in bulk nanostructured metals", The physics and engineering of high pressures, Vol. 10, No. 4, 9-13

Alkorta, J., Rombouts M., De Messemaeker J., Froyen L. and Gil Sevillano J. (2002), Scripta Mater; 47:13

ASM Handbook (1992), "Metal Forming", 10th ed., vol. 14, ASM International, Metals Park, OH

Azushima, A. and Aoki, K. (2002), "Properties of ultrafine-grained steel by repeated shear deformation of side extrusion process", Materials Science and Engineering A 377(1–2):45–49

Belov, N., A., Eskin, D., G., Aksenov, A., A. (2005), "Multicomponent Phase Diagrams: Applications for Commercial Aluminum Alloys", Elsevier Science, New York

Berbon, P.B., Furukawa M., Horita Z., Nemoto, M. and Langdon T.G. (1999), "Influence of pressing speed on microstructural development in equal-channel angular pressing," Metallurgical and Materials Transactions A Vol.30, 1989-1997

Biswas, C.P. (1973), "Strain hardening of titanium by severe plastic deformation, Massachusetts Institute of Technology, MS Thesis

Bozzolo, N., Dewobroto, N., Wenk, H.R. and wagner F. (2007), "Microstructure and micro texture of highly cold-rolled commercially pure titanium, J Mater Sci 42, 2405-2416

Cabibbo, M., Evangelista, E. and Scalabroni, C. (2005), "EBSD FEG-SEM, TEM and XRD techniques applied to grain study of a commercially pure 1200 aluminum subjected to equal-channel angular-pressing", Micron,36,401–414

Cathleen Ruth Hutchins (2007), "Consolidation of copper and aluminum micro and nanoparticles via equal channel angular extrusion." M.S. Thesis, Texas A&M University

Chakkingal, U., Suriadi, A. B. and Thomson P., F. (1998), "Microstructure development during equal channel angular drawing of Al at room temperature", Scripta Materialia, Vol. 39(6), 677-684

Chakkingal, U., Suriadi A.B., Thomson P.F. (1999),"The development of microstructure and influence of processing route during equal channel angular drawing of pure aluminium" Materials Science and Engineering A 266, 241-249

Chakkingal, U., and Thomson, P., F. (2001), "Development of microstructure and texture during high temperature equal channel angular extrusion of aluminum", Journal of Materials Processing Technology, 117, 169–177

Chen, Y.C., Huang, Y.Y., Chang, C.P. and Kao, P.W. (2003), "The effect of extrusion temperature on the development of deformation microstructures in 5052 aluminium alloy processed by equal channel angular extrusion", Acta Materialia, Vol. 51(7), 2005-2015

Christian, J. W. and Mahajan, S.(1995),"Deformation Twinning," Progress in Materials Science, Vol. 39, No. 1-2, 1995, 1-157

Cornwell, L. R., Hartwig, K. T., Goforth, R. E., and Semiatin, S. L. (1996), "The Equal Channel Angular Extrusion Process for Materials Processing", Materials Characterization, 37, 295-300

Courtney T.H. (2000), "Mechanical behavior of materials", second ed., McGraw-Hill, Boston, USA

Dalla Torre F., Lapovok, R., Sandlin, J., Thomson, P.F., Davies, C.H.J. and Pereloma E.V.(2004), "Microstructures and properties of copper processed by equal channel angular extrusion for 1−16 passes", Acta Materialia, Vol.52(16), 4819-4832

Dieter, G. E. (2001), "Mechanical Metallurgy", McGraw-Hill Book Company, 254-258

Djavanroodi, F., and Ebrahimi, M. (2010), "Effect of die channel angle, friction and back pressure in the equal channel angular pressing using 3D finite element simulation", Materials Science and Engineering A 527, 1230–1235

Donachie, M.J. (2000), "Titanium: A Technical Guide", second ed., ASM International, Materials Park, OH.

EI-Danaf, E. A. (2008), "Mechanical properties and microstructure evolution of 1050 aluminum severely deformed by ECAP to 16 passes", Materials Science and Engineering A 487(1-2), 189-200

Fang, D.R., Zhang, Z.F., Wu, S.D., Huang, C.X., Zhang, H., Zhao, N.Q. and Li, J.J. (2006), "Effect of equal channel angular pressing on tensile properties and fracture modes of casting Al–Cu alloys" Materials Science and Engineering A 426, 305–313

Ferrasse, S., Segal, V. M., Hartwig, K.T., and Goforth, R.E. (1997), "Microstructure and properties of copper and aluminum alloy 3003 heavily worked by equal channel angular extrusion" Metallurgical and Material Transactions A, Vol.28, 1047-1057

Ferrasse, S., Alford, F., Grabmeier, S., Du¨ vel, A., Zedlitz, R., Strothers, S., and Evans, J., Daniels, B. (2003), Technology White Paper, Honeywell International Inc.

Ferrasse, S., Segal, V. M., Kalidindi, S.R and Alford, F. (2004), "Texture evolution during equal channel angular extrusion: Part I. Effect of route, number of passes and initial texture", Materials Science and Engineering: A, Vol.368 (1–2), 28-40

Fukuda, Y., Oh-ishi, K., Horita, Z., and Langdon, T. G. (2002),"Processing of a low-carbon steel by equal-channel angular pressing," Acta Mater.,50, 1359–1368

Fukuda, Y., K. Oh-ishi, Furukawa M., Horita Z. and Langdon T.G. (2006), "Influence of crystal orientation on ECAP of aluminum single crystals," Materials Science and Engineering A 420, 79-86

Furukawa, M., Horita Z., Nemoto M. and Langdon T.G. (2001), "Processing of metals by simple shear: principles of equal-channel angular pressing", Journal of Materials Science, Vol.36, 2835-2843

Goloborodko, Sitdikov, O., Kaibyshev R., Miura H., and T. Sakai (2004), "Effect of pressing temperature on fine-grained structure formation in 7475 aluminum alloy during ECAP", Materials Science and Engineering A, 381, 121–128

Gubicza J., Schiller I., Chinh N.Q., Illy J., Horita Z. and Langdon T.G.(2007), "Precipitation microstructure of ultrafine-grained Al-Zn-Mg alloys processed by severe plastic deformation " ,Mater. Sci. Eng. A, 460–461, 77-55

Gupta, R. K., Nayan, N., Ghosh and B., R. (2006), "Design of homogenization cycle for various grain sizes of aluminum alloy AA2219 using diffusion principles", Canadian Metallurgical Quarterly, 45(3), 347-352

Han Jun-Hyun, Hyun-Kwang Seok, Young-Hoon Chung, Myung-Chul Shin, Jae-Chul Lee (2002), "Texture evolution of the strip cast 1050 Al alloy processed by continuous confined strip shearing and its formability evaluation" Materials Science and Engineering: A, Vol. 323(1–2), 342-347

Horita, Z., Fujinami T., Nemoto M., Langdon T. G. (2000), "Equal-channel angular pressing of commercial aluminium alloys: grain refinement, thermal stability and tensile properties", Metallurgical and Materials Transactions A, Vol.31, 691-701

Horita, Z., Fujinami, T. and Langdon T.G. (2001), "The potential for scaling ECAP: effect of sample size on grain refinement and mechanical properties," Materials Science and Engineering A 318, 34-41

Horita Z., Ohashi K., Fujita T., Kaneko K. and Langdon T.G. (2005), "Achieving high strength and high ductility in precipitation-hardened alloys," Advanced Materials 17, 1599-1602

Huang, W.H., Yu C.Y., Kao P.W. and Chang C.P. (2004), "The effect of strain path and temperature on the microstructure developed in copper processed by ECAE", Materials Science and Engineering A, Vol. 366(2), 221-228

Huang J., Zhu Y.T., Jiang H. and Lowe T. C. (2001), "Microstructures and dislocation configurations in nanostructured Cu processed by repetitive corrugation and straightening", Acta Materialia, 49(9), 1497-1505

Islamgaliev, R.K., Yunusova N.F., Sabirov I.N., Sergeeva A.V. and Valiev R.Z. (2001), "Deformation behaviour of nanostructured aluminum alloy processed by severe plastic deformation", Mater. Sci. Eng., Vol. A 319-321, 877-881

Iwahashi, Y., Horita, Z., Nemoto, M. and Langdon, T.G. (1997), "An Investigation of Microstructural Evolution during Equal-Channel Angular Pressing", Metallurgical and Materials Engineering A, 4733–4741

Iwahashi, Y., Horita, Z., Nemoto, M. and Langdon T.G. (1998), "The process of grain refinement in equal-channel angular pressing", Acta Mater., Vol.46, No.9, 3317-3331

Iwahashi, Y., Horita, Z., Nemoto, M. and Langdon, T. G. (1998), "Factors influencing the Equilibrium Grain Size in Equal-Channel Angular Pressing: Role of Mg additions to Aluminum", Metall. Mater. Trans. A, 29, 2503-2510

Iwahashi Yoshinori, Furukawa Minoru, Horita Zenji, Nemoto Minoru and Langdon Terence G., (1998), "Microstructural characteristics of ultrafine-grained aluminum produced using equal-channel angular pressing", Metallurgical And Materials Transaction A, 29, 2245-2252

Iwahashi, Y., Wang, J., Horita, Z., Nemoto, M. and Langdon, T.G. (1996), "Principle of equal-channel angular pressing for the processing of ultra-fine grained materials" Scripta Materialia, 35(2), 143–146

Iwahashi, Y., Horita, Z., Nemoto, M. and Langdon, T.G. (1997), "Equal-channel angular pressing for the processing of superplastic materials", THERMEC'97, (T. Chandra and T. Sakai, eds.), Vol. II, pp. 1945-1951, The Minerals, Metals and Materials Society, Warrendale, PA

Kalidindi, S.R., Salem, A.A. and Doherty, R.D. (2003), "Role of Deformation Twinning on Strain Hardening in cubic and Hexagonal, Polycrystalline", Adv.Eng.Mater. 5(4), 229-232

Kamachi, M., Furukawa M., Horita Z., and Langdon, T.G. (2003), "An Model Investigation of the Shearing Characteristics in Equal-Channel Angular Pressing," Materials Science and Engineering A 347, 223-230

Kamachi, M., Furukawa, M., Horita, Z. and Langdon, T.G. (2003), "Equal-Channel Angular Pressing Using Plate Samples," Materials Science and Engineering A 361, 258-266

Kamachi, M., Takayoshi, F., Horita, Z. and Langdon, T.G. (2004), "Influence of Channel Geometry on Super-plasticity in Equal-Channel Angular Pressing," Materials Science Forum, 447-448, 477-482

Kamachi M., Furukawa M., Horita Z. and Langdon T.G.(2004), "Application of Equal-Channel Angular Pressing for Grain Refinement of Plate Samples," Ultrafine Grained Materials III (Y.T. Zhu, T.G. Langdon, R.Z. Valiev, S.L. Semiatin, D.H. Shin

and T.C. Lowe, eds.), The Minerals, Metals and Materials Society, Warrendale, PA. 407-412

Khan, Z.A., Chakkingal, U. and Venugopal, P.(2003), "Analysis of forming loads, microstructure development and mechanical property evolution during equal channel angular extrusion of a commercial grade aluminum alloy", Journal of Materials Processing Technology, Vol.135, Issue 1,59-67

Kim Inyoung, Won-Sik Jeong, Jongryoul Kim, Kyung-Tae Park, Dong Hyuk Shin (2001), "Deformation structures of pure Ti produced by equal channel angular pressing" Scripta mater.Vol.45, Issue 5, 575-580

Kim, J.K., Jeong, H.G., Hong, S.I., Kim, Y.S and Kim W.J. (2001), "Effect of aging treatment on heavily deformed microstructure of a 6061 aluminium alloy after Equal Channel Angular pressing", Sripta materilia, 45, 901-907

Kim I., Kim J., Shin, D.H., Liao, X.Z., Zhu, Y.T. (2003), "Deformation twins in pure titanium processed by equal channel angular pressing", Scripta Mater. Vol.48, 813–817

Kim, I., Kim, J., Shin, D.H., Lee, C.S., Hwang, S.K.(2003), "Effects of equal channel angular pressing temperature on deformation structures of pure Ti", Materials Science and Engineering: A, Vol. 342, Issues 1–2, 302-310

Koch, C.C. (2003), "Optimization of strength and ductility in nanocrystalline and ultrafine grained metals, Scripta Materialia, Vol.49, Issue7, 657-662

Korbel, A. and Richert, M. (1985), "Formation of shear bands during cyclic deformation of aluminium", Acta Metallurgica, 33, 1971-1978

Langdon, T.G. (2007), "The principles of grain refinement in equal channel angular pressing", Materials Science and Engineering A, 462, 3-11

Langdon, T.G., Furukawa, M., Nemoto, M. and Horita, Z. (2000), "Refining grain size through severe plastic deformation," JOM 52 (4), 30-33

110

Lange, K. (1985), "Hand book of Metal Forming", McGraw-Hill, New Delhi, 15.36 - 15.73

Lapovok, R. (2005), "The role of back-pressure in equal channel angular extrusion", Journal of Material Science, Vol.40 (2), 341-346

Lee, J. W., and Park, J. J. (2002), "Numerical and experimental investigations of constrained groove pressing and rolling for grain refinement", Journal of Materials Processing Technology, 130, 208-213

Lim, S., T., Lee, Y., Y., Eun, I., S. (2006), Mater. Sci. Forum 519-521, 549

Lowe T.C. and Valiev R.Z. (Eds.) (2000), "Investigations and Applications of Severe Plastic Deformation", Kluwer Academia Pub., Dordrecht, 347–56

Ma, A., Suzuki, K., Nishida, Y., Saito, N., Shigematsu, I., Takagi, M., Iwata, H., Watazu, A. and Imura, T. (2005) "Impact Toughness of an Ultrafine-grained Al–11 mass% Si Alloy Processed by Rotary-die Equal-channel Angular Pressing", Acta Materialia 53(1):220–221

Ma, A., Suzuki, K., Saito N., Nishida Y., Takagi, M., Shigematsu, I., and Iwata, H. (2005), "Impact toughness of an Ingot Hypereutectic Al–23 Mass% Si Alloy improved by Rotary-die equal-channel angular pressing", Materials Science and Engineering A, 399 (1–2):181–189

Ma, A., Nishida, Y., Suzuki, K., Shigematsu, I. and Saito, N. (2005), "Characteristics of Plastic Deformation by Rotary-die Equal-channel Angular Pressing", Scripta Materialia 52(6):433–437

Málek, P., Cieslar, M. and Islamgaliev, R.K. (2004), "The influence of ECAP temperature on the stability of Al–Zn–Mg–Cu alloy", Journal of Alloys and Compounds, 378, 237–241

111

Male, A.T. and Cockroft, M.G. (1964), "A method for the determination of the coefficient of friction of metals under condition of bulk plastic deformation", J. Inst. Metals, 93, 38-46

Mallikarjuna, C., Shashidhara, S.M., and Mallik, U.S. (2009), "Evaluation of grain refinement and variation in mechanical properties of equal-channel angular pressed 2014 aluminum alloy", Materials and Design, 30, Issue 5,1638–1642

Matthias Hockauf, Lothar W. Meyer, Daniela Nickel, Gert Alisch, Thomas Lampke, Bernhard Wielage, Lutz Kruger (2008),"Mechanical properties and corrosion behaviour of ultrafine-grained AA6082 produced by equal channel angular pressing", Journal of material science, Vol.43,7409-7417

Matsuki, K., Aida T., Takeuchi, T., Kusui, J. and Yokoe K. (2000), "Microstructural characteristics and superplastic-like behavior in aluminum powder alloy consolidated by equal-channel angular pressing", Acta Materialia, 48 (10):2625–2632

May, J., Höppel, H.W. and Göken, M. (2005), "Strain rate sensitivity of ultrafine-aluminium processed by severe plastic deformation", Scripta Materialia, Vol. 53, 189-194

Minonishi, Y., Morozumi, S., Yoshinaga, H. (1985), "Accommodation around {1011} twins in titanium", Scripta Metallurgica, Vol.19, Issue 10, 1241-1245

Morozumi, Y., and Yoshinaga S., H. (1982), "{1122} <1123> slip in titanium" Scripta Metallurgica, Vol.6, Issue 4, 427-430

Mondal, C., and Mukhopadhyay, A. K. (2005), "On the nature of T($Al_2Mg_3Zn_3$) and S(Al_2CuMg) phases present in as-cast and annealed 7055 aluminum alloy." Materials Science and Engineering, A, Vol.391, 367

Mughrabi H., Höppel, H.W., Kautz, M., and Valiev R.Z. (2003), "Annealing treatments to enhance thermal and mechanical stability of ultrafine-grained metals

produced by severe plastic deformation", Zeitschrift für Metallkunde, Vol.94, No.10, 1079-1083

Murayama, M., Horita, Z. and Hono, K. (2001), "Microstructure of two phase Al-1.7at. % Cu alloy deformed by equal channel angular pressing", Acta mater., 49, 21-29

Nagasekhar, A.V., Chakkingal, U. and Venugopal, P. (2006), "Equal channel angular extrusion of tubular aluminium alloy specimens - Analysis of extrusion pressures and mechanical properties", Journal of Manufacturing Processes, Vol. 8(2), 112-120

Nagasekhar, A.V., Chakkingal, U. and Venugopal, P. (2006), "Candidature of equal channel angular pressing for processing of tubular commercial purity titanium", Journal of Materials Processing Technology, 173, 53–60

Nakashima, K., Horita, Z., Nemoto M. and Langdon, T.G. (1998), "Influence of channel angle on the development of ultrafine grains in equal-channel angular pressing", Acta Mater. 46 (5), 1589-1599

Nakashima Kiyotaka, Zenji Horita, Minoru Nemoto and Terence G. Langdon (2000), "Development of a multi-pass facility for equal-channel angular pressing to high total strains", Materials Science and Engineering A, Vol.281 (1-2), 82–87

Nam, C.Y., Han, J.H., Chung, Y.H. and Shin M.C. (2003), "Effect of Precipitates on Microstructural Evolution of 7050 Al Alloy Sheet during Equal Channel Angular Rolling", Materials Science and Engineering A 347(1–2):253–257

Nasser Nemat, S., Guo, W.G. and Cheng, J.Y. (1999), "Mechanical properties and deformation mechanisms of a commercially pure titanium Acta Materialia, 47, 3705 – 3720

Nemoto, M., Horita, Z., Furukawa, M. and Langdon, T.G. (1998), "Equal-Channel Angular Pressing: A Novel Tool for Microstructural Control", Metals and Materials Vol.4, 1181-1190

Nemoto, M., Horita, Z., Furukawa, M. and Langdon, T.G. (1999), "Microstructural Evolution for Superplasticity using Equal-Channel Angular Pressing", Materials Science Forum, 59, 304-306

Numukara, H. and Koiwa, M. (1998), "Dislocations in metals and alloys with hexagonal close-packed structure", Metall. Sci. Technology, 16 (1-2), 4-19

Oh-Ishi, K., Horita, Z., Furukawa, M., Nemoto, M. and Langdon, T. G. (1998), "Optimizing the rotation conditions for grain refinement in equal-channel angular pressing", Metall. Mater. Trans. A, Vol.29, 2011-2013

Oh-ishi, K., Hashi Y., Sadakata, A., Kaneko, K., Horita, Z. and Langdon, T.G. (2002), "Microstructural control of an Al-Mg-Si alloy using equal-channel angular pressing," Materials Science Forum 396-402, 333-338

Park, K.T., Han, S.Y., Shin, D.H., Lee, Y.K., Lee, K.J. and Lee K.S. (2004), "Effect of heat treatment on microstructures and tensile properties of ultrafine grained C-Mn Steel containing 0.34 mass % V, ISIJ International 44(6):1057–1062

Park, K.T., Lee, H.J., Lee, C.S, Nam, W.J., Shin, D.H. (2004), "Enhancement of High Strain Rate Superplastic Elongation of a Modified 5154 Al by Subsequent Rolling after Equal Channel Angular Pressing", Scripta Materialia, Vol.51 (6):479–483

Paton N.E., and Backofen W.A. (1970), "Plastic deformation of titanium at elevated temperatures, Metallurgical and Materials Transactions B, 1, 2839-2847

Prangnell P.B., Gholinia A., and Markushev V.M. (1999), Proceedings of NATO Advanced research workshop on investigations and applications of severe plastic deformation, 2–6 August, Moscow, Russia

Raab, G.I. (2005), "Plastic flow at equal channel angular processing in parallel channels", Materials Science and Engineering: A, Volumes 410–411, 230-233

Raab, G.J, Valiev, R.Z., Lowe, T.C. and Zhu, Y.T (2004), "Continuous processing of ultrafine grained Al by ECAP-Conform", Materials Science and Engineering A 382(1–2):30–34

Raab, G. I., Soshnikova, E. P. and Valiev, R. Z. (2004), "Influence of temperature and hydrostatic pressure during equal channel angular pressing on the microstructure of commercial purity Ti", Materials Science and Engineering A, 387-389,674-677

Raab, G.I., Krasilnikov, N.A., Alexandrov, I.V. and Valiev, R.Z. (2000), "Structure and properties of copper after ECA-pressing in conditions of elevated pressures", The Physics and Engineering of High Pressures, Vol.10, No.4, pp.73-77

Reed Hill R.E. and Reza Abbaschean, (1994), "Physical Metallurgy", Principles, PWS Publishing, Boston

Rijesh M., Valder J., Geethalakshmi K., and Surendranathan A. O. (2011), "Deformation of Al-5Zn-1Mg in the temperature range of 303 – 673 K", International Journal of Engineering Sciences & Management, Vol. I, Issue II, 18-22

Rokhlin, S.I., Wang, L., Xie, B., Yakovlev, V.A., and Adler, L. (2004), "Modulated angle beam ultrasonic spectroscopy for evaluation of imperfect interfaces and adhesive bonds", Ultrasonics 421037-1047

Rybin, V.V., and Izvestiya Vuzov Fizika (1999), "Proceedings of Institutes of Higher Education. Physics", Vol.3, 7

Saito Y., Tsuji N., Utsunomiya H., Sakai T. and Hong R. G. (1998), "Ultrafine-grained bulk aluminium produced by accumulative roll bonding (ARB) process", Scripta Materialia, 39, 1221-1227

Saito Y., Utsunomiya H., Suzuki H., and Sakai T. (2000), "Improvement in the r-value of aluminum strip by a continuous shear deformation process", Scripta Materialia Vol.42 (12):1139–1144

Sakai, G., Horita, Z. and Langdon, T.G.(2005), "Grain refinement and super plasticity in an aluminium alloy processed by high pressure torsion", Materials Science and Engineering A, 393, 344-351

Salem Ayman A., Surya R. Kalidindi and Roger D. Doherty (2003), "Strain hardening of titanium:role of deformation twinning, Acta Materialia, 51,4225-4237

Salischev, G.A., Valiakhmetov, O.R., and Galeyev, R.M. (1993), "Formation of sub micro crystalline structure in the titanium alloy VT8 and its influence on mechanical properties", Journal of Material Science, 28, 2898-2902

Saray, O. and Purcek G. (2009), "Microstructural evolution and mechanical properties of Al–40 wt. %Zn alloy processed by equal-channel angular extrusion", Journal of Materials Processing Technology, 209, 2488-2498

Saravanan, M., Pillai, R.M. and Pai, B.C. (2005), "Equal channel angular pressing of aluminium alloys and composites – An overview", Aluminium in India, 5(2):3–14

Saravanan, M., Pillai, R. M., Pai, B. C., Brahmakumar, M. and Ravi, K. R. (2006), "Equal Channel angular pressing of pure aluminium-an analysis", Bull. Mater. Sci., Vol.29, 679-684

Segal, V.M. (1995), "Materials processing by simple shear", Mater. Sci. Eng. A, 197, 157–164

Segal, V.M. (2003), "Slip line solutions deformation mode and loading history during equal channel angular extrusion", Mater Sci Eng A, 345 (1–2), 36

Segal, V.M. (2004), "Engineering and commercialization of equal channel angular extrusion (ECAE)", Materials Science and Engineering A 386, 269–276

Segal, V.M., Reznikov, V.I., Drobyshevskiy, A. E. and Kopylov V.I. (1981), "Plastic working of metals by simple shear", Russ. Metall., 1, 99–105

Semiatin, S.L. and DeLo, D.P. (2000), "Equal channel angular extrusion of difficult-to-work alloys", Materials and Design, 21,311-322

Semiatin, S.L., DeLo, D.P., Shell, E.B. (2000), "The effect of material properties and tooling design on deformation and fracture during equal channel angular extrusion", Acta Materialia, Vol.48 (8):1841–1851

Serra, A., Bacon, D. J. and Pond, R. C. (2002), "Twins as barriers to basal slip in hexagonal-close-packed metals", Metallurgical and Materials Transactions A-Physical Metallurgy and Materials Science, Vol. 33, Issue 3, 809-812

Sergueeva, A.V., Stolyarov, V.V., Valiev, R.Z. and Mukherjee, A.K. (2001) "Advanced mechanical properties of pure titanium with ultrafine grained structure", Scripta Mater., Vol.45, 747-752

Sha G., Wang, Y.B., Liao, X.Z., Duan, Z.C., Ringer, S.P. and Langdon, T.G. (2009), "Influence of equal-channel angular pressing on precipitation in an Al–Zn–Mg–Cu alloy", Acta Materialia, 57, 3123–3132

Shan Aidang, In-Ge Moon, Hung-Suk Ko, Jong-Woo Park (1999), "Direct observation of shear deformation during equal channel angular pressing of pure aluminum", Scripta Materialia, Vol.41, Issue 4, 23, 353-357

Shin, D.H., Kim, B.C., Kim, Y.S., and Park, K.T., (2000), "Microstructural evolution in a commercial low carbon steel by equal channel angular pressing", Acta Materialia, Vol.48, 2247-2255

Shin, D.H., Kim, I., Kim, J., Kim, Y. S. and Semiatin S.L. (2003), "Microstructure development during equal-channel angular pressing of titanium", Acta Mater., 51(4):983-996

Shin, D. H., Pak, J.J., Kim, Y.K., Park, K.T. and Kim Y.S.(2002), "Effect of pressing temperature on microstructure and tensile behavior of low carbon steels processed by

equal channel angular pressing", Materials Science and Engineering: A, Vol.323, Issues 1–2, 31,409–415

Shwe, W. H. A., Kay, T. L. and Waing, W. K. K. O. (2008), "The Effect of Ageing Treatment of Aluminum Alloys for Fuselage Structure-Light Aircraft", World Academy of Science, Engineering and Technology 46, 696-699

Sivaraman, A. and Chakkingal, U. (2008), "Flow properties of commercial purity aluminum processed by equal channel angular pressing" Materials Science and Engineering A, 487, 264–270

Stolyarov, V.V., and Lapovok R. (2004), "Effect of backpressure on structure and properties of AA5083 alloy processed by ECAP", Journal of Alloys and Compounds, 378, 233–236

Stolyarov, V.V., Lapovok, R., Brodova I.G. and Thomson P.F. (2003), "Ultrafine-grained Al–5 wt.% Fe alloy processed by ECAP with backpressure", Materials Science and Engineering: A, Vol.357, Issues 1–2,159-167

Stolyarov, V.V., Latysh, V.V., Shundalov, V.A., Salimonenko, D.A., Islamgaliev, R.K. and Valiev, R.Z. (1997), "Influence of severe plastic deformation on aging effect of Al-Zn-Cu-Zr alloy" Mater Sci. Eng. A 339, 234–236

Stolyarov Vladimir V., Zhu Y. Theodore, Alexandrov V. Igor, Terry C. Lowe, and Ruslan Z. Valiev (2001), "Influence of ECAP routes on the microstructure and properties of pure Ti", Materials Science and Engineering A 299, 59–67.

Stolyarov, V.V., Zhu, Y.T., Lowe, T.C. and Valiev, R.Z.(2001), "Microsturcture and properties of pure Ti processed by ECAP and cold extrusion", Mater. Sci. Eng. A303 82–89.

Stolyarov, V.V., Zhu, Y.T., Alexandrov, I.V., Lowe, T.C. and Valiev R.Z.(2003), "Grain refinement and properties of pure Ti processed by warm ECAP and cold rolling" Mater. Sci. Eng. A, Vol. 343, No. 1-2, 43-50

118

Stolyarov, V.V., Zhu, Y.T., Lowe, T.C., Islamgaliev, R.K. and Valiev, R.Z. (1999), "A two step SPD processing of ultrafine-grained titanium", Nanostructured Materials, Vol. 11, No. 7, 947-954

Stolyarov, V.V., Zeipper, L., Mingler, B., Zehetbauer, M. (2008), "Influence of post-deformation on CP-Ti processed by equal channel angular pressing", Materials Science and Engineering A 476, 98–105

Sun Pei-Ling, Po-We Kao, Chih-Pu Chang (2004), "Effect of deformation route on microstructural development in aluminium processed by equal channel angular extrusion", Metallurgical and Materials Transactions A Vol 35A, 1359-1368

Sun, P.L. Yu, C.Y., Kao, P.W. and Chang C.P. (2002), "Microstructural characteristics of ultrafine-grained aluminum produced by equal channel angular extrusion", Scripta Materialia, Vol.47, Issue 6, 377-381

Tjong S.C., Haydn Chen (2004), "Nanocrystalline materials and coatings" Materials Science and Engineering R ,Vol.45, Issues 1–2, 30, 1–88

Utsunomiya, H., Hatsuda, K., Sakai, T., Saito, Y. (2004), "Grain refinement of aluminum strip by conshearing", Materials Science and Engineering A, 372, 199–206

Valiev R.Z. (2003), "Paradoxes of Severe Plastic Deformation" Adv. Eng. Mat., Vol. 5, No. 5, 296-300.

Valiev, R.Z., Alexandrov, I.V., Zhu, Y.T. and Lowe,T.C. (2002), "Paradox of strength and ductility in metals processed by severe plastic deformation" J Mater Res Vol. 17, No. 1, 5-8

Valiev, R. Z., Islamgaliev, R. K. and Alexandrov, I. V. (2000), "Bulk Nanostructured Materials from Severe Plastic Deformation", Progress in Materials Science, Vol. 45,103-189

Valiev, R.Z. and Langdon T.G. (2006), "Principles of equal-channel angular pressing as a processing tool for grain refinement," Progress in Materials Science 51, 881-981

Venugopal, P., Venugopal, S. and Seetharaman V. (1990), "Influence of strain rate and temperature on the cold extrusion of commercially pure titanium", J. Mater. Process. Tech., 22, 163–175

Vidhyasagar, N., Anand K. S., Mithun, A. C. and Srinivasan, K. (2006), "Friction factor of CP aluminium and aluminium–zinc alloys", Bull. Mater. Sci., Vol. 29, No. 7, 685–688

Wang, J., Iwahashi, Y., Horita, Z., Furukawa, M., Nemoto, M., Valiev, R.Z. and Langdon, T.G. (1996),"An investigation of microstructure stability in an Al-Mg alloy with sub-micrometer grain size", Acta Mater., 1996, Vol.44, No.7, 2973-2982

Wang, Z.C. and Prangnell P.B. (2002), "Microstructure refinement and mechanical properties of severely deformed Al–Mg–Li alloys", Materials Science and Engineering: A, Vol.328, Issues1–2, 87-97

Wu, Y., and Baker, I. (1997), "An experimental study of equal channel angular extrusion", Scripta Materialia, Vol.37, Issue 4, 437-442

Xia, K., and Wu, X. (2005), "Back Pressure equal channel angular consolidation of pure Al particles", Scripta Materialia, Vol.53 (11):1225–1229

Xicheng Zhao, Wenjie Fu, Xirong Yanga and Terence G. Langdon (2008), "Microstructure and properties of pure titanium processed by equal-channel angular pressing at room temperature", Scripta Materialia, Vol.59, 542–545

Xirong Yang, Zhao Xicheng, Fu Wenjie (2009),"Deformed microstructures and mechanical properties of CP-Ti processed by multi-pass ECAP at room temperature", Rare Metal Materials and Engineering, Vol.38,955-957

Xu, C. and Langdon T.G. (2003), "Influence of a round corner die on flow homogeneity in ECA pressing," Scripta Materialia, Vol.48, 1-4

Xu, C., Furukawa, M., Horita, Z. and Langdon, T.G.(2005), "The Evolution of Homogeneity and Grain Refinement during Equal-Channel Angular Pressing: A

Model for Grain Refinement in ECAP," Materials Science and Engineering A, Vol.398, 66-76

Xu, C., Furukawa, M., Horita, Z. and Langdon, T.G. (2005), "Influence of ECAP on precipitate distributions in a spray-cast aluminum alloy," Acta Materialia, Vol. 53, 749-758

Yamaguchi, D., Horita, Z., Nemoto, M. and Langdon, T.G. (1999), "Significance of adiabatic heating in equal-channel angular pressing", Scripta Materialia, Vol. 41, 791-796

Yamashita, A., Yamaguchi, D. Horita, Z. and Langdon, T.G. (2000), "Influence of Pressing Temperature on Microstructural Development in Equal-Channel Angular Pressing," Materials Science and Engineering A, Vol.287, 100-106

Yoo, M.H. (1981), "Slip, twinning and fracture in hexagonal close-packed metals", Metallurgical and Materials Transactions A, Vol.12, 409-418

Yu Eunji, Inyoung Kim, Dong Hyuk Shin and Jongryoul Kim (2008), "The Japan Institute of Metals-Deformation Mechanism of Severely Deformed CP-Titanium by Uniaxial Compression Test", Materials Transactions, Vol.49, No.01, 38-40

Zeipper, L., Zehetbauer, M., Mingle, B., Schafler, E., Korb, G. and Karnthaler, H. P. (2002),"Nanomaterials by severe plastic deformation", Proceedings of the Conference – Nanospd 2, 810-816

Zhang, S., Hu, W., Berghammer, R., Gottstein, G. (2010), "Microstructure evolution and deformation behavior of ultrafine-grained Al–Zn–Mg alloys with fine ή precipitates", Acta Materialia, 58, 6695–6705

Zhao,Y.H., Liao X.Z., Cheng S., Ma E. and Zhu Y.T.,(2006),"Simultaneously increasing the ductility and strength of nanostructured alloys ", Adv Mater;18:2280

Zhao, Y.H., Liao, X.Z., Jin, Z., Valiev, R.Z. and Zhu, Y. T.(2004), "Microstructures and mechanical properties of ultrafine-grained 7075Al alloy processed by ECAP and their evolutions during annealing", Acta Materialia, 52: 4589–4599

Zhao Xicheng, Wenjie Fu, Xirong Yang and Langdon, T.G.(2008), "Microstructure and properties of pure titanium processed by equal channel angular pressing at room temperature, Scripta Materialia, 59, 542-545

Zhilyaev, A.P., Kim, B.K., Szpunar, J.A., Baró M.D. and Langdon, T.G. (2005), "The microstructural characteristics of ultrafine-grained nickel," Materials Science and Engineering A, Vol.391, 377-389

Zhu, Y.T., Huang, J.Y., Gubicza, J., Ungár, T., Wang, Y.M., Ma, E. and Valiev, R.Z. (2003),"Nanostructures in Ti processed by severe plastic deformation", J. Mater. Res., Vol. 18, No. 8, 1908-1917

Zhu, Y.T., and Langdon, T.G. (2004), "Fundamentals of nanostructured materials processed by severe plastic deformation," JOM, 56(10), 58-63

Zhu, Y.T. and Lowe, T. C. (2000), "Observations and issues on mechanisms of grain refinement during ECAP process", Materials Science and Engineering: A, Vol. 291, 1–2, 46-53

APPENDIX – I

1. VARIATION OF MICRO VICKERS HARDNESS ALONG THE LONGITUDINAL AND RADIAL DIRECTION OF CP-Al TUBE
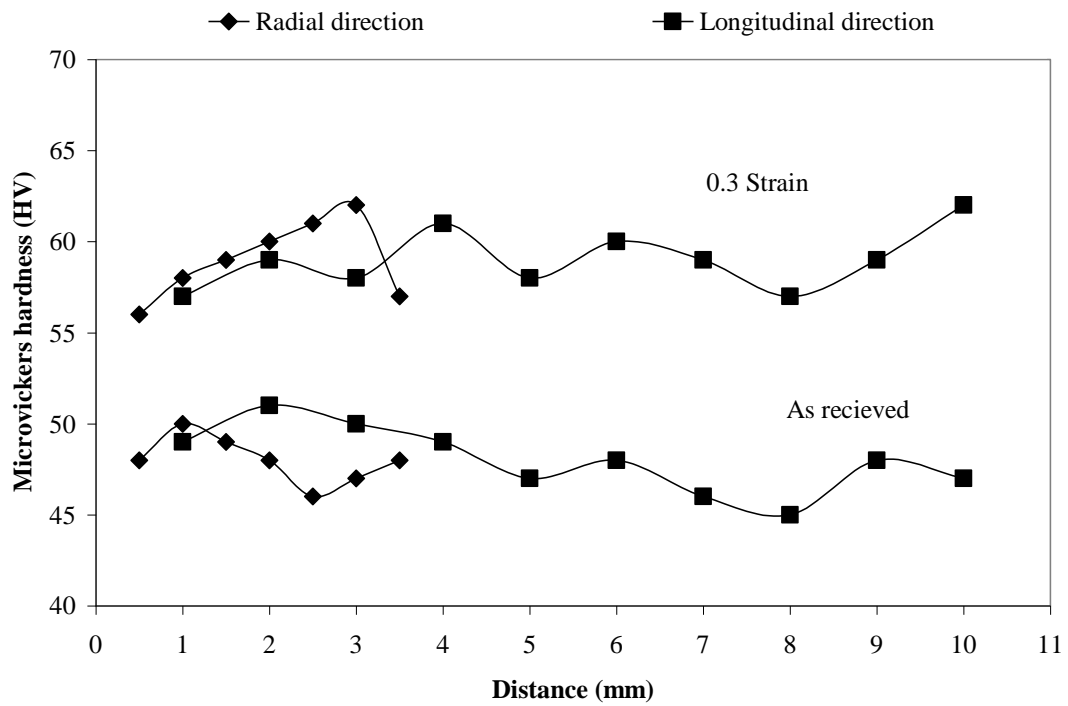

Fig.1 Hardness variation in radial and longitudinal direction of an as –received and as-pressed CP-Al tube
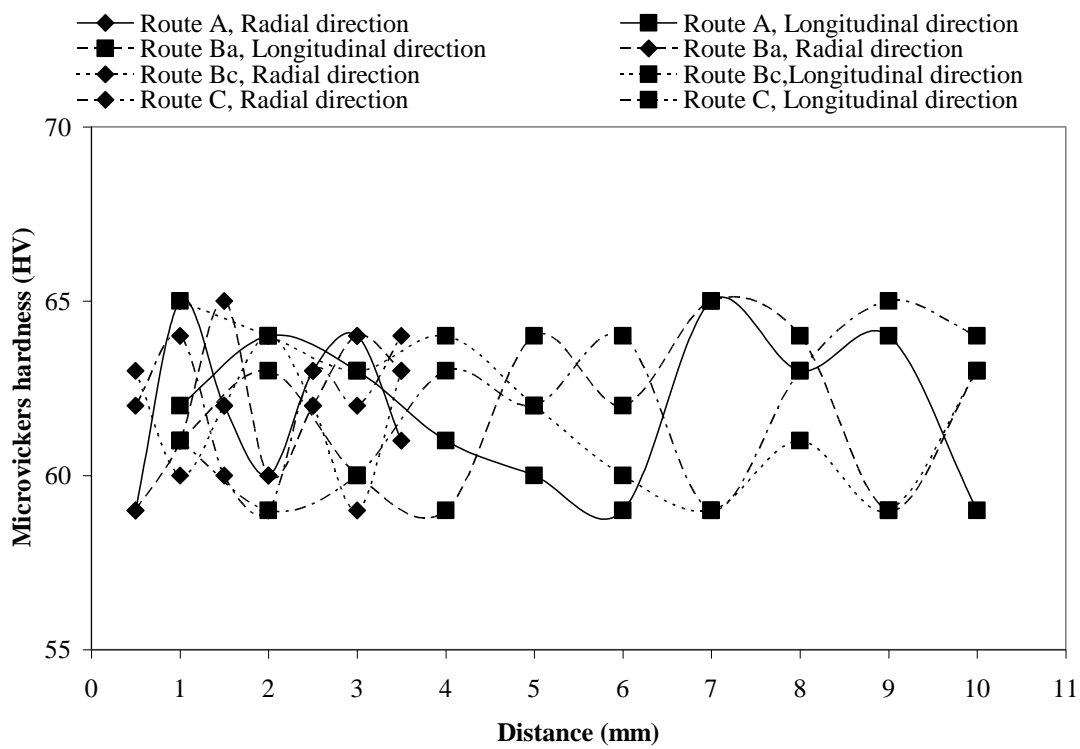
Fig.2 Hardness variation in radial and longitudinal direction of a CP-Al tube after
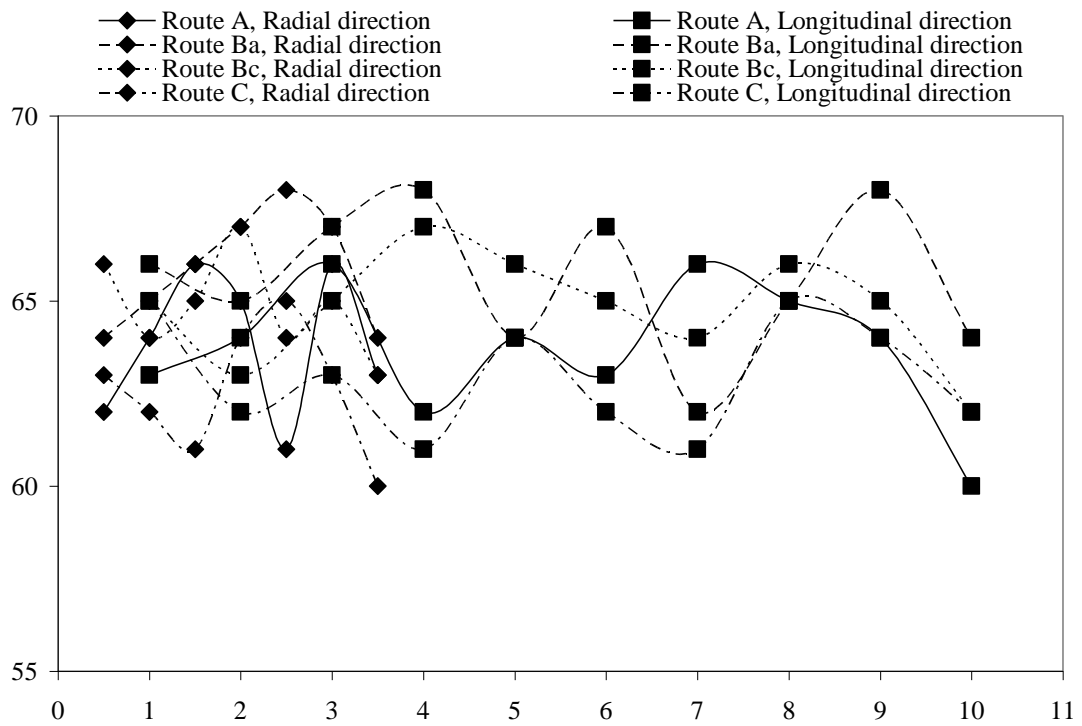
ECAP second pass processed by various routes

Fig. 3 Hardness variation in radial and longitudinal direction of a CP-Al tube after
ECAP third pass processed by various routes

2. CALCULATION OF SHAPE DIFFICULTY FACTOR FOR CP-Al TUBE AFTER EACH PASS OF ECAP

Shape difficulty factor is defined as the ratio of the surface area to volume of the extruded specimens. After each pass of ECAP, the end of sample, i.e. un-extruded portion of 5 mm sample was cut off. This causes a reduction in length of the specimen after each pass, so there will be a change in shape difficulty factor too which is shown in Table 1 below.

2.1 Surface area calculations

Surface area of a tube = $2 \times \pi$ [(Outer radius)^2 – (Inner radius)^2] + ($2 \times \pi \times$ Outer radius $\times$ Length of specimen) + ($2 \times \pi \times$ Inner radius $\times$ Length of specimen)

2.2 Volume calculations

Volume of a tube = $\pi \times$ Length of specimen [(Outer radius)^2 – (Inner radius)^2]

Table.1 Shape difficulty factor of CP-Al tube after successive pass
(When un-extruded portion of 5 mm sample was cut off after each pass)

No of passes	Length of the tube (mm)	Surface area of the tube	Volume of the tube	Shape difficulty factor (SDF)
1	60	6579.87	10880.1	0.604
2	55	6061.77	9973.43	0.608
3	50	5543.67	9066.75	0.611

LIST OF PUBLICATIONS (Based on Ph.D. Research Work)

International journals

Rijesh M., **James Valder**, Geethalakshmi K., and A. O. Surendranathan (2011), "Deformation of Al-5Zn-1Mg in the temperature range of 303 – 673 K", International Journal of Engineering Sciences & Management, Vol. I, Issue II, 18-22

James Valder, Rijesh M.,and A. O. Surendranathan (2012), "Forming of tubular commercial purity aluminium by ECAP", Materials and Manufacturing Processes, 27:986-989.

James Valder, Rijesh M., and A. O. Surendranathan (2012), "Determination of forming loads of Al-5Zn-1Mg using ECAE at various temperatures", International Journal of Engineering Sciences & Management, Vol. II, Issue I, 10-14

Rijesh M, **James Valder**, and A. O. Surendranathan (2012) "Determination of friction factor by ring compression test for Al-5Zn-1Mg using graphite and MoS_2 lubricants", Thammasat International Journal of Science and Technology, Vol. 17, No. 3, 13-19

Conference Proceedings and Presentations

James Valder and K. Srinivasan (2008), "The FEM Die design for ECAP of Ti-Ta-Nb Alloys", International Conference on Advances in Manufacturing Technology (ICAMT 2008) for Young Engineers, IIT Madras, Chennai, 6-8 February, p144.

Rajesh R, **James Valder**, K. Srinivasan, P.Parameswaran and M.Vijayalakshmi (2008),"Die design for equal channel angular pressing", International Conference on Towards Global Leadership in Minerals and Metals, 46th National Metallurgist Day & 62nd Annual Technical Meeting of the Indian Institute of Metals, Greater Noida, New Delhi, 14-16 November, p312.

James Valder, Rijesh M and A. O. Surendranathan (2009), *"*Determination of friction factor by Ring Compression Test for Al-5Zn-1Mg using graphite and MoS$_2$ lubricants", National Conference on Recent Trends in Advanced Materials(RTAM-2009), KVGCE, Sullia, Karnataka, 18th December, p168.

James Valder, Rijesh M and A. O. Surendranathan (2010), "Analysis of forming loads of Al-5Zn-1Mg using ECAE at various temperatures ", National Conference on Advances in New Engineering Materials and Characterization (AMC-2010), KVGCE, Sullia, Karnataka, 28th December, p15.

James Valder, Rijesh M and A. O. Surendranathan (2011), "Processing of tubular commercial purity aluminium by ECAP", Golden Jubilee National Conference on, Advances in Mechanical Engineering (AIM ENGG – 2011), MIT, Manipal, 3-5 January, p39

James Valder, Rijesh M and A. O. Surendranathan (2012), *"*Difficulties in processing cast Al-5Zn-1Mg tubular specimens at room temperature by Equal Channel Angular Pressing (ECAP)" National Conference on Emerging Trends in Materials for Advanced Technology (NETMAT-2012), KVGCE, Sullia, Karnataka, 20-21, March, p21.

BIO-DATA

Name	:	James Valder
Permanent address	:	Panjottu House, Pilimogaru Village, Vamadapadavu Post, Bantwal Taluk, D.K – 574324, Karnataka State, India
Email	:	jamesvalder@gmail.com, james_valder@yahoo.com
Contact Number	:	+919972717540

Academic qualification

B.E (Mechanical Engineering)	:	Bangalore University, Bangalore, India
M.Tech (Materials Engineering)	:	National Institute of Technology Karnataka, Surathkal, P.O. Srinivasanagar -575025, India
Experience	:	2.8 years of teaching and 3 years of research experience as senior research fellow (SRF)
Date of Joining for Ph.D	:	10.07.2007